Prediction of Multicomponent Equilibrium Diagrams

PREDICTION OF MULTICOMPONENT EQUILIBRIUM DIAGRAMS

by

BARTON A. THOMSON, B. Eng.

A Thesis

Submitted to the School of Graduate Studies

in Partial Fulfillment of the Requirements

for the Degree

Master of Engineering

McMaster University

April, 1978

MASTER OF ENGINEERING (1978) McMaster University
(Metallurgy) Hamilton, Ontario

TITLE: Prediction of Multicomponent Equilibrium Diagrams

AUTHOR: Barton A. Thomson, B.Eng., McMaster University

SUPERVISOR: Professor J.S. Kirkaldy

NUMBER OF PAGES: xi, 163

Abstract

Published standard free energy changes and activity data for iron and its binary and ternary alloys have been used to evaluate the general linear series (Wagner) expansion of the activity coefficient and these were employed in turn for the accurate thermodynamic determinations of the liquidus line and the field in steels with additions of Mn, Si, Ni, Cr, Mo, Cu, W, V, Nb and Co. Computer programs based on several derived analytic formulae were used to predict multicomponent constant composition and isothermal phase diagrams for total alloy additions up to 5 wt%.

Acknowledgements

The author is indebted to his supervisor, Dr. J.S. Kirkaldy, for suggesting the problems treated here and for his continuing guidance. The author also wishes to thank the staff and graduate students of the Department of Metallurgy and Materials Science for their advice and assistance.

TABLE OF CONTENTS

LIST OF TABLES

LIST OF FIGURES

CHAPTER I

INTRODUCTION

For more than a century studies have been undertaken to characterize the important transformation parameters for steels. Due to the large number of components that are added to or are naturally found in steel, this is a very complex task.

In this chapter the old empirical methods for determining the transformation temperatures are reviewed. The chapter also contains a brief review of the early approximate thermodynamic formulae.

I.1 Review of Empirical Methods

Since most of the metallurgically important transformations in steel occur at austenitising temperatures and below, the bulk of the work undertaken on the phase diagrams and transformation temperatures in the Fe-C-X and Fe-X systems is found in this range.

The important quantities that one finds discussed in the literature are: the Ae_3 temperature or the temperature under equilibrium conditions at which austenite (f.c.c. iron) begins to decompose to ferrite (b.c.c. iron); the Ac_3 temperature or the temperature at which the apparent transformation occurs on heating; the Ar_3 temperature or the temperature

of the apparent transformation on cooling. The latter two transition temperatures are normally dilatometrically determined and can vary widely with heating and cooling rates. The Ae_3 temperature is very difficult to measure accurately because of the slow heating rates and long times involved to ensure equilibrium.

The majority of efforts at predicting these temperatures have taken the form of empirical relations derived via regression analysis of the steel compositions versus the determined temperature. All of these formulae assume linear terms:

$$Ae_3(Ac_3) = \text{constant} + \sum_i A_i W_i$$

with constant coefficients to be sufficient. Baganis (1) has shown by thermodynamic analysis that this constancy assumption is inadequate in the ranges over which these relations are employed.

The best known and most widely used empirical formulae are:

(1) Andrews' (2) Formula:

$$Ac_3(^{\circ}C) = 910 - 230\sqrt{C} - 15.2\ Ni + 44.7\ Si + 104\ V + 31.5\ Mo + 131\ W - 30\ Mn - 11\ Cr - 20\ Cu + 700\ P$$

This was derived from 155 steels over the composition range up to 0.6% C, 5% Cr, 5% Ni, 5.4% Mo and 4% V.

(2) Kunitake and Ohtani's (3) Formula:

$$Ac_3(^{\circ}C) = 881 - 206\ C + 53.1\ Si - 15\ Mn - 20.1\ Ni - 0.7\ Cr - 26.5\ Cu + 41.1\ Mo$$

This was derived from 85 steels and assumed valid up to 1.70% Cr, 1.05% Mo, 0.98% Cu, 3.09% Ni and in the ranges 0.10 to 0.55% C, 0.30 to 1.67% Mn and 0.13 to 1.68% Si.

(3) Grange's (4) Formula:

$$Ae_3(^{\circ}C) = 854 - 179\ C - 14\ Mn + 22\ Si - 15\ Ni - 23\ Cr$$

derived from careful determinations of 19 steels in the composition range 0.35 to 0.63% C, 0.37 to 1.85% Mn, 0.15 to 0.30% Si, and up to 3.41% Ni, 0.93% Cr and 0.23% Mo.

(4) Andrews' (2) Formula:

$$Ae_3(^{\circ}C) = 913 - \Delta T - 25\ Mn + 11\ Cr - 20\ Cu + 60\ Si + 60\ Mo + 40\ W + 100\ V + 700\ P$$

derived from the results of Grange (4) in conjunction with the binary Fe-X phase diagrams. ΔT accounts for the undercooling due to C and Ni where:

$$C_{effective} = C + \frac{Ni}{10}$$

I.2 Approximate Thermodynamic Formulae

Since the available empirical linear regression formulae give varying results for the same steel composition and have limited ranges of application it was evident that some of the alloy effects could not be treated using a linear formula and that more fundamental thermodynamic data should be used for an adequate quantitative treatment.

The necessary form of the thermodynamic analysis began with Wever (5,6,7) who classified the binary Fe-X phase diagrams by type. This work was built upon by Zener (8) who expressed the thermodynamic quantities (such as free energy) in a form similar to that in use today. Zener's analysis was modified by Andrews (2) to try to predict the effect of alloying elements on the Ae_3 temperature.

The lack of good thermodynamic data and the cumbersome calculations involved in these early methods resulted in poor acceptance and inadequate quantitative results.

CHAPTER II

THERMODYNAMIC ANALYSIS FOR PHASE BOUNDARIES IN THE Fe-C-X_i SYSTEM

II.1 Introduction

If the thermodynamic data were available, it was thought that it would be possible to predict the effect of adding alloying elements to steel by describing their effect on the Fe-C binary phase diagram. This chapter outlines such an analysis which is applicable to all the phases which are present in the binary Fe-C system.

II.2 The Effect of Alloying Elements on the Phase Boundaries of the Fe-C System.

In this section is described a rigorous precedure for predicting dilute two phase regions similar to that of Baganis and Kirkaldy (9) for the deviation of the Ae_3 temperature of steels from Fe-C binary values.

If any two phases are in equilibrium at any temperature, T, then the partial molar free energies or chemical potentials of the alloying elements and the solvent are equal in the two phases. Analytically we have:

$$\begin{aligned} \bar{G}_i^{\gamma} &= \bar{G}_i^{\alpha} \\ \bar{G}_i^{\delta} &= \bar{G}_i^{\gamma} \\ \bar{G}_i^{L} &= \bar{G}_i^{\delta} \\ G_i^{L} &= \bar{G}_i^{\delta} \end{aligned} \qquad \text{(II-1)}$$

for the various equilibria in steel where $\bar{G}_i^{\phi}$ is the partial molar free energy of element i in the phase ϕ and ϕ is delta iron (b.c.c.), gamma iron (f.c.c.), alpha iron (b.c.c.) or the liquid state. This latter quantity can be rewritten:

$$\bar{G}_i^{\phi} = {}^{o}G_i^{\phi} + RT\ln a_i^{\phi} \qquad \text{(II-2)}$$

where ${}^{o}G_i^{\phi}$ is the standard free energy and a_i is the activity of component i in phase ϕ or alternatively:

$$\bar{G}_i^{\phi} = {}^{o}G_i^{\phi} + RT(\ln x_i^{\phi} + \ln \gamma_i^{\phi}) \qquad \text{(II-3)}$$

where x_i^{ϕ} is the mole fraction and γ_i^{ϕ} the activity coefficient. This relation can also be expressed in terms of an ideal solution contribution and an excess free energy term to account for the observed departure from ideality:

$$\bar{G}_i^{\phi} = {}^{o}G_i^{\phi} + RT\ln x_i + EG_i^{\phi} \qquad \text{(II-4)}$$

Wagner (10) recognized that the excess free energy can be described by a Taylor expansion in the solute concentrations about $x_o = 1$ (pure solvent, infinitely dilute solutes), viz.,

$$\ln\gamma_i = \ln\gamma_i^o + \left[x_i\left(\frac{\partial \ln\gamma_i}{\partial x_i}\right)_{\text{all } x_k=0} + x_j\left(\frac{\partial \ln\gamma_i}{\partial x_j}\right)_{\text{all } x_k=0} + \ldots\right] \tag{II-5}$$

It is usual to define the standard states of all solutes at infinite dilution and to introduce the coefficients:

$$\varepsilon_{ii} = \left(\frac{\partial \ln\gamma_i}{\partial x_i}\right)_{\text{all } x_k=0} \tag{II-6}$$

$$\varepsilon_{ij} = \left(\frac{\partial \ln\gamma_i}{\partial x_j}\right)_{\text{all } x_k=0} \tag{II-7}$$

evaluated at infinite dilution. These are often called Wagner interaction coefficients. The magnitude and sign of these quantities expresses the attractive or repulsive forces between atoms of element i or j in solvent iron. Further simplification is allowed by the symmetry properties of the interaction parameter (10):

$$\varepsilon_{ij}^{\phi} = \varepsilon_{ji}^{\phi} \tag{II-8}$$

Kirkaldy and Purdy (94) and De Brion (95) have applied the Gibbs-Duhem to this expansion at infinite dilution to obtain the corresponding relation for the solvent:

$$\ln\gamma_o^{\phi} = -\frac{1}{2}\sum_{i=1}^{n}\sum_{j=1}^{n}\varepsilon_{ij}^{\phi}x_i^{\phi}x_j^{\phi} \tag{II-9}$$

It is now possible to evaluate the equality of chemical potentials (equation (II-1)) to yield the expressions (rigorous up to linear terms in the solute concentrations) for any two phases, 1 and 2:

$$ {}^{o}G_i^1 + RT(\ln x_i^1 + \ln \gamma_i^1) = {}^{o}G_i^2 + RT(\ln x_i^2 + \ln \gamma_i^2) \qquad \text{(II-10)} $$

or:

$$ \frac{{}^{o}G_i^1 - {}^{o}G_i^2}{RT} = \ln \frac{x_i^1}{x_i^2} + \ln \frac{\gamma_i^1}{\gamma_i^2} \qquad \text{(II-11)} $$

or finally:

$$ \frac{\Delta^{o}G_i^{2\to 1}}{RT} = \ln \frac{x_i^1}{x_i^2} + \sum_j^n \epsilon_{ij}^1 x_i^1 - \sum_j^n \epsilon_{ij}^2 x_i^2 \qquad \text{(II-12)} $$

and:

$$ \frac{\Delta^{o}G_o^{2\to 1}}{RT} = \ln \frac{x_0^1}{x_0^2} + \frac{1}{2} \sum_{j=1}^{n} \sum_{i=1}^{n} \epsilon_{ij}^1 x_i^1 x_j^1 - \frac{1}{2} \sum_{j=1}^{n} \sum_{i=1}^{n} \epsilon_{ij}^2 x_i^2 x_j^2 \qquad \text{(II-13)} $$

$\Delta^{o}G_i^{2\to 1}$ is the shorthand notation of the standard free energy change for the transformation from phase 1 to phase 2 at equilibrium, viz.,

$$ \Delta^{o}G_i^{2\to 1} = {}^{o}G_i^1 - {}^{o}G_i^2 \qquad \text{(II-14)} $$

Neglecting the cross interaction terms between alloying elements other than carbon since these ultimately appear in a higher order, one obtains for the transformation from γ to L:

$$\frac{\Delta^o G_o^{\gamma-L}}{RT} = \ln\left[\frac{1-x_1^\gamma - \sum_2^n x_i^\gamma}{1-x_1^L - \sum_2^n x_i^L}\right] - x_1^\gamma \sum_2^n \varepsilon_{1i}^\gamma x_i^\gamma + x_1^L \sum_2^n \varepsilon_{1i}^L x_i^L - \frac{\varepsilon_{11}^\gamma}{2}(x_1^\gamma)^2$$

$$+ \frac{\varepsilon_{11}^1}{2}(x_1^L)^2 \qquad \text{(II-15)}$$

$$\frac{\Delta^o G_1^{\gamma-L}}{RT} = \ln\left[\frac{x_1^\gamma}{x_1^L}\right] + \varepsilon_{11}^\gamma x_1^\gamma - \varepsilon_{11}^L x_1^L \quad \text{For carbon (n=1)} \qquad \text{(II-16)}$$

$$\frac{\Delta^o G_i^{\gamma-L}}{RT} = \ln\left[\frac{x_i^\gamma}{x_i^L}\right] + \varepsilon_{1i}^\gamma x_1^\gamma - \varepsilon_{1i}^L x_1^L \quad \text{For component i, i=2,11}$$

$$\text{(II-17)}$$

Utilizing, in the linearization of this set of eleven equations, the partition coefficient of component i in any two phases:

$$k_i = \frac{x_i^\gamma}{x_i^L} = \frac{\exp\left[\frac{\Delta^o G_i^{\gamma\to L}}{RT} + \varepsilon_{1i}^L x_1\right]}{1 + \varepsilon_{1i}^\gamma x_1^L \exp\left[\frac{\Delta^o G_1^{\gamma\to L}}{RT}\right]} \qquad \text{(II-18)}$$

it is possible to arrive at an analytic formula for the temperature change from the binary iron-carbon phase diagram with the addition of alloying elements that is rigorous up to the linear terms in the solute concentrations:

$$\Delta T = RT_o^2 \sum_{i=2}^{11} A_i X_i^L \qquad \text{(II-19)}$$

where

$$A_i = \frac{[A_i^o - \{1+X_1^L(1-X_1^L)(\varepsilon_{1i}^L - \varepsilon_{1i}^\gamma A_1^o A_i^o)\} \exp\{\frac{\Delta^o G_o}{RT_o} - \frac{(X_1^L)^2}{2}(\varepsilon_{11}^L - \varepsilon_{11}^\gamma A_1^{o2})\}]}{X_1^L \Delta^o H_1 A_1^o + (1-X_1^L)\,\Delta^o H_o \exp\{\frac{\Delta^o G_o}{RT_o} - \frac{(X_1^L)^2}{2}(\varepsilon_{11}^L - \varepsilon_{11}^\gamma A_1^{o2})\}}$$

The full derivation is given in Appendix (1).

II.3 The Effect of Alloying on the Carbide Equilibrium in the Fe-C System

Although studies of the $\delta \rightarrow L$, $\gamma \rightarrow L$, $\gamma \rightarrow \delta$ and $\alpha \rightarrow \gamma$ transformations in the binary and ternary systems provide sufficient experimental information on the respective free energies to support evaluation in the above manner, the carbide phase equilibria do not. As a consequence, it became necessary to derive another form of the above equation so as to utilize the experimental partition coefficient information available.

Starting with the Gibbs-Duhem equation for any two phases, 1 and 2, at constant temperature and pressure, where phase 1 is the metal and phase 2 the carbide one obtains:

$$x_o^1 d\mu_o + x_1^1 d\mu_1 + \sum_2^n x_i^1 d\mu_i = 0 \qquad \text{(II-20)}$$

$$x_o^2 d\mu_o + x_1^2 d\mu_1 + \sum_2^n x_i^2 d\mu_i = 0 \qquad \text{(II-21)}$$

From these relations one obtains, using the Wagner expansion and expanding about the empirical binary iron-carbon phase diagram, the expression for the change in carbon content of the metal-carbide phase boundary at any temperature, T:

$$\Delta x_1 = \frac{-x_1^c \sum_{i=2}^{n} x_i\{k_i - 1 + (1+\epsilon_{1i})(x_i^2 - x_1^c)\}}{x_1^2 + x_1^c\{(x_1^2 - x_1^c)(1+\epsilon_{11}) - 1\}} \qquad \text{(II-22)}$$

where the partition coefficient, $k = \frac{x_i^2}{x_i^1}$ and x_1^c is the composition of carbon, in mole fraction of the binary Fe-C metal/carbide phase boundary. The full derivation is given in Appendix (II).

II.4 Dependence of T_o Temperature on Alloying

The method used to determine the analytic expression for the temperature deviation of the phase boundary can be extended for use in determining the change in the T_o temperature with alloy additions. This temperature is defined in Figure (1) according to the requirement that the integral free energy curves of the two phases present at equilibrium intersect. This corresponds to the conditions:

$$G_i^I = G_i^{II} \qquad \text{(II-23)}$$

$$x_1^I = x_1^{II} \qquad \text{(II-24)}$$

where I and II refer to phases I and phase II respectively. Using this equality of free energies and expanding about the Fe-C binary phase diagram one obtains the following expression for the T_o temperature of an iron-carbon alloy with dilute additions of other elements:

$$T_o^{alloy} = T_o^{Fe-C}\left\{1 + \frac{1}{R(T_o^{Fe-C})^2} \sum_{2}^{n} \frac{x_i^I \Delta^o G_i^{I\to II}}{x_1^I \Delta^o H_1 + (1-x_1^I)\Delta^o H_o}\right\} \qquad \text{(II-25)}$$

The full derivation of this formula is to be found in Appendix (III).

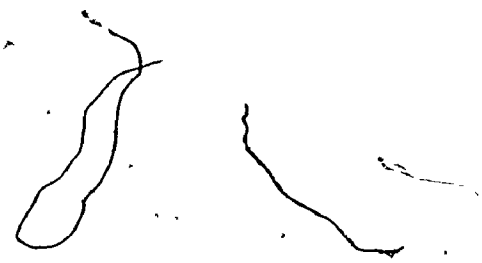

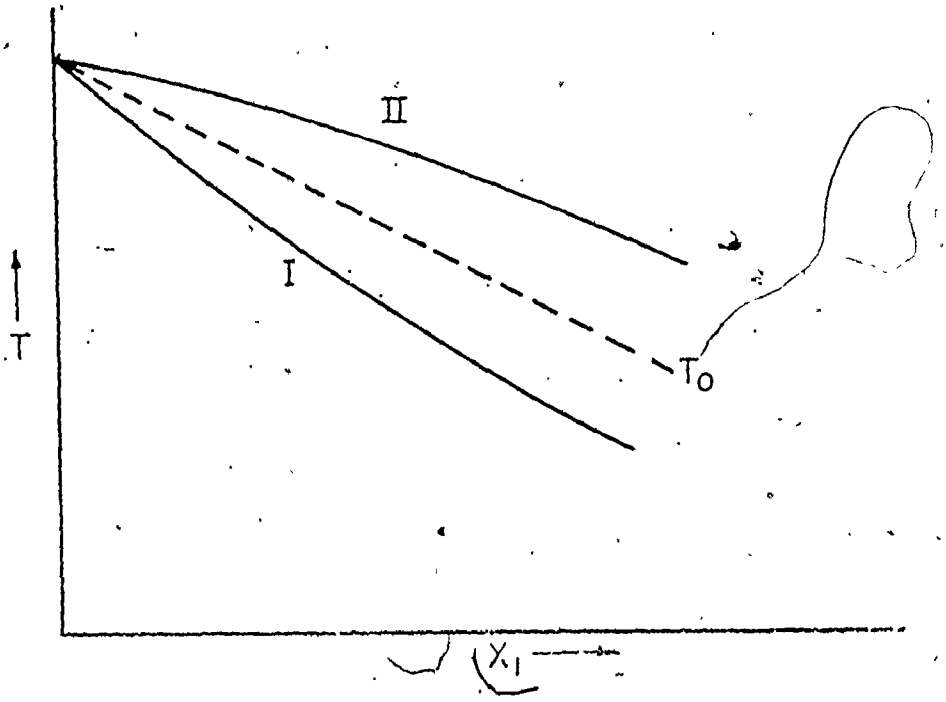

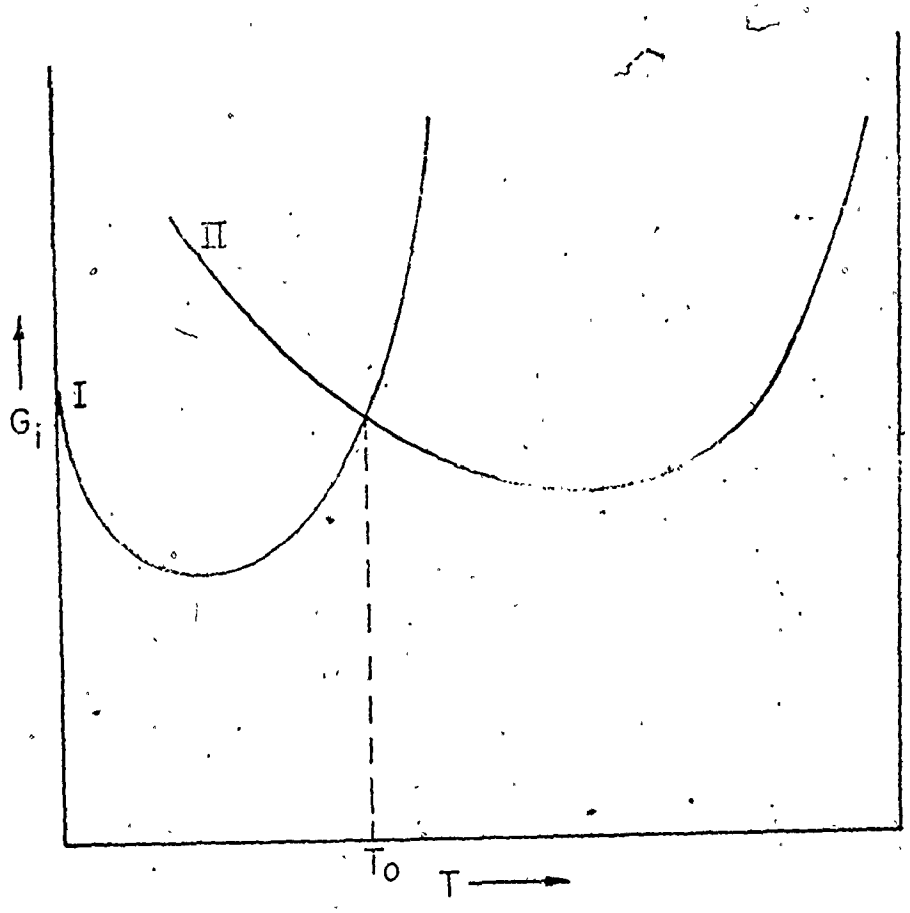

Figure 1 Schematic of T_o temperature.

CHAPTER III

THE THERMODYNAMIC DATA SET

III.1 Introduction

Although it is a relatively simple matter to derive thermodynamic equations to describe phase diagrams, it is much more difficult to obtain the thermodynamic quantities necessary to use them.

In this chapter, the free energy and interaction parameter data necessary for the utilization of our formulae are summarized and reviewed. Since it was not always possible to find information in the exact form required, it was sometimes necessary to obtain a method of conversion. The major conversion methods and their thermodynamic background are also included in order to give a comprehensive idea of the problems encountered (and their solutions) when this type of search for data is attempted.

III.2 Free Energies: Thermodynamic Analysis

Since free energy data referred to a standard state at infinite dilution was not available for all of the transformations in all of the binary Fe-X systems encompassed by this study, it was necessary to convert some free energy information in the literature from the pure component

or one weight percent standard states to the infinite dilution or Henrian standard state. In other cases it was necessary to estimate the free energy from the experimental iron binary phase diagrams.

As in Chapter II the Wagner interaction parameter formalism in conjunction with the equality of chemical potentials was used as a basis for the thermodynamic analysis of binary phase diagrams, viz.,

$$\frac{\Delta^{o}G_i^{1\to 2}}{RT} = \ln \frac{x_i^1}{x_i^2} + \ln \frac{\gamma_i^1}{\gamma_i^2} \qquad \text{(III-1)}$$

which by Taylor expansion of $\ln\gamma_i$ yields:

$$\frac{{}^{o}G_i^2 - {}^{o}G_i^1}{RT} = \ln \frac{x_i^1}{x_i^2} + \varepsilon_{ii}^1 x_i^1 - \varepsilon_{ii}^2 x_i^2 \qquad \text{(III-2)}$$

where component i is the solute and $\ln\gamma_i^{o} \to 0$ as $\gamma_i^{o} \to 1$ in the limit of infinite dilution.

The decision as to whether or not this form or the Henrian approximation to it ($\varepsilon_{ii} = 0$) would be used depended upon the reliability of the phase diagram and the size of the interaction parameters in each phase at temperature. This procedure of fitting experimental phase boundary points to the equation and solving for $\Delta^{o}G_i^{1\to 2}$ as a function of temperature was employed for the $\alpha\to\gamma$ transformation in Fe-Co and the $\alpha\to L$ transformations in the Fe-Si, Fe-Nb and Fe-V systems.

Often the free energies available were expressed in terms of a pure component standard state, e.g., all that data compiled for use

with the thermodynamic model developed by Hillert (10) and coworkers. In the Hillert model the molar free energy is expressed in the form:

$$G_M = \sum_i (x_i {}^oG_i) + RT(\sum_i x_i \ln x_i) + {}^EG_M \qquad \text{(III-3)}$$

where ${}^oG_i$ is for the pure component. By applying the equality of chemical potentials and employing the rule (11):

$$\Delta\bar{G}_i = \Delta G_M + \sum_j x_j \left[\left(\frac{\partial \Delta G_M}{\partial x_j}\right)_{x_k} + \left(\frac{\partial \Delta G_M}{\partial x_i}\right)_{x_k}\right] \qquad \text{(III-4)}$$

where x_k indicates that the ratios between other components are kept constant and $\Delta\bar{G}_i$ is the free energy of component i at infinite dilution, ΔG_M being the free energy for the pure component, substitution yields:

$$\Delta {}^oG_i^{1\to 2}\ (\text{inf.dil.}) = \Delta {}^oG_i^{1\to 2}\ (\text{pure comp.}) + RT[\ln x_i^{o1} - \ln x_i^{o2}] \qquad \text{(III-5)}$$

The temperature, T, is in degrees Kelvin and the free energies are expressed in cal/mole.

If the excess free energy term in equation (III-3) is expressed as a polynomial of the form (11):

$$E_{G_M}^1 = A_{ij}^1 x_i^1 x_j^1 = A_{ij}^1 x_i^1 (1 - x_i^1) \qquad \text{(III-6)}$$

for the binary i-j system in phase 1, this can be transformed, using

equation (III-4) to

$$\bar{E}G_i^1 = A_{ij}^1 (1-x_i^1)^2 \qquad \text{(III-7)}$$

for solvent i. This excess free energy, referenced to the pure component can now be compared with that for the infinite dilution standard state:

$$\bar{E}G_i^1 = RT\ln\gamma_i^1 \qquad \text{(III-8)}$$

$$\bar{E}G_i^1 = RT\ln\gamma_i^{o1} + RT\varepsilon_{ii}^1 x_i^1 \qquad \text{(III-9)}$$

From the comparison of equations (III-7) and (III-9) as $x_i \to 0$ it can be seen that:

$$\ln\gamma_i^{o1} = \frac{A_{ij}}{RT} \qquad \text{(III-10)}$$

Substitution back into equation (III-5) gives the transformation necessary to change standard states as a function of the regular solution parameters defined for this model, viz.,

$$\Delta^o G_i^{1\to 2} \text{ (inf.dil)} = \Delta^o G_i^{1\to 2} \text{ (pure comp.)} - A_{ij}^1 + A_{ij}^2 \qquad \text{(III-11)}$$

where A_{ij}^1 and A_{ij}^2 are the regular solution parameters in phase 1 and 2 respectively.

This type of analysis was used for the $\alpha\to L$ transformations of the Fe-Mo, Fe-Mn and Fe-W as well as the $\alpha\to\gamma$ transformations for the Fe-W, Fe-Mo, Fe-Cr and Fe-Mn systems.

The information from the data set of Elliott et al. (12) which was used for comparison purposes had to be transformed from common logarithms and the one weight percent (1 wt.pct.) standard state. For this purpose, the transformation formula given by Gaskell (13) was used. This is:

$$\Delta^{o}G_{i}^{1,2}\ (\text{inf.dil.} \rightarrow 1\ \text{wt.pct.}) = RT\ln\left(\frac{MW_j}{100\ MW_i}\right) \qquad \text{(III-12)}$$

where j is the solvent, i is the solute and MW is the molecular weight of component i or j.

III.3 Free Energies: Particular Systems

III.3.2. Fe-C

The free energy change for the $\alpha \rightarrow \gamma$ transition in iron carbon was critically analysed by Harvig (14) using the model of Hillert and Staffansson (11) and the free energy difference for α-Fe and γ-Fe determined by Orr and Chipman (15) and confirmed by Wada et al. (16). The transformed values of $\Delta^{o}G_{o}^{\alpha \rightarrow \gamma}$ are shown in Table (I), from 900 to 1820 K. The values from 1800 K to 1820 K were determined by interpolation. The free energy for the $\gamma \rightarrow \delta$ transition was obtained by assuming:

$$\Delta^{o}G_{o}^{\gamma \rightarrow \delta} = -\Delta^{o}G_{o}^{\alpha \rightarrow \gamma} \qquad \text{(III-13)}$$

since the α and δ phases both have a body centred cubic structure.

The free energy for the $\alpha \rightarrow L$ transformation was derived from the tabulated values of $\Delta^{o}G_{o}^{\alpha \rightarrow \gamma}$ and the experimental value for $\Delta^{o}G_{o}^{\gamma \rightarrow L}$ of Orr

and Chipman (15). Both are tabulated from 1600 to 1800 K in Table (I).

Utilizing the carbon free energy for $\alpha \rightarrow \gamma$ from Harvig (14), referenced to graphite:

$$ {}^{o}G_{c}^{\gamma} - {}^{o}G_{c}^{g} = 11030 - 4.594T \text{ cal/mole} \qquad \text{(III-14)} $$

$$ {}^{o}G_{c}^{\alpha} - {}^{o}G_{c}^{\gamma} = 15670 - 5.692 \text{ cal/mole} \qquad \text{(III-15)} $$

the free energy change at infinite dilution due to Sharma and Kirkaldy (17):

$$ {}^{o}G_{c}^{\alpha} - {}^{o}G_{c}^{\gamma} = -15323 + 7.686T \text{ cal/mole} \qquad \text{(III-16)} $$

and the values for the dissolution of graphite in liquid iron due to Sigworth and Elliott (18) and J. Chipman (19), (C(gr.) → C(inf.dil. in Fe)):

$$ \Delta^{o}G_{j}^{l,gr} = 5400 - 4.0T \text{ cal/mole} \qquad \text{(III-17)} $$

one obtains by rearrangement:

$$ \Delta^{o}G_{1}^{\alpha \rightarrow L} = -21300 + 6.3T \text{ cal/mole} \qquad \text{(III-18)} $$

$$ \Delta^{o}G^{\gamma \rightarrow L} = -5630 + 0.6T \text{ cal/mole} \qquad \text{(III-19)} $$

which are consistent with the Fe-C liquidus of Benz and Elliott (20).

The enthalpy values, when unrecorded, were obtained by differentiating the analytic free energy functions:

$$ \Delta^{o}H = \Delta^{o}G - T\left(\frac{\partial \Delta^{o}G}{\partial T}\right) \qquad \text{(III-20)} $$

All of the enthalpies concerning carbon were obtained in this fashion. $\Delta^{o}G_{o}^{\alpha\rightarrow\gamma}$ was fitted in the temperature range 1000 K to 1184 K by Baganis and Kirkaldy (9) and the $\Delta^{o}H_{o}^{\alpha\rightarrow\gamma}$ determined by this method is:

$$\Delta^{o}H_{o}^{\alpha\rightarrow\gamma} = \Delta^{o}G_{o}^{\alpha\rightarrow\gamma} + T(0.79 - 0.00461[T-1000]^{0.96} + 0.058\cos(0.034[T-1000])) \qquad \text{(III-21)}$$

Fischer et al. (21) report:

$$\Delta^{o}H_{o}^{\alpha\rightarrow\gamma} = -0.81T + 1183 \text{ cal/mole} \qquad \text{(III-22)}$$

in the range 1184 K to 1165 K and this agrees favourably with the preceeding formula at 1184 K. For temperatures of 900 K to 1000 K the enthalpy was assumed to be independent of temperature, the value adopted being that at 1000 K from the Baganis and Kirkaldy formula.

The experimental $\Delta^{o}H_{o}^{\gamma\rightarrow\delta}$ shows a wide scatter. Bench and Kubaschewski (22) found 200 cal/mole. Ferrier and Olette (23) reported 263 cal/mole and this was corrected by Orr and Chipman (15) to 192 cal/mole. The value adopted here was 200 cal/mole, independent of temperature.

Values for $\Delta^{o}H_{o}^{\delta\rightarrow L}$ have been reported by Ferrier and Olette (23) who found 3292 ± 80 cal/mole, Morris et al. (24) who found 3298 ± 100 cal/mole and Vollmer et al. (25) who report 3435 ± 50 cal/mole, all at 1809 K. The value chosen was 3300 cal/mole, independent of temperature. The value of $\Delta^{o}H_{o}^{\gamma\rightarrow L}$ obtained by subtraction is about 3500 cal/mole at 1809 K. The enthalpy values for iron and carbon are listed in Table (I).

Table I. Thermodynamic Functions of Iron and Carbon ($\frac{cal}{mole}$)

T(K)	$\Delta G^{\alpha\rightarrow\gamma}$	T(K)	$\Delta G^{\alpha\rightarrow\gamma}$	$\Delta G^{\delta\rightarrow L}$
900	191.1	1500	-13.95	
1000	80.80	1600	- 7.20	387.8
1100	22.22	1700	4.08	195.4
1200	-2.40	1800	19.98	16.0
1300	-12.87	1820	23.32	-7.34
1400	-16.10			

	Iron	Carbon*	References
$\Delta^{o}G^{\alpha\rightarrow\gamma}$	Tabulated		14
$\Delta^{o}H^{\alpha\rightarrow\gamma}$	-0.81T + 692	-15323	21
$\Delta^{o}G^{\delta\rightarrow\gamma}$	Tabulated		14
$\Delta^{o}H^{\gamma\rightarrow\gamma}$	200	-15323	15
$\Delta^{o}G^{\delta\rightarrow L}$	$-2646+39.1693T-5.27T\ln T+0.001T^{2}$		14,15
$\Delta^{o}H^{\gamma\rightarrow L}$	3600	-5630	15
$\Delta^{o}G^{\delta\rightarrow L}$	$\Delta^{o}G^{\gamma\rightarrow L}-\Delta^{o}G^{\alpha\rightarrow\gamma}$		
$\Delta^{o}H^{\delta\rightarrow L}$	3300	-21300	15

*$\Delta^{o}H_{1} = \Delta^{o}G_{1} - T[\frac{\partial\Delta^{o}G_{1}}{\partial T}]$

III.3.B Fe-Mn

Virtually all the work done on the $\alpha \rightarrow \gamma$ transformation in this system was based on the binary phase diagram of Troiano and McGuire (26) which contained no experimental points on the phase boundaries or in the two phase region. The only true equilibrium point in this system is that of Kirchner et al. (27) on the $\alpha/\alpha+\gamma$ phase boundary at 0.015 mole fraction manganese and 1075 K. Utilizing this point and the A^{α}-A^{γ} temperature dependence of Kirchner et al., the free energy of Baganis and Kirkaldy was corrected in an attempt to produce a $\Delta^{o}G_2^{\alpha \rightarrow \gamma}$ that would behave correctly out to 2 w/o Mn.

Plots of predicted Ae_3 temperature versus the experimentally determined values for selected steels (from reference (28)), Figures 2 and 3, show a marked systematic deviation from expected behaviour at lower carbon and higher manganese contents. This was traced back to the uncertainty in the binary phase diagram.

From the experimental phase diagram of Hellawell and Hume-Rothery (29), Kirchner et al. and Hillert and Staffansson (30) demonstrated that it was not possible to extend the $\Delta^{o}G_2^{\alpha \rightarrow \gamma}$ obtained for the Ae_3 temperature range up into the $\gamma \rightarrow \delta$ transformation because of the non-linear nature of the regular solution parameters over this range of temperature.

$\Delta^{o}G_2^{\alpha \rightarrow L}$ and $\Delta^{o}G^{\gamma \rightarrow \delta}$ were taken from reference (30) and converted to the infinite dilution standard state using the regular solution parameters suitable to the temperature ranges from references (27) and (30). The values obtained are similar to those reported by Sigworth and

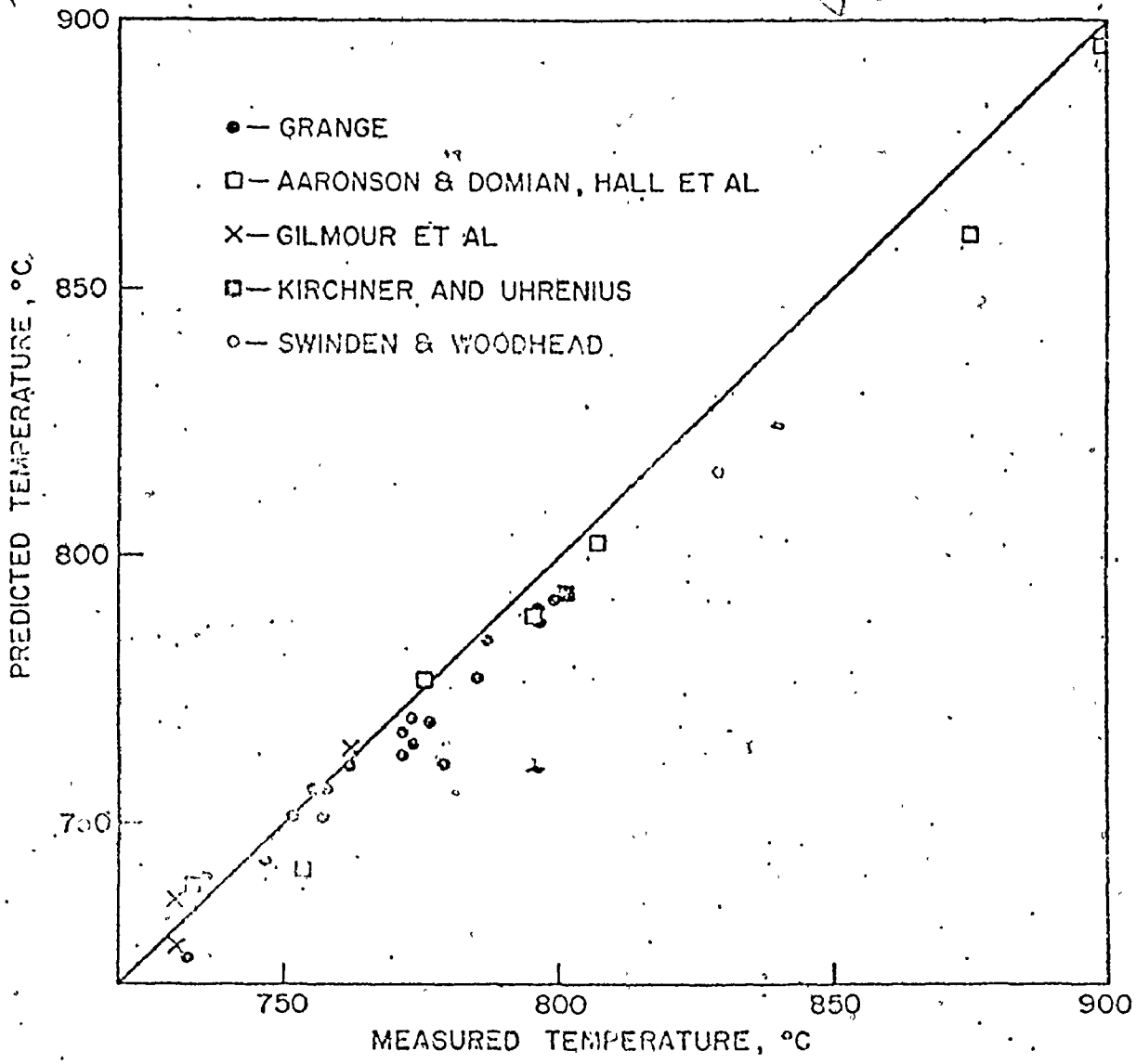

Figure 2. Predicted versus measured Ae_3 temperature for a set of low-alloy steels. Steels identified in reference (28).

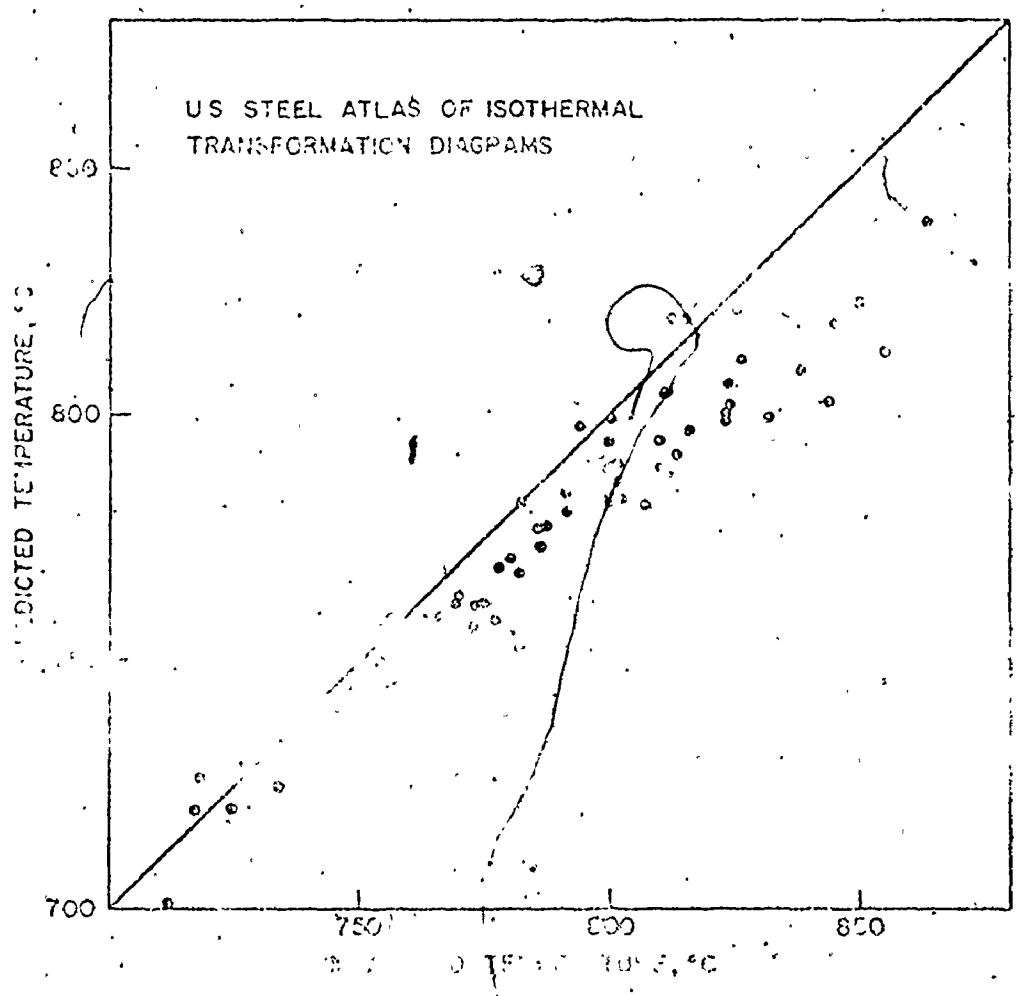

Figure 3 Predicted versus measured Ae_3 temperature for a set of low alloy steels. Steels identified in reference (28).

Elliott (18). $\Delta^{o}G^{\gamma\rightarrow L}$ was deduced by subtraction.

III.3.C Fe-Si

The free energy and regular solution parameters determined by Fridberg and Harvig (32) allowed the calculation of a $\Delta^{o}G_{3}^{\alpha\rightarrow\gamma}$ value at infinite dilution which reproduces the gamma loop of the Fe-Si phase diagram of Übelacker (31) up to 1.8 w/o Si.

Since there was insufficient reliable data on $\Delta^{o}G_{3}^{\alpha\rightarrow L}$ at infinite dilution this value was deduced by thermodynamic analysis of the phase diagram of Übelacker in the range 0 to 4 w/o Si. The solidus and liquidus are essentially linear out to this point and assumptions of both ideal solution and regular solution behaviour produced similar results. $\Delta^{o}G_{3}^{\gamma\rightarrow L}$ was obtained by subtraction.

III.3.D Fe-Ni

The $\alpha\rightarrow\gamma$ transformation was studied by Brown and Kirkaldy (17) whose results were adopted and extended up to 1800 K. For the $\gamma\rightarrow\delta$ transformation $\Delta^{o}G_{4}^{\alpha\rightarrow L}$ was a combination of Sigworth and Elliott's results and those of Kaufman and Nesor (33). Since Kaufman and Nesor reported a value for the L - f.c.c. transformation in pure nickel it was possible to obtain independent results for the $\alpha\rightarrow L$ and $\gamma\rightarrow L$ transitions.

III.3.E Fe-Cr

The free energy for the $\alpha\rightarrow\gamma$ transformation was first suggested by Kaufman (34) and used by Kirchner et al. (27) who reported the necessary

regular solution parameters for conversion to the infinite dilution standard state. Since the value of the quantity $(A^{\gamma}-A^{\alpha})$ decreased linearly with temperature in the range 1100 K to 1700 K, the $\Delta^{o}G_{5}^{\alpha\rightarrow\gamma}$ was extrapolated for use in the $\gamma\rightarrow\delta$ region (cf. equation (III-4)).

Information on the $\alpha\rightarrow L$ transformation was obtained from Reese et al. (35) who reported $\Delta^{o}G_{5}^{\alpha\rightarrow L}$ as a function of x_{Fe} (x_{Fe} = 1 at infinite dilution), Kaufman and Nesor (33), Belton and Freuhan (36) and Sigworth and Elliott (18). The adopted value was from Kaufman and Nesor and Sigworth and Elliott, assuming an ideal solution in the liquid. $\Delta^{o}G_{5}^{\gamma\rightarrow L}$ was obtained from $\Delta^{o}G_{5}^{\alpha\rightarrow\gamma}$ and $\Delta^{o}G_{5}^{\alpha\rightarrow L}$.

III.3.F Fe-Mo

The $\alpha\rightarrow\gamma$ free energy was suggested by Kaufman (34) and converted to the infinite dilution standard state using the regular solution parameters of Kirchner et al. (37). Since these parameters were well behaved with respect to temperature, the values obtained were extrapolated for use in the $\gamma\rightarrow\delta$ transformation as well. With this $\Delta^{o}G_{6}^{\alpha\rightarrow\gamma}$ it was possible to reproduce the gamma loop of Sinha et al. (38) up to 2 w/o molybdenum.

Little data was available for the free energy of the $\alpha\rightarrow L$ transformation but the value from Sigworth and Elliott, calculated assuming an ideal solution produces a good fit between the computed liquidus and that reported by Gibson et al. (39). $\Delta^{o}G_{6}^{\gamma\rightarrow L}$ was obtained from the above results.

III.3.G Fe-Cu

The value of $\Delta^{o}G_{7}^{\alpha\rightarrow\gamma}$ was reported by Baganis and Kirkaldy (9) who fitted the data of Weiss and Tauer (40). By means of a method similar to that used for manganese, Harvig et al. (41), using the phase diagram of Hellawell and Hume-Rothery (29), demonstrated that the temperature dependence of the regular solution parameters were such that $\Delta^{o}G_{7}^{\alpha\rightarrow\gamma}$ would not be valid if extrapolated out of the range of this transformation. $\Delta^{o}G_{7}^{\gamma\rightarrow\delta}$ was determined by using the free energy of the pure component suggested by Kaufman (45) for the $\alpha\rightarrow\gamma$ transition and converting it to the infinite dilution standard state using the regular solution parameters of Harvig et al. evaluated in the region of 1800 K.

Activity measurements through the temperature range of the $\alpha\rightarrow L$ transformation were performed by Morris and Zellars (43) and Wooley and Elliott (44). The $\Delta^{o}G_{7}^{\alpha\rightarrow L}$ obtained, when converted to the correct standard state could not reproduce the iron-rich portion of the phase diagram of Hellawell and Hume-Rothery (29) as well as the value of Geiss et al. (45). This latter $\Delta^{o}G_{7}^{\alpha\rightarrow L}$, although independent of temperature was chosen and $\Delta^{o}G_{7}^{\gamma\rightarrow L}$ was obtained from it and the $\gamma\rightarrow\delta$ values chosen.

III.3.H Fe-W

When the $\alpha\rightarrow\gamma$ free energy of Kaufman (34) was converted to the infinite dilution standard state by utilizing the regular solution parameters of Kirchner et al. (37) it was found that the resulting expression:

$$\Delta^{o}G_{8}^{\alpha\rightarrow\gamma} = 3710 - 0.3T \qquad \text{(III-23)}$$

was a poorer fit to the gamma loop of the Fe-W phase diagram of Sinha and Hume-Rothery (46) than could be obtained by assuming that the self-interaction parameters, ε_{ww}, are equal in ferrite and austenite. It was assumed, because of insufficient information, that the $\Delta^{o}G_{8}^{\alpha\rightarrow\gamma}$ so derived was also applicable to the $\gamma\rightarrow\delta$ transformation.

The free energy for the $\alpha\rightarrow$ L transformation was reported by Kaufman (57) and Sigworth and Elliott (18). The latter value will reproduce the phase diagram of Sinha and Hume-Rothery to 3 w/o tungsten. $\Delta^{o}G_{8}^{\gamma\rightarrow L}$ was derived with the use of the above values.

III.3.I Fe-V

$\Delta^{o}G_{9}^{\alpha\rightarrow\gamma}$ was derived from a thermodynamic analysis of the Fe-V binary phase diagrams of Kirchner and Gemmel (47), Lucas and Fishel (48) and Fischer et al. (21), using the self interaction coefficient, ε_{vv}, deduced by Wada et al. (49) and assuming the self interaction in ferrite to be negligible. Since no other information was available, the α-γ free energy was extrapolated for use in describing the $\gamma\rightarrow\delta$ transformation.

The $\alpha\rightarrow$L transformation was studied by Myles and Aldred (50) over the entire range 0 to 1 mole fraction vanadium and by Fruehan (51) who was able to estimate the activity coefficient of liquid vanadium at infinite dilution. This information was sufficient to attempt a thermodynamic analysis of the liquidus, which yielded $\Delta^{o}G_{9}^{\alpha\rightarrow L}$ up to 2 w/o V. $\Delta^{o}G_{9}^{\gamma\rightarrow L}$ was obtained from the above information.

III.3.J Fe-Nb

The $\alpha \rightarrow \gamma$ transformation in this binary system differs from those so far mentioned because of the addition of an intermediate phase field into the gamma loop. In this analysis it was assumed that this extra phase field does not exist and the gamma loop is treated as a normal one. The $\Delta^{o}G_{10}^{\alpha \rightarrow \gamma}$ adopted is reported by Hudd et al. (52) and is not to be used over 0.2 w/o Nb. Due to lack of data, this free energy was extrapolated for use in the $\gamma \rightarrow \delta$ transformation up to 0.2 w/o Nb.

The phase diagram of Ferrier et al. (55) utilized to check the free energy for the $\alpha \rightarrow L$ transition derived by assuming an ideal solution seemed anomolous because of the narrow width of the solidus-liquidus region. For an ideal solution of an element i in iron it can be shown that:

$$\ln\left(\frac{1-x_i^1}{1-x_i^2}\right) = \frac{\Delta^{o}G_{Fe}^{1\rightarrow 2}}{RT} \qquad \text{(III-21)}$$

for the transformation from phase 1 to phase 2. If x_i^1 and x_i^2 are sufficiently dilute this expression may be approximated (29) by performing a Taylor series expansion on $\ln(1-x_i)$:

$$x_i^2 - x_i^1 = \frac{\Delta^{o}G_{Fe}^{1\rightarrow 2}}{RT} \qquad \text{(III-25)}$$

In this case of the $\alpha \rightarrow L$ transformation, this means that for small additions of alloying element, the width of the $\alpha + L$ phase field is independent of the element added at any given temperature.

Comparison with the phase diagrams of Fe-Mo, Fe-Cr, Fe-Si and Fe-Mn demonstrated that since these phase fields had almost constant widths, the Fe-Nb phase diagram was probably wrong. As a result, the thermodynamic analysis for $\Delta^{o}G_{10}^{\alpha\rightarrow L}$ was carried out on a phase diagram constructed with the width of the solidus-liquidus region of the Fe-Mo system which straddled (i.e. contained) the measured Fe-Nb phase region. The adopted free energy lies between that of an ideal solution and that necessary to reproduce this particular phase diagram using the self interaction parameter of Sigworth and Elliott.

It must be emphasised that this free energy, while similar to that of Sigworth and Elliott is not strictly based on the experimental information.

III.3.K Fe-Co

Analysis by Harvig et al. (41) showed that $\Delta^{o}G_{11}^{\alpha\rightarrow\gamma}$ ranged from -90 cal/mole at 1688 K to 0 cal/mole at 1184 K. The value of the free energy for the $\alpha\rightarrow\gamma$ transformation was taken to be 0 cal/mole, independent of temperature because it would reproduce the phase diagram of Fischer et al. (21) up to .02 atom fraction cobalt. Since -90 cal/mole is of the same order or smaller than the error normally encountered on free energy measurements at higher temperatures, the value of zero was also adopted for the $\gamma\rightarrow\delta$ transformation.

$\Delta^{o}G_{11}^{\alpha\rightarrow L}$ and $\Delta^{o}G_{11}^{\gamma\rightarrow L}$ were reported by Kaufman and Nesor (33) and adopted assuming an ideal solution behaviour. These free energy values

reproduced the phase diagram of Harris and Hume-Rothery (54) out to .06 atom fraction cobalt.

All of this themrodynamic free energy data is summarized in Tables I to IV.

III.4 Interaction Coefficients

As previously mentioned it has been common practice to express the interaction parameters in terms of common logarithms and the one weight percent standard state or as mole fractions at infinite dilution and natural logarithms:

$$e_{ij} = \left(\frac{\partial \log f_i}{\partial w/o\ J}\right)_{w/o_i = w/o_j = 0} \qquad \text{(III-26)}$$

$$\varepsilon_{ij} = \left(\frac{\partial \ln \gamma_i}{\partial x_j}\right)_{x_i = x_j = 0} \qquad \text{(III-27)}$$

Since both forms occur in the literature, the conversion from the weight percent form to the mole fraction form required here was accomplished using the method given by Lupis and Elliott (58):

$$\varepsilon_{ij} = 230 \frac{m_j}{m_o} e_{ij} + \frac{m_o - m_j}{m_o} \qquad \text{(III-28)}$$

where m is the respective molecular weights of the elements of a ternary system with $x_i \to 0$ and $x_j \to 0$ in solvent "0" (iron).

Table II. $\Delta G_i^{\alpha\to\gamma}$ as Functions of Temperature*

	$\Delta G_i^{\alpha\to\gamma}$ (cal/mole)	References
C	$-15323 + 7.686T$	14,17
Mn**	$-26650 + 42.69T - 0.17T^{2}$†	9,27,29,30,55
Si	$-5964 + 38.799T - 4.7244T\ln T$	32
Ni	$-4545 + 3.233T$	17
Cr	$-367 - 4.656T + 0.6568T\ln T$	27,34
Mo	$565 + 0.15T$	34,37
Cu***	$-25500 + 41.183T - 0.17T^{2}$	9,41
W	$2500 + 0.15T$	37
V	$-8357 + 13.8T - 0.0031T^{2}$	derived from 47,50
Nb	$14.34 - 0.00131T$	52
Co	0	41

*$\Delta G_i^{\gamma\to\delta} = -\Delta G_i^{\alpha\to\gamma}$

**$\Delta G_{Mn}^{\gamma\to\delta} = 650 + 0.305T$

†Because of a systematic deviation between observations and predictions we have taken this as 0.687 times the value given in reference 27.

***$\Delta G_{Cu}^{\gamma\to\delta} = 1450 - 0.8T$ 21,24

Table III. $\Delta G_i^{\alpha \rightarrow L}$ as Functions of Temperature

	$\Delta G_i^{\alpha \rightarrow L}$ (cal/mole)	References
C	-21300 + 6.3T	14,19,56
Mn	3100 - 2.308T	30
Si	3.9T - 8200	31, ideal solution
Ni	-2120 - 0.38T	18,33
Cr	2.19T - 4600	
Mo	2.29T - 6600	18, ideal solution
Cu	-1200	45, ideal solution
W	3.65T - 7500	18,57
V	-5100 + 2.5T	18,51, ideal solution
Nb	2.3 - 5500	18, ideal solution
Co	3550 - 2.19T	18,33

Table IV. $\Delta G_i^{\gamma \to L}$ as Functions of Temperature

	$\Delta G_i^{\gamma \to L}$ (cal/mole)	References
C	-5360 + 0.6T	14,29
Mn	2860 - 2.03T	30
Si	-2236 - 34.9T + 4.7244TlnT	*
Ni	-790 - 0.64T	18,32
Cr	-4233 + 6.89T - 0.6568TlnT	*
Mo	2.14T - 7165	*
Cu	1.39T - 3150	*
W	3.50T - 10000	*
V	3257 - 11.5T + $0.0051T^2$	*
Nb	2.3T - 5500	*
Co	3950 - 2.19T	18,19

$$\Delta G_i^{\gamma \to L} = \Delta G^{\alpha \to L} + \Delta G^{\gamma \to \delta}$$

Dealy and Pehlke (59) investigated the temperature dependence of the interaction parameter:

$$\frac{\partial \epsilon_{ij}}{\partial T} = -\frac{1}{RT^2}\left(\frac{\partial^2 H}{\partial x_i \partial x_j}\right)_{x_i=x_j=0} \qquad \text{(III-29)}$$

where the derivative of the molar enthalpy can in principle be deduced from tabulated heat of solution data. Provided that the derivative of the enthalpy as written above for the two solutes at infinite dilution is not a strong function of temperature, it is possible to write equation (III-29) as:

$$\frac{\partial \epsilon_{ij}}{\partial(\frac{1}{T})} = \frac{1}{R}\left(\frac{\partial^2 H}{\partial x_i \partial x_j}\right)_{\text{all } x_k=0} \qquad \text{(III-30)}$$

which indicates that a relationship of the form:

$$\epsilon_{ij} = \frac{A}{T} + B \qquad \text{(III-31)}$$

would be valid for the interaction coefficients. Where data from more than one source or at more than one temperature was used, the values were averaged or a least squares method was used for evaluation, fitting a curve of the above type. Since the greater portion of the data was available at only one temperature, the integration constant was assumed zero and a reciprocal temperature relationship used for determining the value at a different temperature. Where data came from a regular solution model or was used in the form necessary to be used in such a model,

the conversion formula of Nishizawa (60) was utilized:

$$C^1 = +RT\epsilon_{cj} \qquad \text{(III-32)}$$

where C^1 is the regular solution ternary "correction" for the interaction between carbon and solute j in solvent iron in phase 1.

The majority of the liquid alloy cross interaction parameters were reported by Sigworth and Elliott (18), with newer or different information being referenced in Table V.

There is much more information available for the cross interaction between carbon and transition metals in austenite than in ferrite or the liquid state. Where more than one reference is listed for ϵ_{1i} in Table VI, the value adopted was an average over all the reported ones. A case in point is molybdenum, where different researchers (49, 60-66) arrived at similar $\epsilon^{\gamma}_{cm_o}$ values for the temperature range 1000 K to 1273 K but the large variation with temperature outside this range was such that any one determination could not be used for the γ-δ transformation.

Little information exists on the cross-interaction parameters for the δ and α phases. The δ phase interaction parameter was assumed equal to the austenite interaction parameter extrapolated to the temperature of interest. All high temperature extrapolations were checked for consistency of sign with the liquid interaction values at 1800 K and to ensure that, the adopted values were of the same order of magnitude, e.g.:

$$\varepsilon^{L}_{CMo} = -4.2 \text{ at } 1800 \text{ K} \qquad \text{(III-33)}$$

$$\varepsilon^{\gamma}_{CMo} = -6.1 \text{ at } 1800 \text{ K} \qquad \text{(III-34)}$$

For ferrite, the mole fraction of carbon, x_1, is sufficiently small that assuming $\varepsilon^{\gamma}_{1} = \varepsilon^{\alpha}$ leads to negligible error.

III.5 Partition Coefficients

Because interaction coefficients and free energies have not been reliably evaluated for the carbide phase, it became necessary to adopt the partition coefficients between austenite and cementite:

$$k_i = \frac{x_i^{cem}}{x_i^{\gamma}} \qquad \text{(III-35)}$$

as the experimental inputs, where x_i^{cem} is the mole fraction of element i in the Fe_3C carbide phase at any temperature.

The only temperature dependent partition coefficients available were those of Uhrenius (78). These are expressed in terms of weight percent of solute i, at temperature T, viz:

$$k'_i = \frac{\text{wt.pct. i in cementite}}{\text{wt.pct. i in austenite}} \qquad \text{(III-36)}$$

The transformation from k' to k is possible knowing x_i^{γ} and wt.pct. i in austenite, if equation (III-36) is expressed as

$$[w/o_i \text{ in cementite}] = k'[w/o_i \text{ in austenite}] \qquad \text{(III-37)}$$

Table V. ε^{L}_{ci} as Functions of Temperature

	ε^{L}_{ci}	References
C	0.389 + 7810/T	12,19,20,65
Mn*	-5060/T	18,30,66
Si	-0.428 + 18740/T	18,65
Ni*	5340/T	18,67
Cr*	-9500/T	18
Mo*	-7490/T	18
Cu*	7586/T	18
W*	-12230/T	18
V*	-30100/T	18
Nb*	-46615/T	18
Co*	3550/T	18,66,67

*Assumed inverse temperature relationship

Table VI. $\varepsilon_{ci}^{\gamma}$ as Functions of Temperature*

	$\varepsilon_{ci}^{\gamma}$	References
C**	8910/T	68
Mn**	-5070/T	16,30,61,68
Si	4.84 - 7370/T	16,68,69
Ni	-2.2 + 7600/T	70,71,72,73
Cr	24.4 - 38400/T	49,61,62,71,74
Mo	3.855 - 17870/T	49,60,61,62,63,64
Cu**	4200/T	70
W	23.4 - 36214/T	62
V**	-24660/T	49,56
Nb**	-28770/T	62
Co**	+2800/T	75,76,77

*Assumed $\varepsilon^{\gamma} = \varepsilon^{\alpha}$ and $\varepsilon^{\gamma} = \varepsilon^{\delta}$

**Assumed inverse temperature relationship.

Now, when the weight percent of element i in cementite is converted to mole fraction, it can be put into equation (III-35) which can then be solved for the necessary partition coefficient. The values obtained by this method of analysis for the chromium partition data of Uhrenius were found to be in good agreement with the experimental chromium partition coefficients calculated from the data of Sharma (79). The zero partition coefficient of silicon is reported by Uhrenius (80) and is used here as independent of temperature. This data is listed in Table VII.

III-6 Empirical Fe-C Phase Diagram

The iron-carbon phase diagram in the range 1000 to 1809 K has been reviewed and revised by Benz and Elliott (20) and more recently by Ban-Ya et al. (82). Both papers have extensively searched and commented upon the literature, eventually publishing phase diagrams. The empirical equations of Table IX describe the phase diagram of Fig. (4) and are based on the experimental determinations and the corrected experimental values of previous investigators from Benz and Elliott. For temperatures below 1000 K the extrapolation of the Ae_3 line was taken from Kaufman et al. (81) and the carbide lines are simply linearly extended according to the equation in Table (VIII).

Table VII. Partition Coefficients as Functions of Temperature

	k = wt%C in Fe_3C/wt%C in $\gamma \rightarrow Fe$	References
Mn	-0.00284T + 5.44	78
Ni	0.0004T - 0.249	78
Cr	163.4 - 22.781nT	78,79
Mo	121 - 16.91nT	78
Si	≈0	

Table VIII. Analytic Formula for Fe-C Phase Diagram

		References	
$\gamma \rightarrow \gamma+\alpha$	$T = 1115 - 150.3\ wt\%C + 216[0.765-wt\%C]^{4.26}$	9	$1000 \leq T \leq 1184$ K
	$T = 1083 - 108.46\ wt\%C$	81	$T \leq 999$ K
$L \rightarrow L+\gamma$	$T = 1804.3 - 61.3\ wt\%C - 4.6(wt\%C)^2$	20	
$L \rightarrow L+\delta$	$T = 1809 - 29.56\ wt\%C - 86(wt\%C)^2$	20	
$\gamma \rightarrow \gamma+\delta$	$T = 1666 + 981\ wt\%C - 1790(wt\%C)^2$	20	
$\gamma \rightarrow \gamma+Fe_3C$	$T = 641.3 + 530\ wt\%C - 78.4(wt\%C)^2$	20	

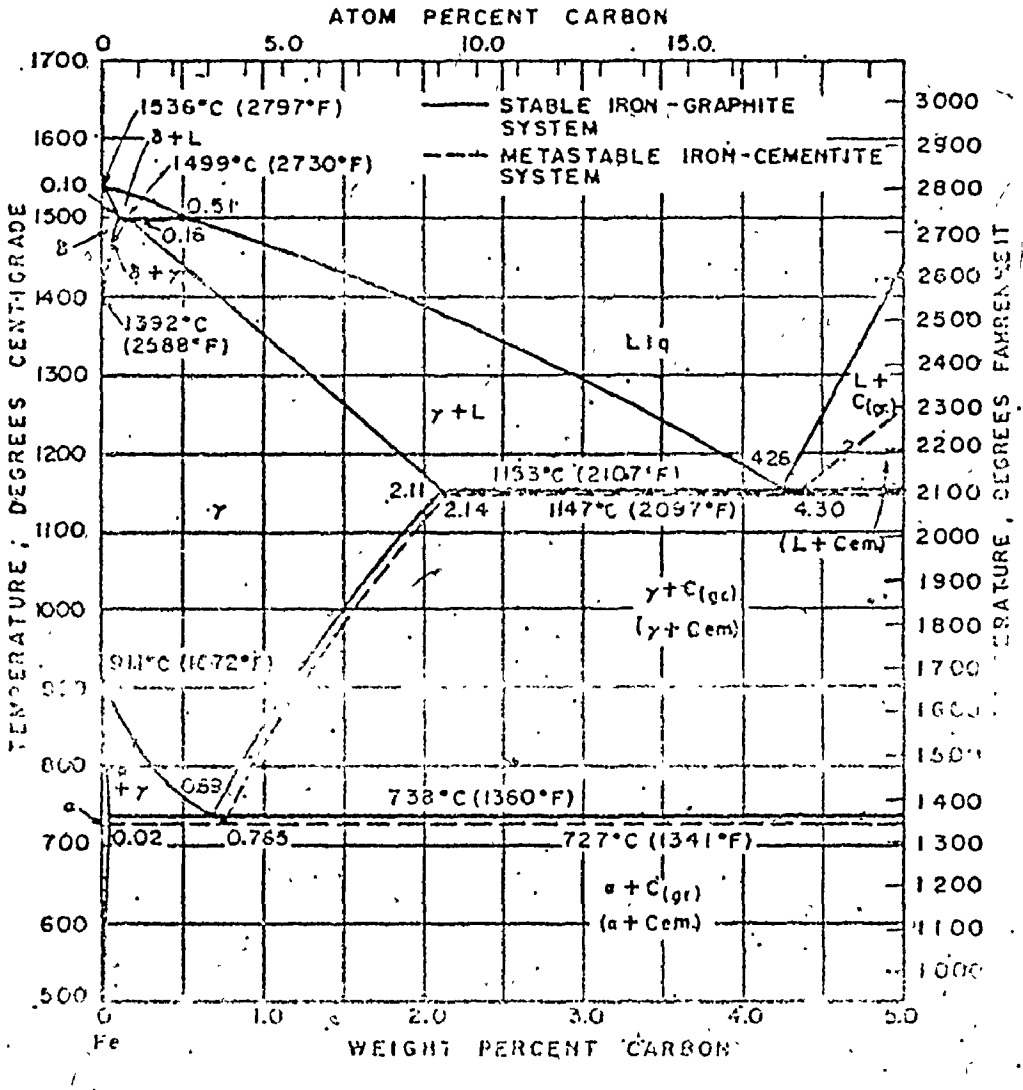

Figure 4 The Fe-C Phase Diagram According to Ref. 20.

CHAPTER IV

CALCULATIONS, DISCUSSION AND RESULTS

IV.1 Introduction

In this chapter we review the major sources of verification for our predictive formulae, from the early Ae_3 determinations to latter day experimental equilibria. Although we are forced to centre on the $\alpha+\gamma$ transformation information to demonstrate the validity of the method, due to lack of reliable experimental and thermodynamic data for the other regions, the formulae are not limited to this range. Also included, is a summary of the computational methods and problems overcome to extend the simple predictive formulae to the prediction of phase diagrams.

IV.2 Computer Calculations

IV.2.A Constant Composition Sections of the Fe-C Phase Diagram

Constant composition sections were calculated and plotted by computer for the temperature range 950 K to 1850 K and the composition range 0 to 2.5 wt.pct. carbon. As shown in Figure (5) for carbon compositions x_1 and x_2, both the stable phase boundaries and metastable extensions had to be calculated indiscriminately. Since both the stable

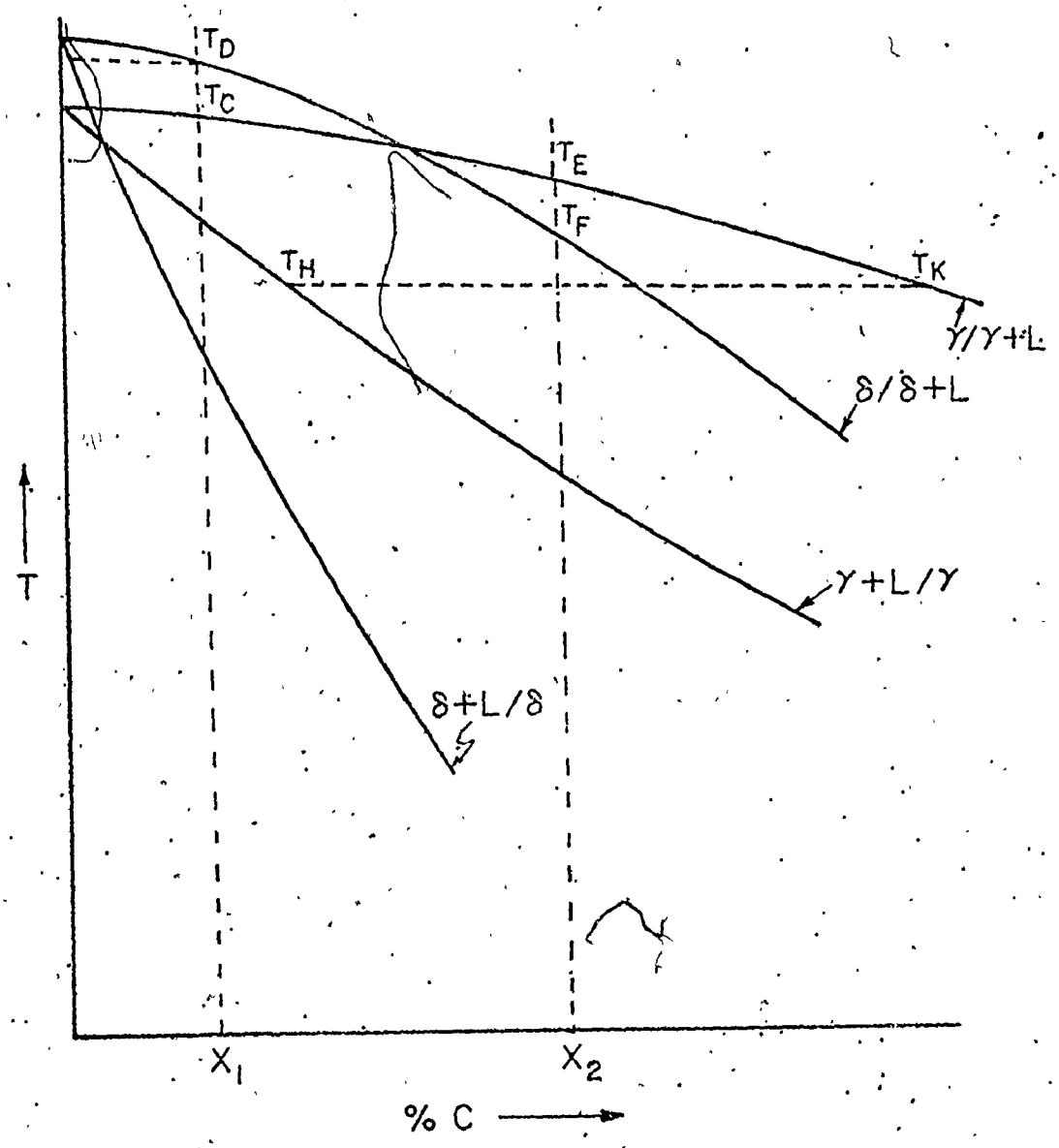

Figure 5 Schematic of an Fe-C-X Liquidus and Solidus.

phase temperature and the temperature of the metastable phase at any temperature was known, it was possible to determine which phase would be plotted in the following manner.

As shown in Figure (5) for carbon content x_1, the $\delta/\delta+L$ line (i.e. δ-liquidus) is the stable phase boundary at a temperature T_D. The metastable phase boundary, the γ-liquidus is denoted by temperature T_C. As x_1 approaches x_2, the two phase boundaries cross over and the stable phase is now the γ-liquidus at T_E and the metastable phase boundary is the δ-liquidus at temperature T_G. Thus the calculation of all phase temperatures results in a form of "memory" of the phase boundary plotted to that point.

This method was used to determine which phase should be plotted for the $\delta+\gamma/\delta+L$ and $\delta+\gamma/\gamma+L$ cross overs as well. Once it was determined which was the stable phase at any temperature, the partition coefficient (cf. equation (II-18)) was used to calculate the carbon composition on the other side of the two phase region. For instance, with reference to Figure (5), when the $\delta+L/\delta$ phase boundary at x_1 is stable, the composition of carbon of the $\delta/\delta+L$ phase boundary is given by point c, and when the $\gamma/\gamma+L$ phase boundary is stable, at T_K, the carbon composition of the $\gamma/\gamma+L$ boundary is given by the carbon content at point H. This method was used for determining the carbon composition of one side of a two phase region when that of the other side is known for the $\alpha+\gamma$, $\delta+\gamma$, $\delta+L$ and $\gamma+L$ regions.

The actual plots, as shown in Figures (6 to 9) are contours of

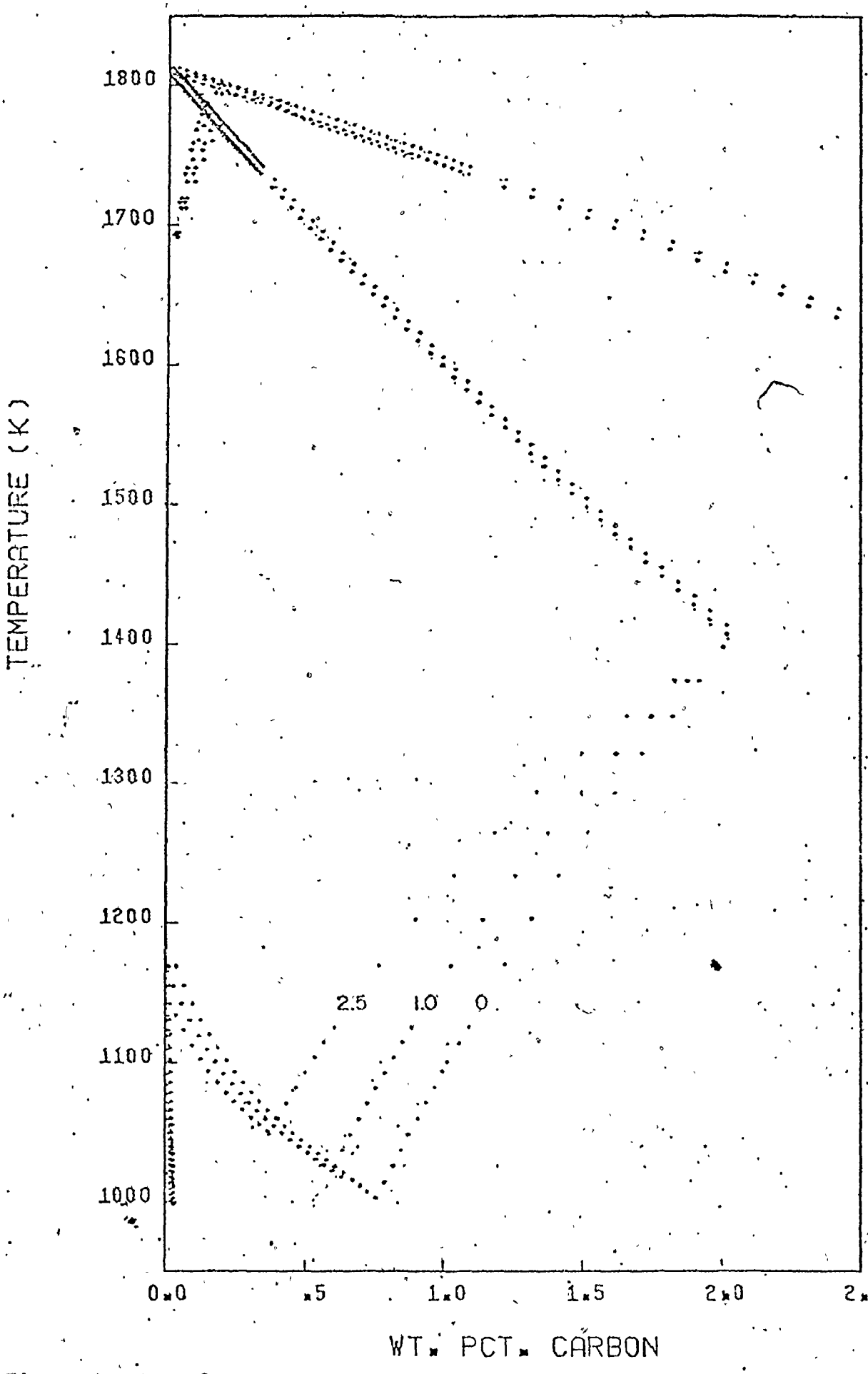

Figure 6 Set of constant Cr sections through the Fe-C-Cr phase diagram.

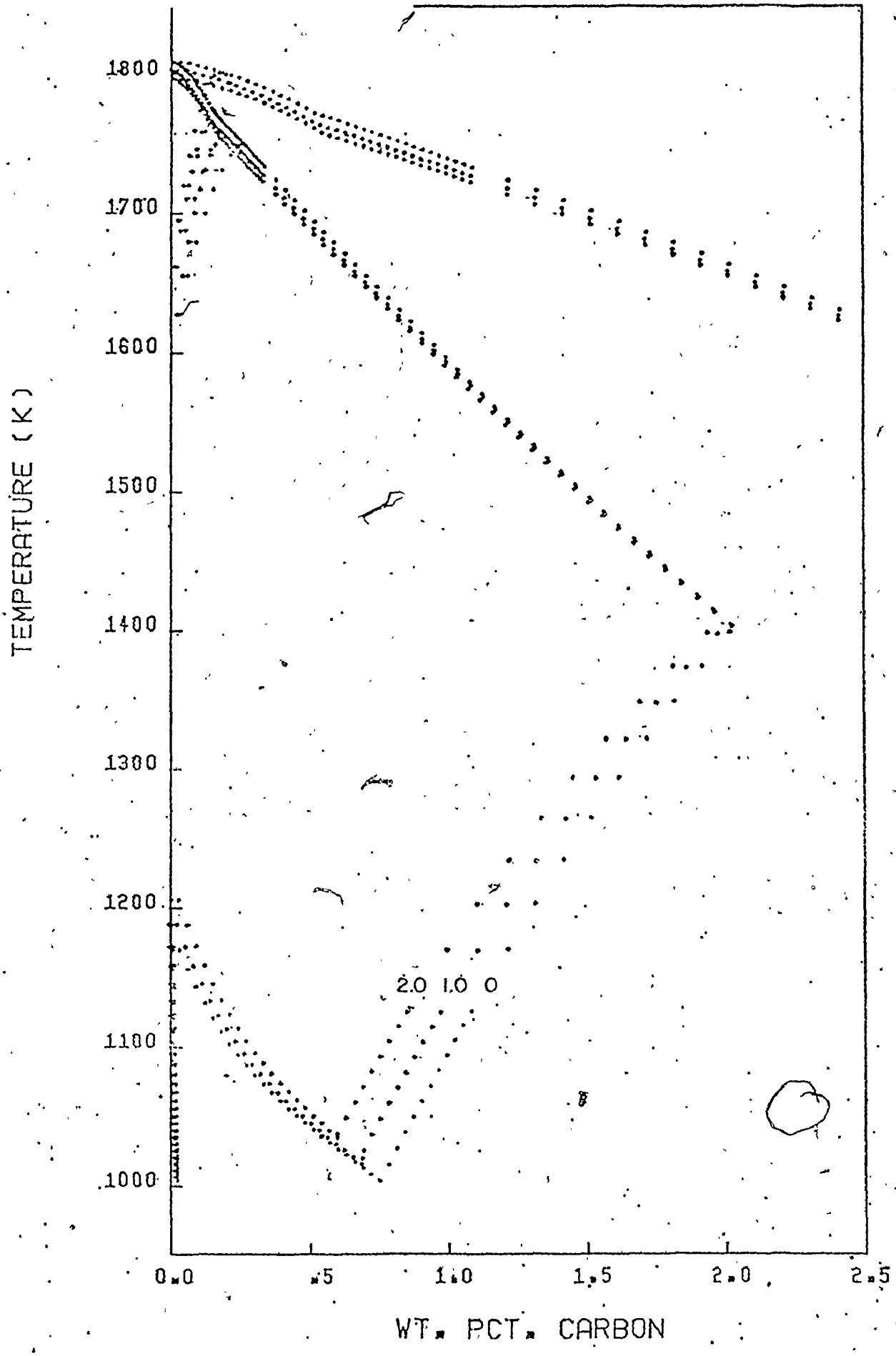

Figure 7 Set of constant Mo sections through the Fe-C-Mo phase diagram.

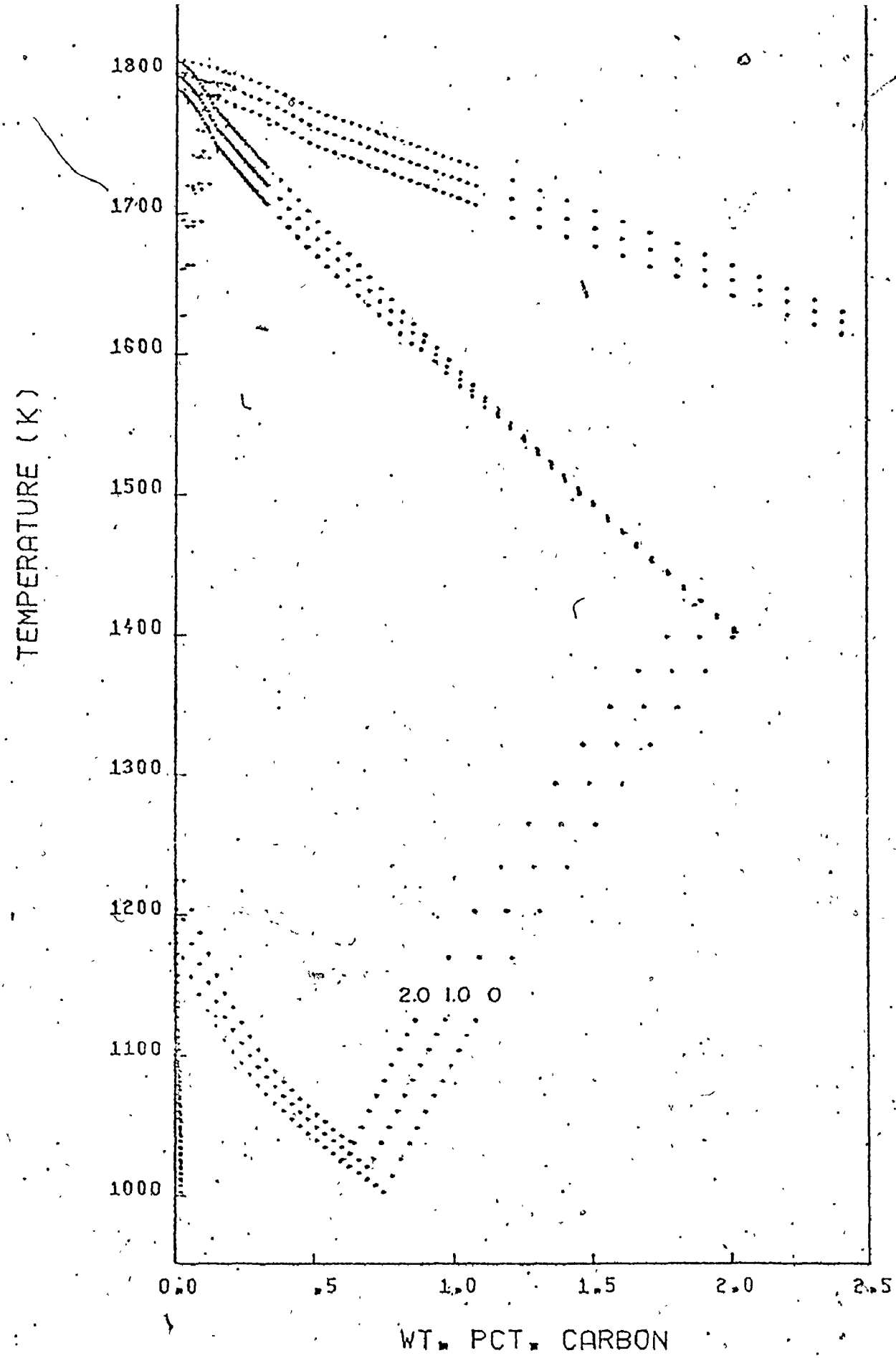

Figure 8 Set of constant Si sections through the Fe-C-Si phase diagram.

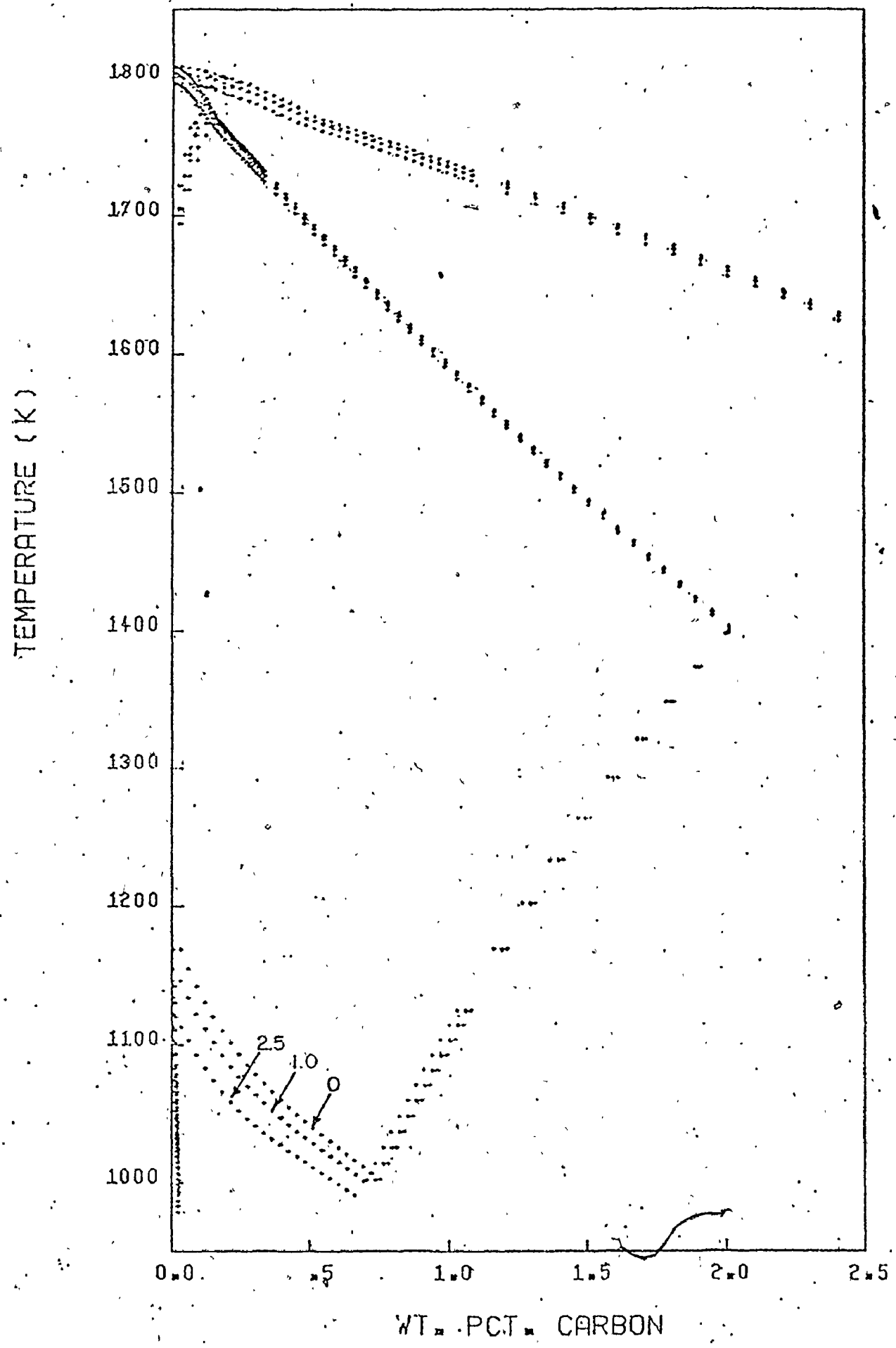

Figure 9 Set of constant Mn sections [illegible] the Fe-C-Mn phase dia

the Fe-C binary phase diagrams; each contour representing a different amount of the specified alloy. For example, in Figure (6) the contours represent the following constant composition contours:

Fe-C-0 wt.pct. Cr

Fe-C-1.0 wt.pct. Cr

Fe-C-2.5 wt.pct. Cr

IV.2.B Isothermal Ternary and Ternary Constant Composition Sections

There are many isothermal ternary systems documented in the literature, especially for the temperature range 950 to 1350 K where the stable phases are austenite, ferrite and cementite. Since the best thermodynamic data also exists in this temperature regime, this was the one chosen to test the formulae.

Two methods were used for predicting this type of phase diagram. The first consists of setting up a grid of values, say for carbon between 0 and 2 mole percent and alloying element i between 0 and 4 mole percent, holding the composition of the other elements constant. For each point, the temperature at which it exists is calculated and compared with the temperature of interest. This method is expensive in computer time but allows one to gauge the effect of uncertainties in temperature or thermochemical data (see Figure (10)).

The second, and preferable method of prediction was to transform equations (II-19) and (II-22) to a form whereby the deviation in the carbon content rather than the change in temperature from the binary iron

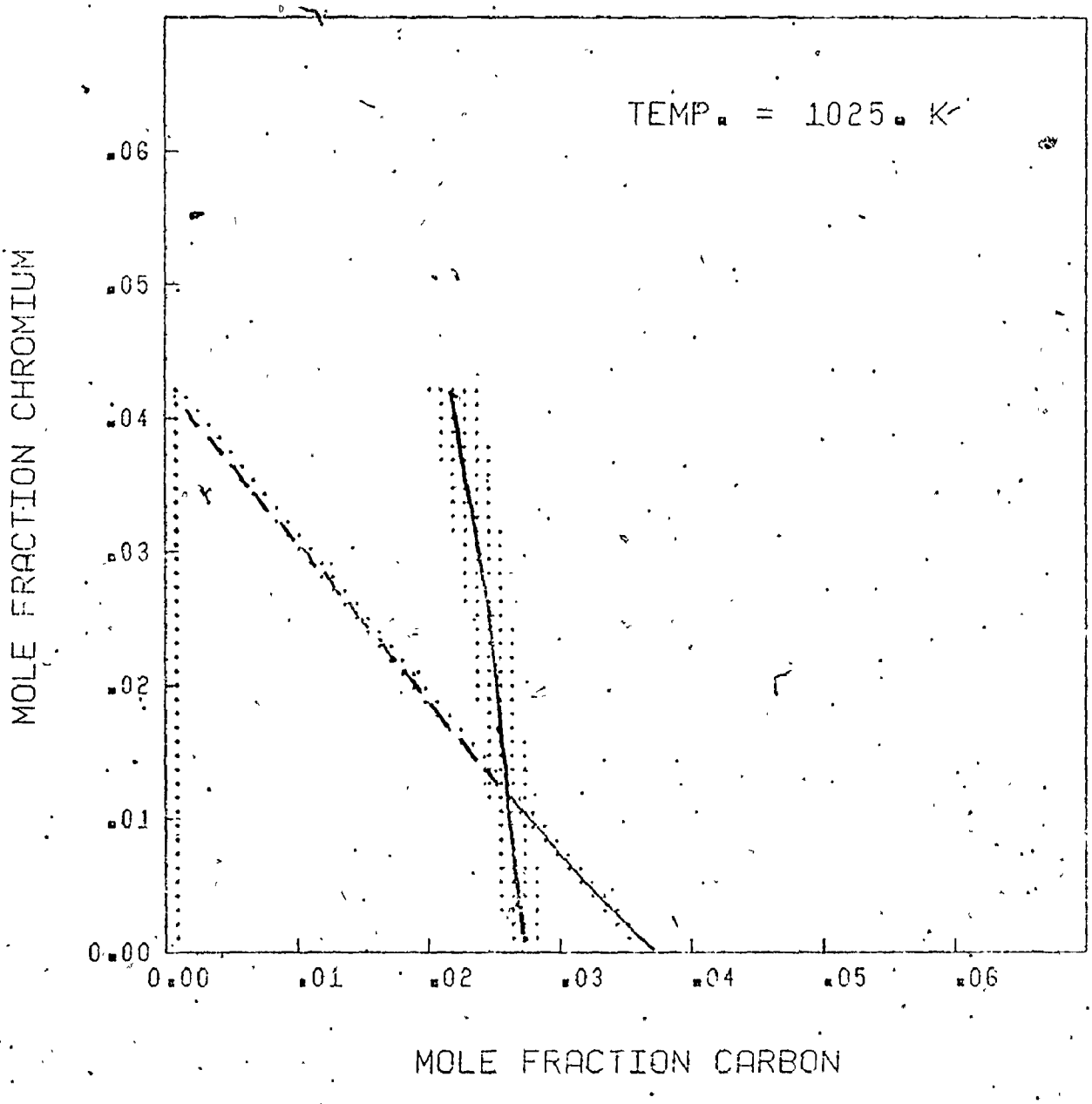

Figure 10 Fe-C-Cr ternary phase diagram for 1025±5 K.

carbon phase diagram is calculated:

$$x_1^{alloy} = x_1^{Fe\text{-}C} + \frac{\Delta T}{m_g} \qquad \text{(IV-1)}$$

for the Ae_3 temperature, where m_g is the slope of the binary Fe-C $\alpha/\alpha+\gamma$ phase boundary at this temperature, evaluated from the first derivative of its empirical equation. The shift in the carbide line needed no further transformation since it already existed in the required form.

In order to determine if a three phase region existed, it was necessary to evaluate the existence of a ternary eutectic in the plotted equation. An exact equation was derived for this by Kirkaldy et al. (93):

$$T_{eutectic}^{alloy} = \frac{T_E\left(1-\frac{m_g}{m_c}\right) + \Delta T + m_g \Delta x_1}{1 - \frac{m_g}{m_c}} \qquad \text{(IV-2)}$$

where m_g and m_c are the slopes of the binary Ae_3 and carbide lines and T_E is the binary eutectic temperature.

In the program, the $\alpha+\gamma/\gamma$ and carbide lines were fitted by quadratic equations and these were solved to find the ternary eutectic, rather than introduce this linear expression.

As in the constant composition sections, the $\alpha/\alpha+\gamma$ phase boundary is calculated using the partition coefficient evaluated within the program. In an analogous manner, the corners of the three phase region are determined and lines computed and plotted between them.

Equations IV-1 and IV-2 are derived in Appendix (IV). Examples of this type of plot, are found in Figures (11) to (13) for the system Fe-Ni-C at 973 K, 1073 K and 1173 K. Following each Figure, is a table (Table IX-XI) containing the coordinates of the plotted points in wt. percent.

IV.3 Results and Comparison with Experiment

It was decided the most effective manner for demonstrating the generality of our predictive formulae was to calculate and plot complete constant composition sections of the iron-carbon binary phase diagram as in Figures (6) to (9). These phase diagrams encompass the entire range of temperatures and phases (except higher carbides) of hardenability steels. Although a diagram of this scope may become more than qualitatively useful, at present there are insufficient experimental results available to verify the entire range of this study.

By far the most extensive data set was available for the Ae_3 temperature of low alloy steels. Comparison between experimental and predicted Ae_3 temperatures provide a check on one carbon value of the corresponding constant composition section in this limited temperature range. The exhaustive work on this single temperature by Baganis and Kirkaldy (9) made the perfect proving ground for the accuracy of the formulae and programming techniques.

Shown in Figure (2) were those steels which were thought to approach closest to equilibrium. For the most part, these were chosen

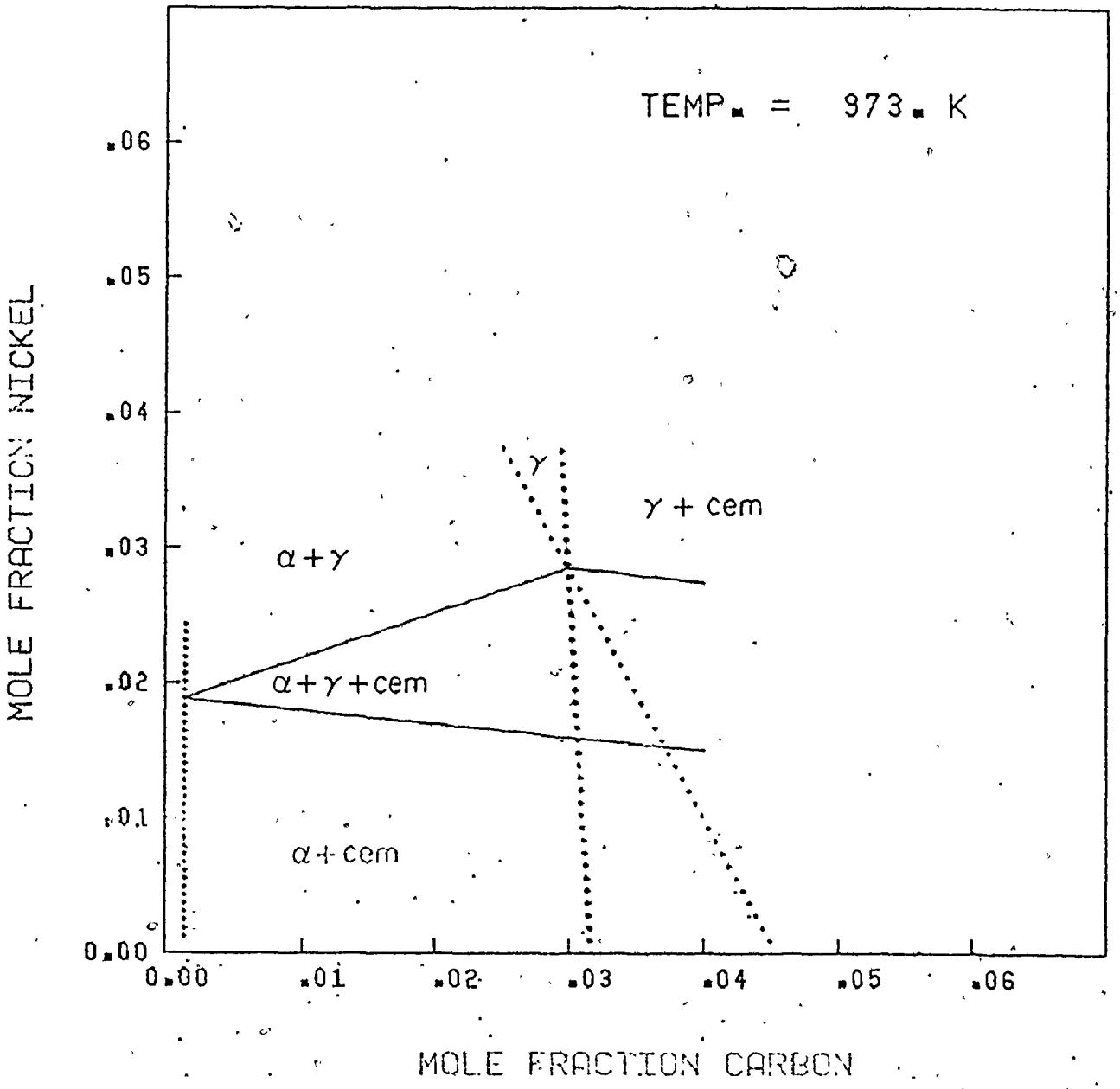

Figure 11 Fe-Ni-C system at 973 K.

Table IX. Fe-Ni-C at 973 K in wt.%

ELEMENT NO 4

ELEMENT	GAMMA	CARBIDE	TEMP
.100000	1.00259	.69659	973.00
.200000	.99099	.69528	973.00
.300000	.97938	.69398	973.00
.400000	.96777	.69268	973.00
.500000	.95616	.69138	973.00
.600000	.94455	.69008	973.00
.700000	.93294	.68878	973.00
.800000	.92132	.68748	973.00
.900000	.90971	.68618	973.00
1.000000	.89809	.68489	973.00
1.100000	.88647	.68359	973.00
1.200000	.87486	.68229	973.00
1.300000	.86324	.68099	973.00
1.400000	.85161	.67969	973.00
1.500000	.83999	.67839	973.00
1.600000	.82837	.67709	973.00
1.700000	.81674	.67579	973.00
1.800000	.80511	.67449	973.00
1.900000	.79349	.67319	973.00
2.000000	.78186	.67189	973.00
2.100000	.77023	.67059	973.00
2.200000	.75859	.66930	973.00
2.300000	.74696	.66800	973.00
2.400000	.73533	.66670	973.00
2.500000	.72369	.66540	973.00
2.600000	.71205	.66410	973.00
2.700000	.70042	.66280	973.00
2.800000	.68878	.66150	973.00
2.900000	.67714	.66021	973.00
3.000000	.66549	.65891	973.00
3.100000	.65385	.65761	973.00
3.200000	.64221	.65631	973.00
3.300000	.63056	.65501	973.00
3.400000	.61891	.65372	973.00
3.500000	.60726	.65242	973.00
3.600000	.59561	.65112	973.00
3.700000	.58395	.64982	973.00
3.800000	.57230	.64853	973.00
3.900000	.56063	.64723	973.00
4.000000	.54897	.64593	973.00

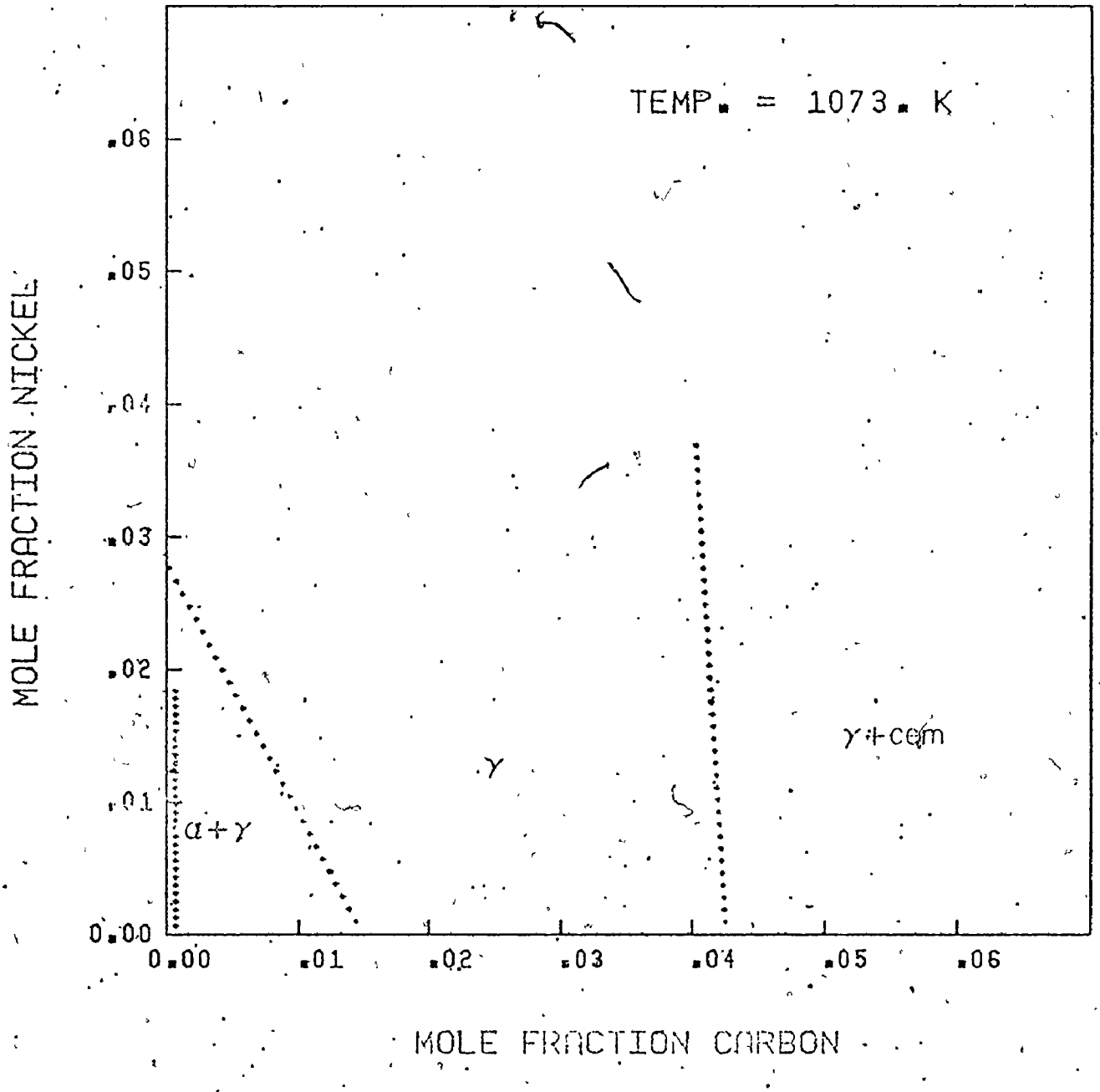

Figure 12 Fe-Ni-C System at 1073 K

Table X. Fe-Ni-C at 1073 K in wt.%

ELEMENT NO 4

ELEMENT	GAMMA	CARBIDE	TEMP
.10000	.31263	.97588	1073.00
.20000	.30159	.96451	1073.00
.30000	.29056	.95315	1073.00
.40000	.27951	.94179	1073.00
.50000	.26847	.93043	1073.00
.60000	.25743	.91907	1073.00
.70000	.24639	.90770	1073.00
.80000	.23534	.89634	1073.00
.90000	.22429	.88498	1073.00
1.00000	.21325	.87362	1073.00
1.10000	.20220	.86226	1073.00
1.20000	.19115	.85090	1073.00
1.30000	.18010	.83954	1073.00
1.40000	.16905	.82818	1073.00
1.50000	.15799	.81682	1073.00
1.60000	.14694	.80546	1073.00
1.70000	.13588	.79410	1073.00
1.80000	.12483	.78274	1073.00
1.90000	.11377	.77138	1073.00
2.00000	.10271	.76002	1073.00
2.10000	.09165	.74866	1073.00
2.20000	.08059	.73730	1073.00
2.30000	.06952	.72594	1073.00
2.40000	.05846	.71458	1073.00
2.50000	.04740	.70322	1073.00
2.60000	.03633	.69186	1073.00
2.70000	.02526	.68050	1073.00
2.80000	.01419	.66914	1073.00
2.90000	0.00000	.65778	1073.00
3.00000	0.00000	.64643	1073.00
3.10000	0.00000	.63507	1073.00
3.20000	0.00000	.62371	1073.00
3.30000	0.00000	.61235	1073.00
3.40000	0.00000	.60099	1073.00
3.50000	0.00000	.58964	1073.00
3.60000	0.00000	.57828	1073.00
3.70000	0.00000	.56692	1073.00
3.80000	0.00000	.55556	1073.00
3.90000	0.00000	.54421	1073.00
4.00000	0.00000	.53285	1073.00

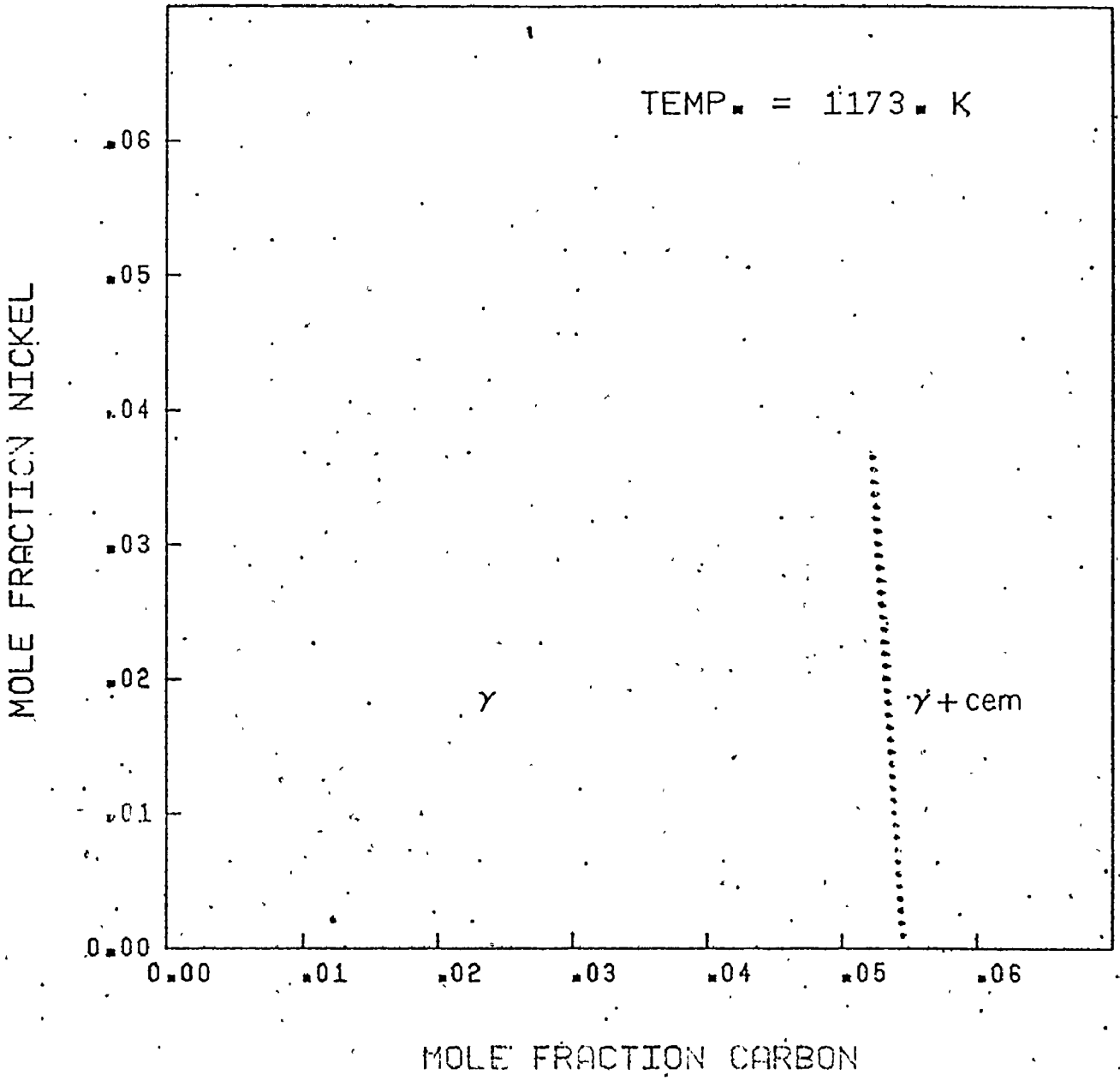

Figure 13 Fe-Ni-C at 1173 K

Table XI. Fe-Ni-C at 1173 K in wt.%

ELEMENT NO

ELEMENT	GAMMA	CARBIDE	TEMP
.10000	0.00000	1.22391	1173.00
.20000	0.00000	1.22257	1173.00
.30000	0.00000	1.22123	1173.00
.40000	0.00000	1.21989	1173.00
.50000	0.00000	1.21855	1173.00
.60000	0.00000	1.21721	1173.00
.70000	0.00000	1.21587	1173.00
.80000	0.00000	1.21453	1173.00
.90000	0.00000	1.21319	1173.00
1.00000	0.00000	1.21185	1173.00
1.10000	0.00000	1.21051	1173.00
1.20000	0.00000	1.20917	1173.00
1.30000	0.00000	1.20784	1173.00
1.40000	0.00000	1.20650	1173.00
1.50000	0.00000	1.20516	1173.00
1.60000	0.00000	1.20382	1173.00
1.70000	0.00000	1.20248	1173.00
1.80000	0.00000	1.20115	1173.00
1.90000	0.00000	1.19981	1173.00
2.00000	0.00000	1.19847	1173.00
2.10000	0.00000	1.19714	1173.00
2.20000	0.00000	1.19580	1173.00
2.30000	0.00000	1.19446	1173.00
2.40000	0.00000	1.19313	1173.00
2.50000	0.00000	1.19179	1173.00
2.60000	0.00000	1.19045	1173.00
2.70000	0.00000	1.18912	1173.00
2.80000	0.00000	1.18778	1173.00
2.90000	0.00000	1.18645	1173.00
3.00000	0.00000	1.18511	1173.00
3.10000	0.00000	1.18378	1173.00
3.20000	0.00000	1.18244	1173.00
3.30000	0.00000	1.18111	1173.00
3.40000	0.00000	1.17977	1173.00
3.50000	0.00000	1.17844	1173.00
3.60000	0.00000	1.17711	1173.00
3.70000	0.00000	1.17577	1173.00
3.80000	0.00000	1.17444	1173.00
3.90000	0.00000	1.17310	1173.00
4.00000	0.00000	1.17177	1173.00

from ternary Fe-C-X experiments. The Ae_3 temperatures of those steels of Aaronson and Domion (83) and Hall et al. (84) were determined by heating the steels to 1300°C, quenching to martensite, then reheating and holding at a temperature thought to be near the Ae_3. The Ae_3 temperature was taken as that intermediate between the highest holding temperature at which ferrite remained in the microstructure and the lowest at which it did not (measured in 5°C increments). Gilmour (85) and Kirchner and Uhrenius (86) were studying isothermal Fe-C-X sections and subjecting their samples to long periods at carefully controlled temperatures (a method similar to that used by Grange (4)). The results of Swinden and Woodhead (87) were determined dilatometrically with a heating rate of 22°C/hr. It is interesting to note that the predicted results lie below the experimental results, even for the leaner steels (low carbon, high Ae_3 temperature).

Figure (3) showed the results for the steels from the U.S.S. Atlas of Isothermal Transformations (88). It was argued that these are not a true Ae_3 temperature (28) since the predictor, while quite good on experimental steels, was predicting consistently low on these commercial steels. Figure (14) shows the Ac_3 and Ar_3 temperatures for 15 steels from the A.S.M. Data Sheets (89) as compared with the predicted Ae_3 temperature. As would be expected, the Ac_3 is below and the Ar_3 above the predicted value. However, as the carbon content decreases (temperature increases) the Ar_3 crosses the predicted value diagonal.

The above irregularities necessitated a further check of the data and closer scrutiny of sources to be made. It was observed that

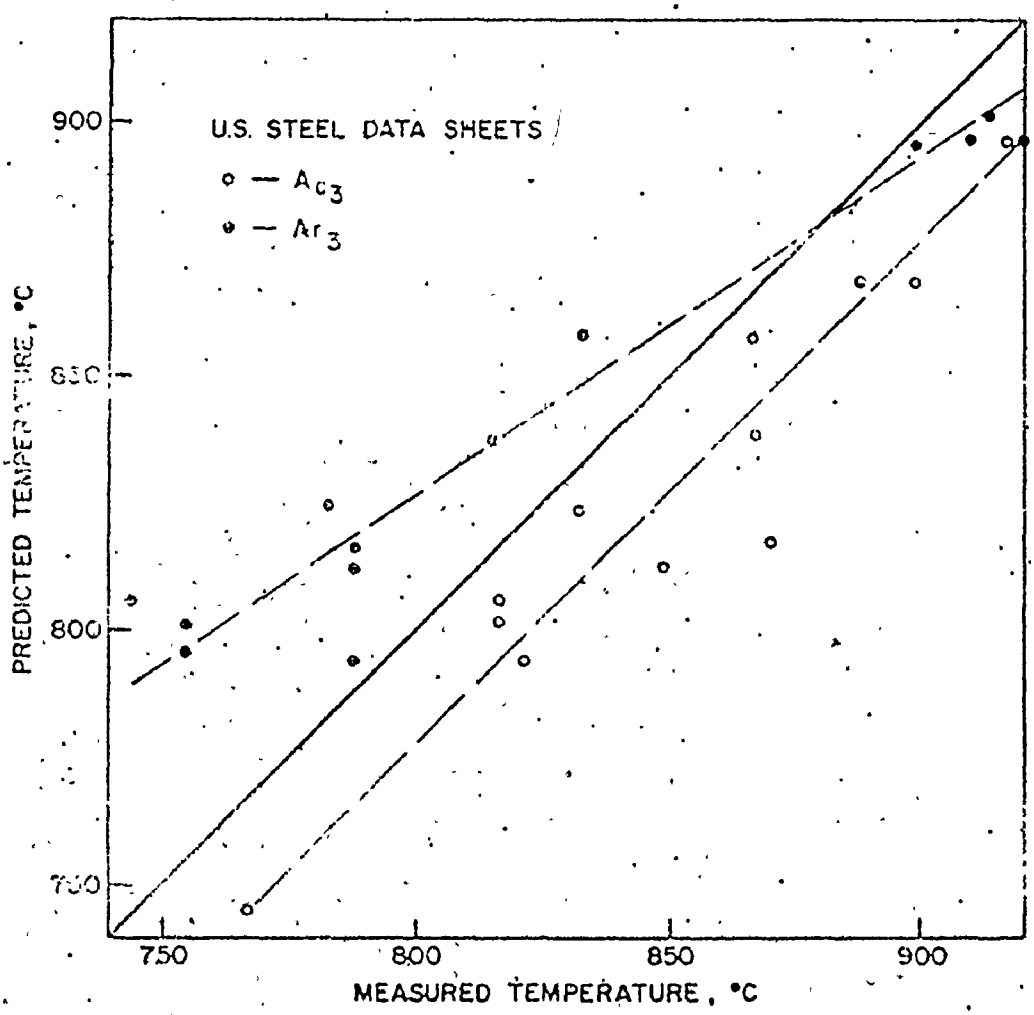

Figure 14 Predicted Ae_3 versus Ac_3 and Ar_3 temperature for low alloy steels. Steels identified in Reference (28).

manganese was present in most of the steels that deviated strongly at low carbon contents, along with lesser amounts of chromium and nickel. It was also discovered that the $\Delta G_{Mn}^{\alpha \rightarrow \gamma}$ being used would not adequately reproduce the Fe-Mn phase diagram; the main reason being the availability of true experimental equilibrium data. $\Delta G_{Mn}^{\alpha \rightarrow \gamma}$ was accordingly adjusted to the value in Table II. It is possible that the Cr and Ni equilibrium data are also insufficiently precise.

Although it is possible to verify at least one point on the Ae_3 line for constant composition sections, there exists no similar data set for the δ/L, δ/γ, γ/L or carbide transformations. However, it is our view that since the formulae and the program are performing adequately on the Ae_3 portion of the diagram and since the other input data are presumably correct, the other calculated portions should have fair reliability. The only check we have on the validity of the input data is the program's ability to reproduce the respective binary Fe-Y phase diagrams. All data tabulated were checked and the program does indeed reproduce all required binary phase diagrams.

Once the binary limits were established, the program and predictive formulae for constant composition isothermal "quasi-ternary" phase diagrams were verified by accurately reproducing, using identical data, the iron-rich portions of the ternary Fe-C-X phase diagrams (where X is one of: Mn, Si, Ni, Mo, W, V or Cu) published by Uhrenius (80) for temperatures above and below the binary eutectoid. His diagrams are the best self-consistent fit between regular solution theory and the data. The method of comparison used is illustrated in Figure (15). This is an isothermal

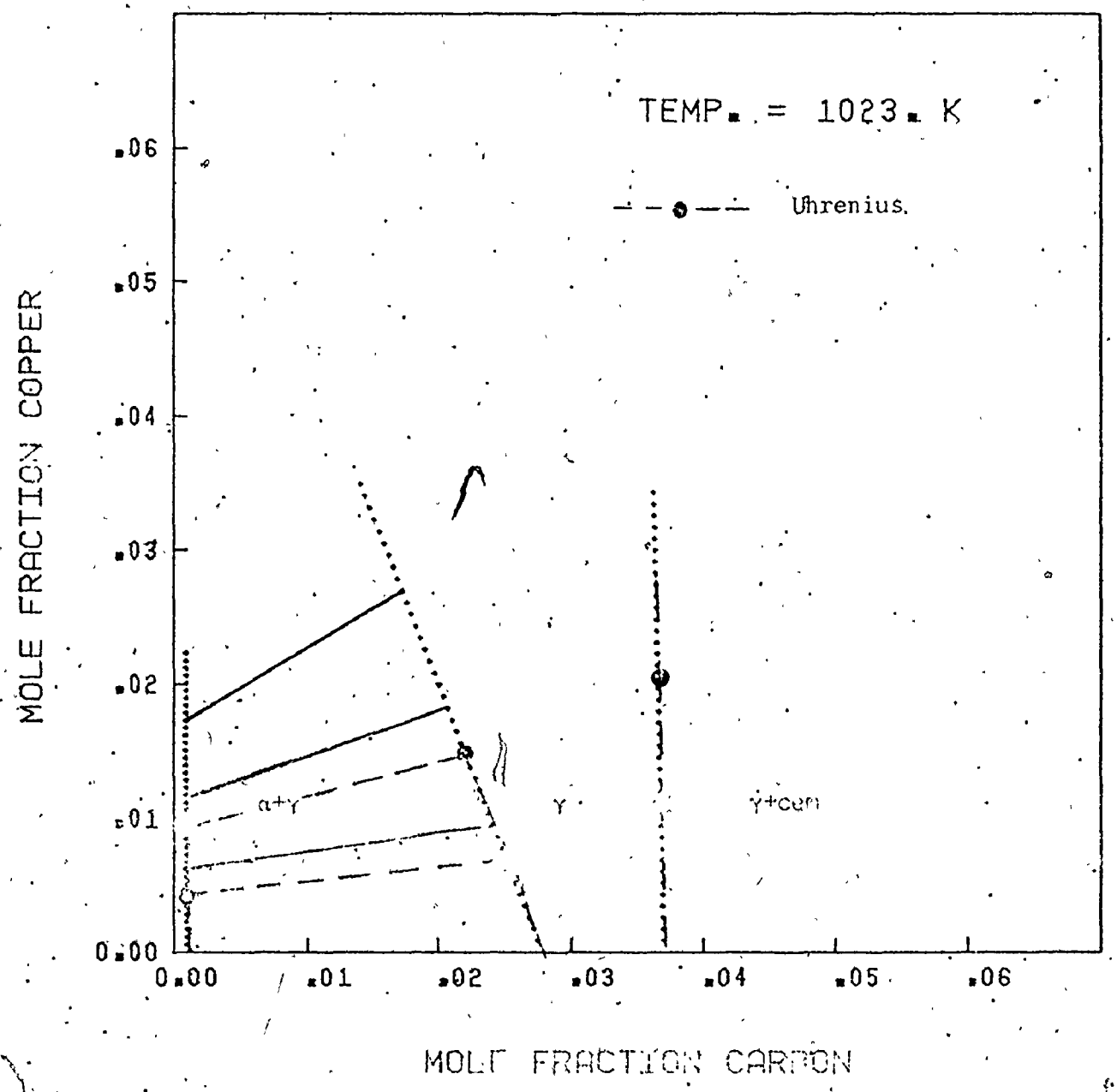

Figure 15 Comparison of the Fe-Cu-C system at 1023 K with that of Uhrenius (80)

section of the Fe-Cu-C system at 1023 K plotted by our program with points from Uhrenius' phase diagram superimposed. The equilibrium tie lines (broken) calculated by Uhrenius and those calculated by our program (full lines) are drawn in for comparison purposes. This was the method of comparison used for every phase diagram plotted (Figures (10) to (13) and (15) to (30)) and good agreement was obtained for Cu, Mn, Ni and Si and for the α-γ equilibrium, for all other elements treated by Uhrenius. Some deviation was found for the γ-carbide equilibrium in the Cr and Mo cases, and this is not unexpected because of the extreme sensitivity of the results to the precise values of k and ε_{ci} used in these cases. The co-ordinates of the plotted points, in wt.pct. for Figures (17) to (29) are in the tables immediately following the respective phase diagrams, i.e.: Tables XII to XXIV.

Figure (16) and (17) contain the comparison between our calculated phase diagrams and the experimental points of Sharma (79) for the Fe-Cr-C system. It was found that there was good agreement at 1023 K and 1043 K, the temperatures at which this work was undertaken. Sharma also reported partition coefficient data for the iron-rich region of this system. Table (XXV) shows the agreement between our calculated α/γ partition coefficients and the experimental ones. The α/γ partition coefficients for the other elements are tabulated in Table (XXVI).

Since all points of the isothermal phase diagrams were calculated, we automatically obtained the eutectoid temperature and composition and the effects of alloying elements on them. The experimental verification

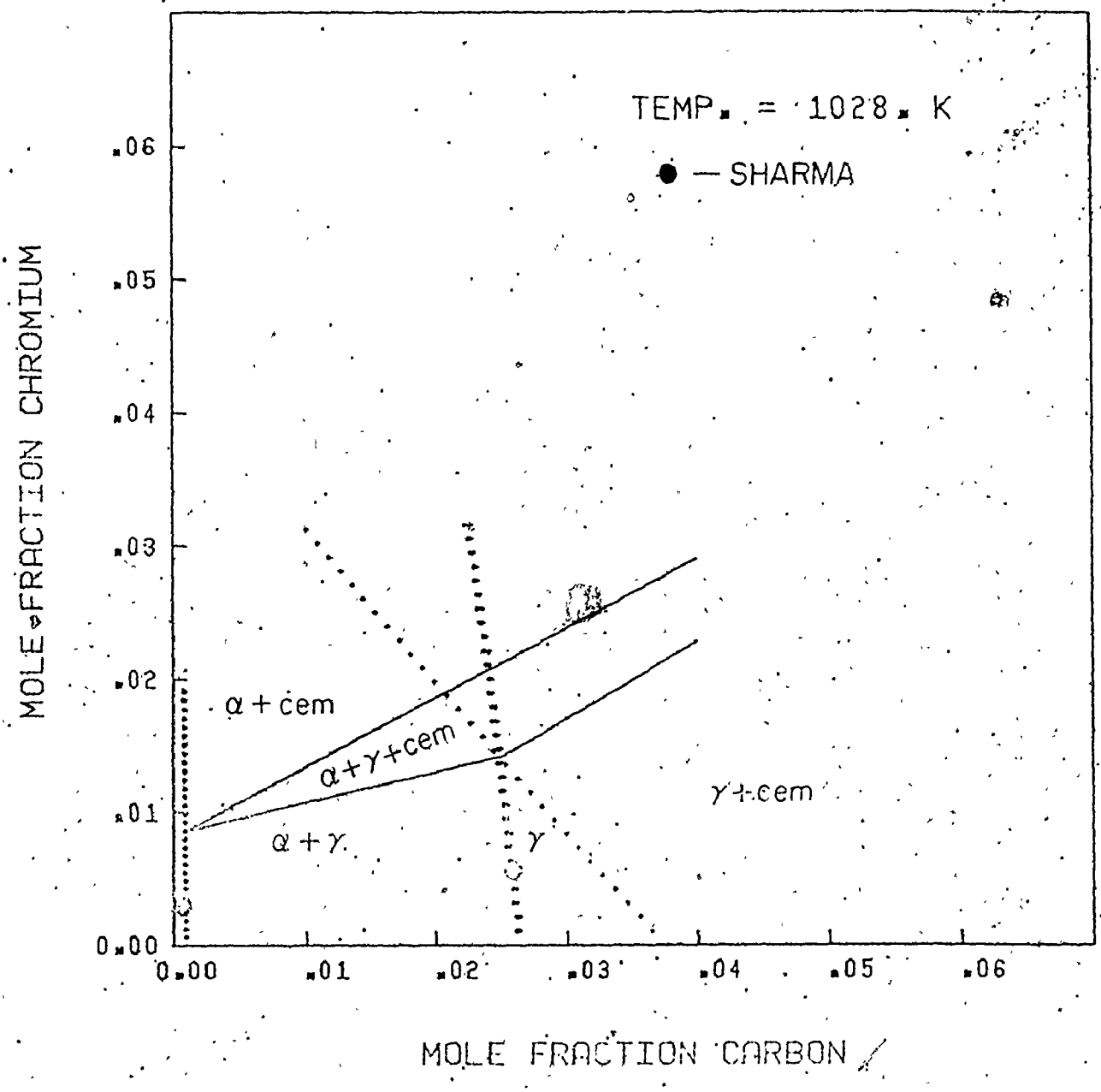

Figure 16 Fe-Cr-C system at 1028 K with the experimental points of Sharma (79).

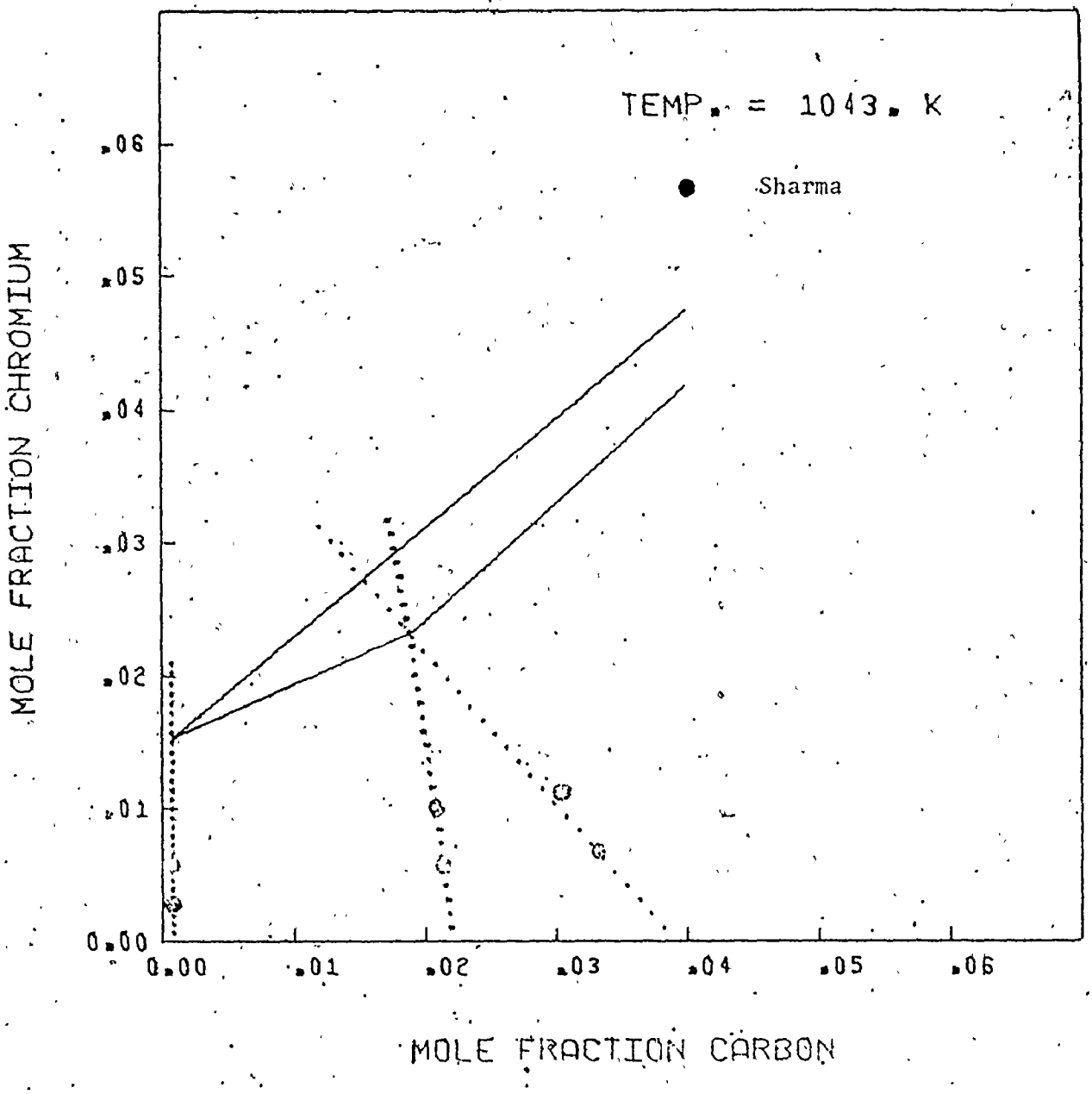

Figure 17 Fe-Cr-C system at 1043 K with the experimental points of Sharma (79)

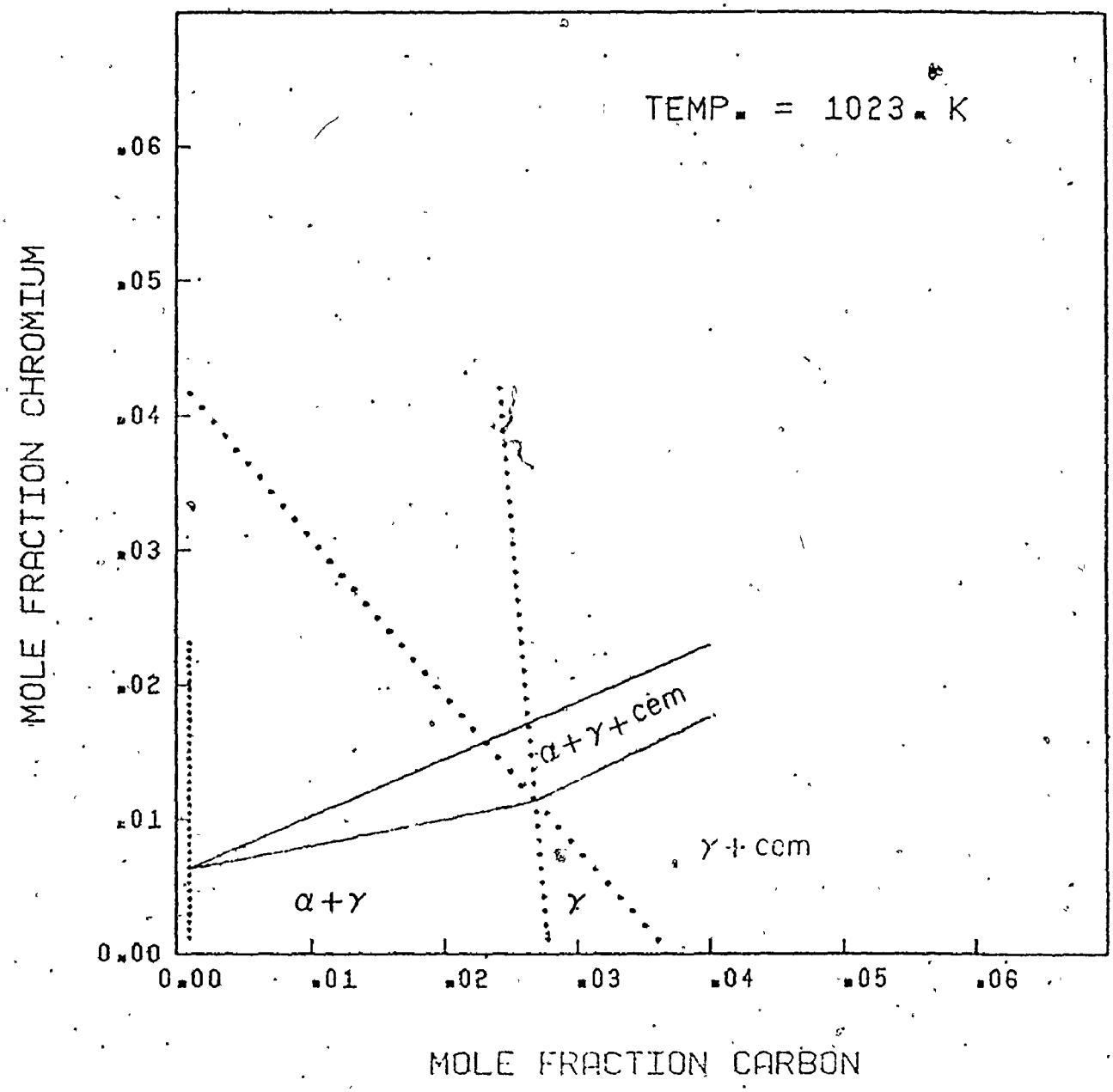

Figure 18 Fe-Cr-C system at 1023 K

Table XII. Fe-Cr-C at 1023 K in wt.%

ELEMENT NO 5

ELEMENT	GAMMA	CARBIDE	TEMP
.100000	.61956	.79811	1023.00
.200000	.60859	.77677	1023.00
.300000	.60651	.76951	1023.00
.400000	.60449	.73433	1023.00
.500000	.60246	.71323	1023.00
.600000	.60044	.69221	1023.00
.700000	.59841	.67126	1023.00
.800000	.59639	.65040	1023.00
.900000	.59436	.62961	1023.00
1.000000	.59233	.60890	1023.00
1.100000	.59030	.58826	1023.00
1.200000	.58827	.56770	1023.00
1.300000	.58623	.54722	1023.00
1.400000	.58420	.52681	1023.00
1.500000	.58217	.50648	1023.00
1.600000	.58014	.48622	1023.00
1.700000	.57812	.46604	1023.00
1.800000	.57609	.44593	1023.00
1.900000	.57406	.42589	1023.00
2.000000	.57203	.40593	1023.00
2.100000	.57003	.38604	1023.00
2.200000	.56801	.36622	1023.00
2.300000	.56598	.34648	1023.00
2.400000	.56396	.32681	1023.00
2.500000	.56192	.30721	1023.00
2.600000	.55989	.28768	1023.00
2.700000	.55787	.26822	1023.00
2.800000	.55584	.24883	1023.00
2.900000	.55381	.22951	1023.00
3.000000	.55178	.21026	1023.00
3.100000	.54975	.19108	1023.00
3.200000	.54772	.17197	1023.00
3.300000	.54569	.15293	1023.00
3.400000	.54367	.13396	1023.00
3.500000	.54164	.11505	1023.00
3.600000	.53961	.09621	1023.00
3.700000	.53758	.07745	1023.00
3.800000	.53555	.05874	1023.00
3.900000	.53352	.04011	1023.00
4.000000	.53149	.02154	1023.00

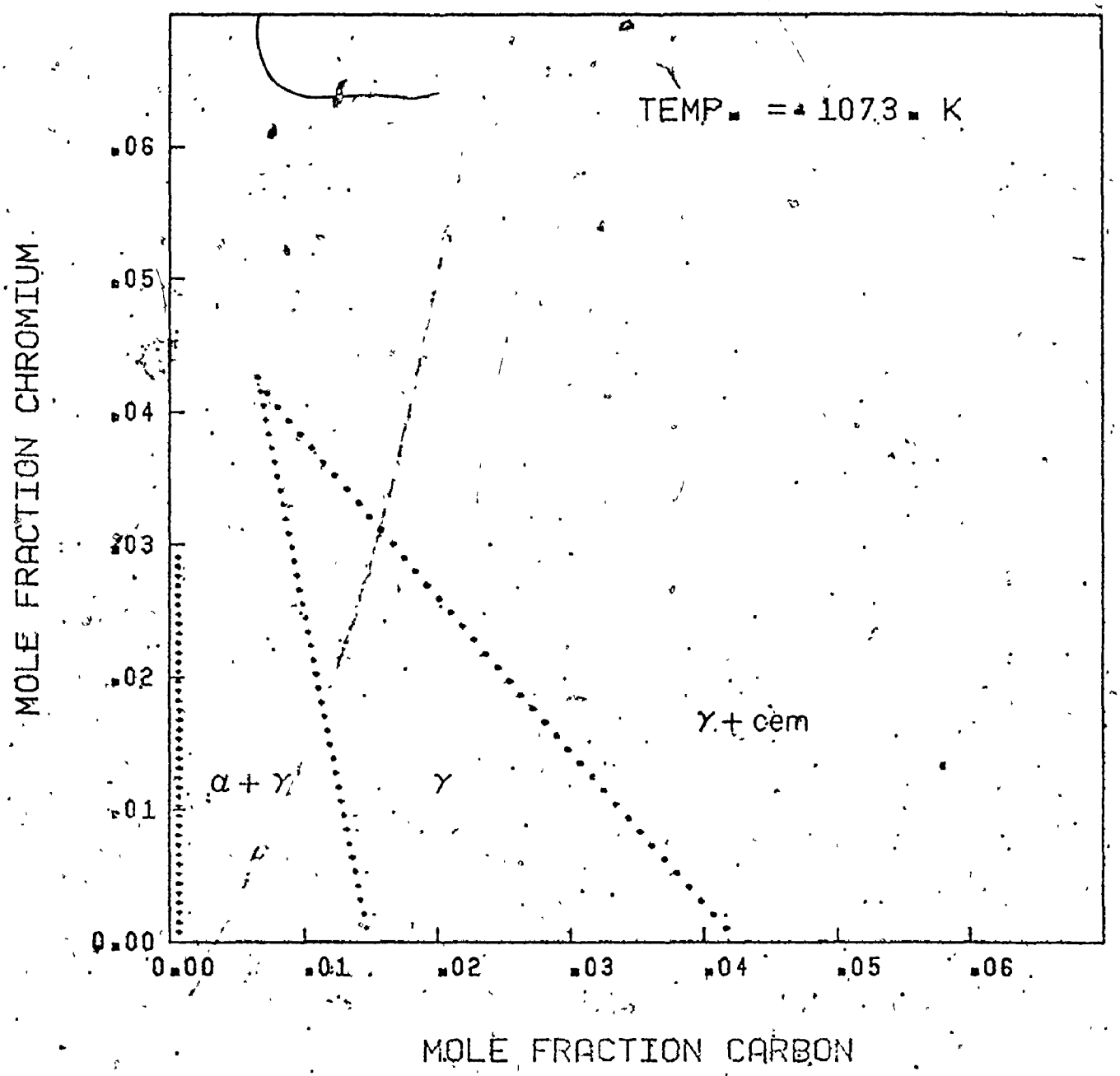

Figure 19 Fe-Cr-C system at 1073 K

Table XIII.. Fe-Cr-C at 1075 K in wt.%

ELEMENT NO 5

ELEMENT	GAMMA	CARBIDE	TEMP
1	3.9913	9.2613	1077.3
2	3.1460	9.0513	1077.3
3	3.1066	8.8413	1077.3
4	3.0555	8.6312	1077.3
5	3.0096	8.4212	1077.3
6	2.9646	8.2112	1077.3
7	2.9169	8.0012	1077.3
8	2.8739	7.7912	1077.3
9	2.8283	7.5812	1077.3
10	2.7833	7.3712	1077.3
11	2.7374	7.1612	1077.3
12	2.6924	6.9512	1077.3
13	2.6468	6.7412	1077.3
14	2.6021	6.5312	1077.3
15	2.5564	6.3212	1077.3
16	2.5115	6.1112	1077.3
17	2.4662	5.9012	1077.3
18	2.4209	5.6912	1077.3
19	2.3755	5.4812	1077.3
20	2.3304	5.2712	1077.3
21	2.2851	5.0612	1077.3
22	2.2398	4.8512	1077.3
23	2.1946	4.6412	1077.3
24	2.1494	4.4312	1077.3
25	2.1041	4.2212	1077.3
26	2.0588	4.0112	1077.3
27	2.0136	3.8012	1077.3
28	1.9684	3.5912	1077.3
29	1.9231	3.3812	1077.3
30	1.8777	3.1712	1077.3
31	1.8327	2.9612	1077.3
32	1.7875	2.7512	1077.3
33	1.7423	2.5412	1077.3
34	1.6971	2.3312	1077.3
35	1.6518	2.1212	1077.3
36	1.6067	1.9112	1077.3
37	1.5615	1.7012	1077.3
38	1.5163	1.4912	1077.3
39	1.4711	1.2812	1077.3
40	1.4259	1.0712	1077.3

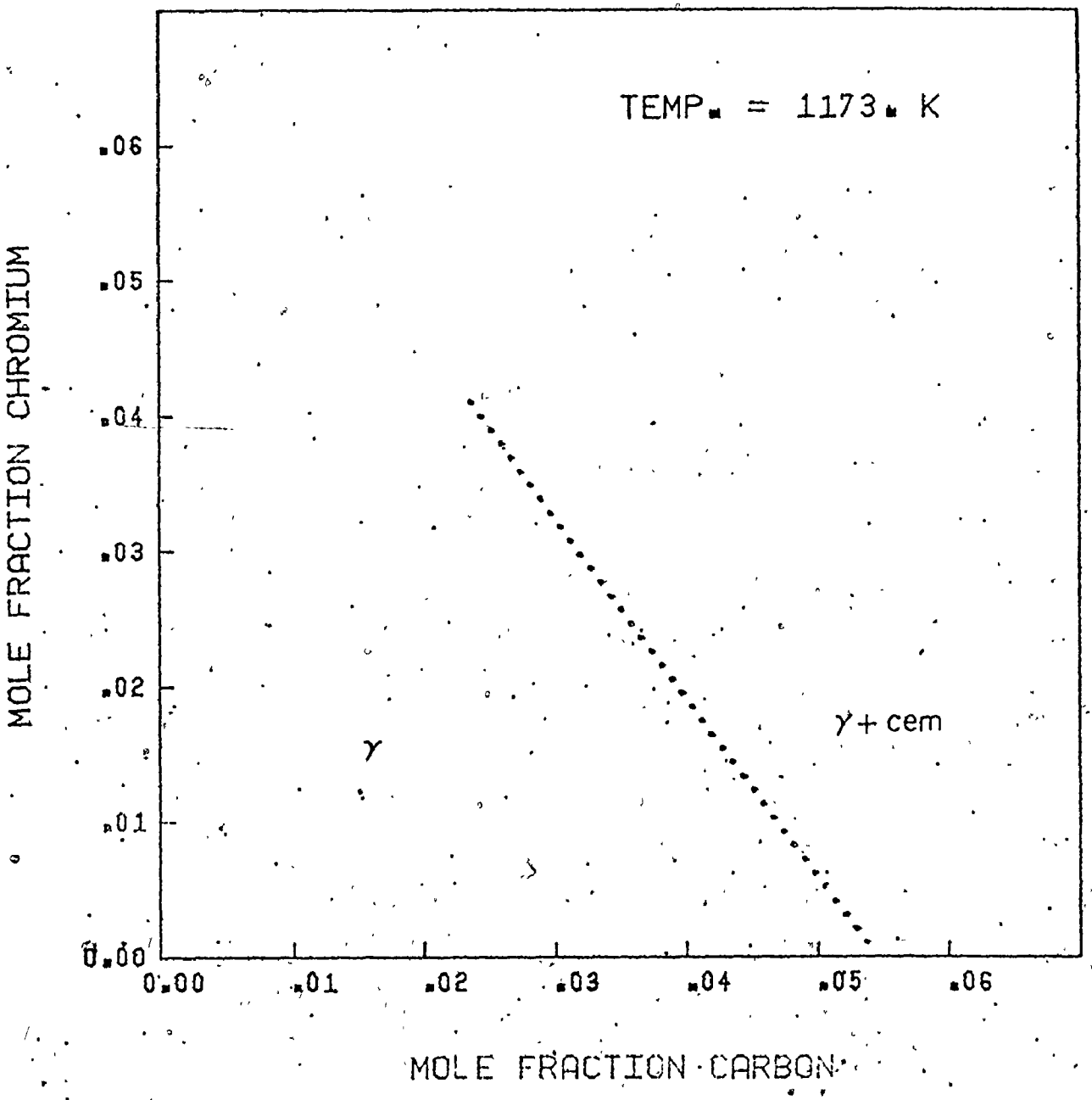

Figure 20 Fe-Cr-C system at 1173 K

TABLE XIV. Fe-Cr-C at 1173 K in wt.%

ELEMENT NO 5

ELEMENT	GAMMA	CARBIDE	TEMP
.100000	0.000000	1.20669	1173.00
.200000	0.000000	1.18817	1173.00
.300000	0.000000	1.16971	1173.00
.400000	0.000000	1.15129	1173.00
.500000	0.000000	1.13293	1173.00
.600000	0.000000	1.11461	1173.00
.700000	0.000000	1.09635	1173.00
.800000	0.000000	1.07813	1173.00
.900000	0.000000	1.05996	1173.00
1.000000	0.000000	1.04184	1173.00
1.100000	0.000000	1.02377	1173.00
1.200000	0.000000	1.00574	1173.00
1.300000	0.000000	.98777	1173.00
1.400000	0.000000	.96984	1173.00
1.500000	0.000000	.95196	1173.00
1.600000	0.000000	.93412	1173.00
1.700000	0.000000	.91634	1173.00
1.800000	0.000000	.89860	1173.00
1.900000	0.000000	.88090	1173.00
2.000000	0.000000	.86326	1173.00
2.100000	0.000000	.84566	1173.00
2.200000	0.000000	.82811	1173.00
2.300000	0.000000	.81060	1173.00
2.400000	0.000000	.79314	1173.00
2.500000	0.000000	.77572	1173.00
2.600000	0.000000	.75835	1173.00
2.700000	0.000000	.74103	1173.00
2.800000	0.000000	.72375	1173.00
2.900000	0.000000	.70652	1173.00
3.000000	0.000000	.68933	1173.00
3.100000	0.000000	.67219	1173.00
3.200000	0.000000	.65509	1173.00
3.300000	0.000000	.63804	1173.00
3.400000	0.000000	.62103	1173.00
3.500000	0.000000	.60406	1173.00
3.600000	0.000000	.58714	1173.00
3.700000	0.000000	.57027	1173.00
3.800000	0.000000	.55343	1173.00
3.900000	0.000000	.53664	1173.00
4.000000	0.000000	.51990	1173.00

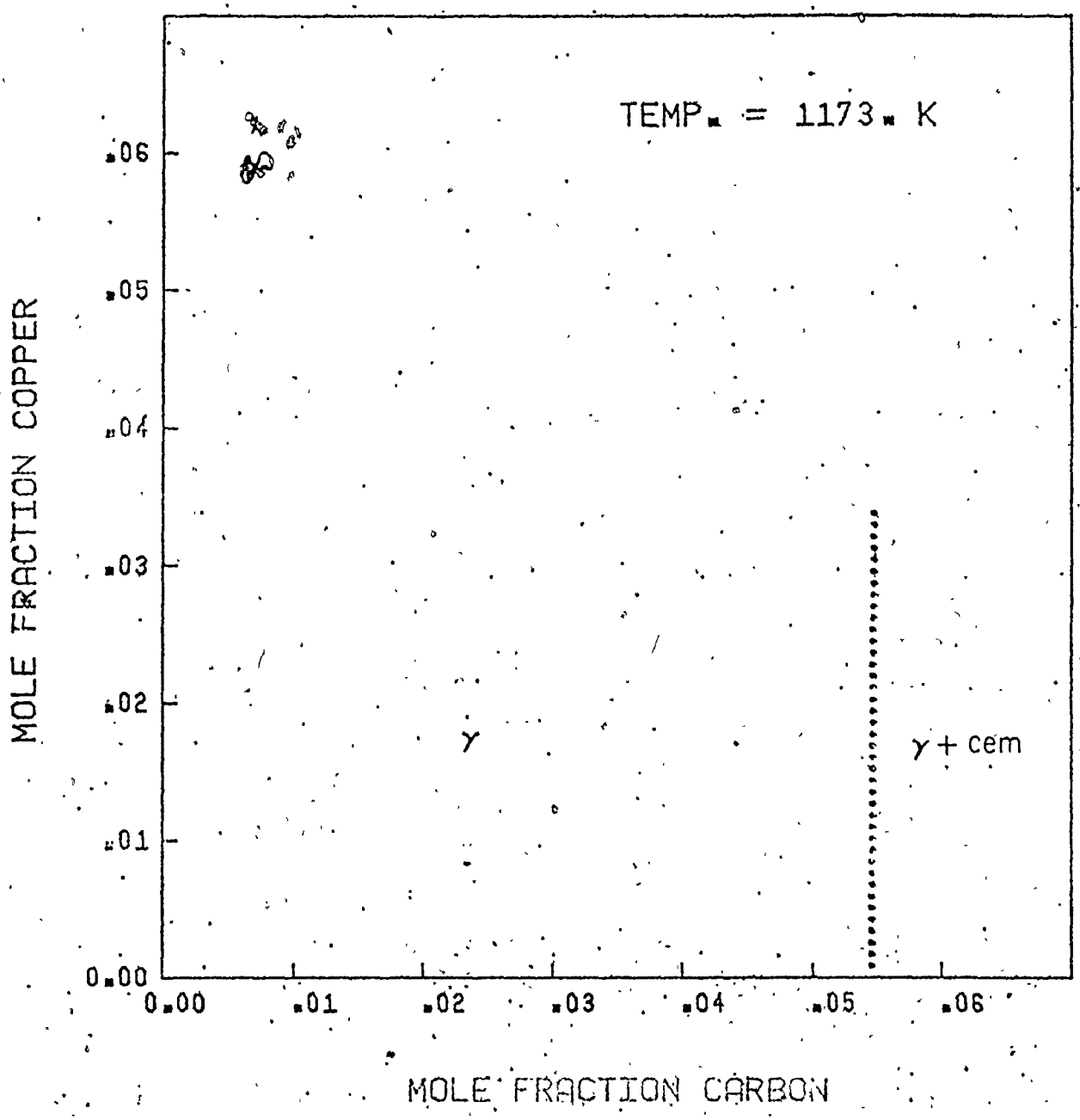

Figure 21 Fe-Cu-C system at 1173 K

TABLE XV. Fe-Cu-C at 1173 K in wt.%

ELEMENT NO 7

ELEMENT	GAMMA	CARBICE	TEMP
.10000	0.000000	1.225524	1173.00
.20000	0.000000	1.225524	1173.00
.30000	0.000000	1.225523	1173.00
.40000	0.000000	1.225523	1173.00
.50000	0.000000	1.225522	1173.00
.60000	0.000000	1.225522	1173.00
.70000	0.000000	1.225521	1173.00
.80000	0.000000	1.225521	1173.00
.90000	0.000000	1.225521	1173.00
.00000	0.000000	1.225520	1173.00
.10000	0.000000	1.225520	1173.00
.20000	0.000000	1.225520	1173.00
.30000	0.000000	1.225519	1173.00
.40000	0.000000	1.225519	1173.00
.50000	0.000000	1.225519	1173.00
.60000	0.000000	1.225519	1173.00
.70000	0.000000	1.225518	1173.00
.80000	0.000000	1.225518	1173.00
.90000	0.000000	1.225518	1173.00
.00000	0.000000	1.225518	1173.00
.10000	0.000000	1.225518	1173.00
.20000	0.000000	1.225518	1173.00
.30000	0.000000	1.225518	1173.00
.40000	0.000000	1.225518	1173.00
.50000	0.000000	1.225518	1173.00
.60000	0.000000	1.225518	1173.00
.70000	0.000000	1.225518	1173.00
.80000	0.000000	1.225518	1173.00
.90000	0.000000	1.225518	1173.00
.00000	0.000000	1.225518	1173.00
.10000	0.000000	1.225518	1173.00
.20000	0.000000	1.225518	1173.00
.30000	0.000000	1.225519	1173.00
.40000	0.000000	1.225519	1173.00
.50000	0.000000	1.225519	1173.00
.60000	0.000000	1.225519	1173.00
.70000	0.000000	1.225520	1173.00
.80000	0.000000	1.225520	1173.00
.90000	0.000000	1.225520	1173.00
.00000	0.000000	1.225521	1173.00

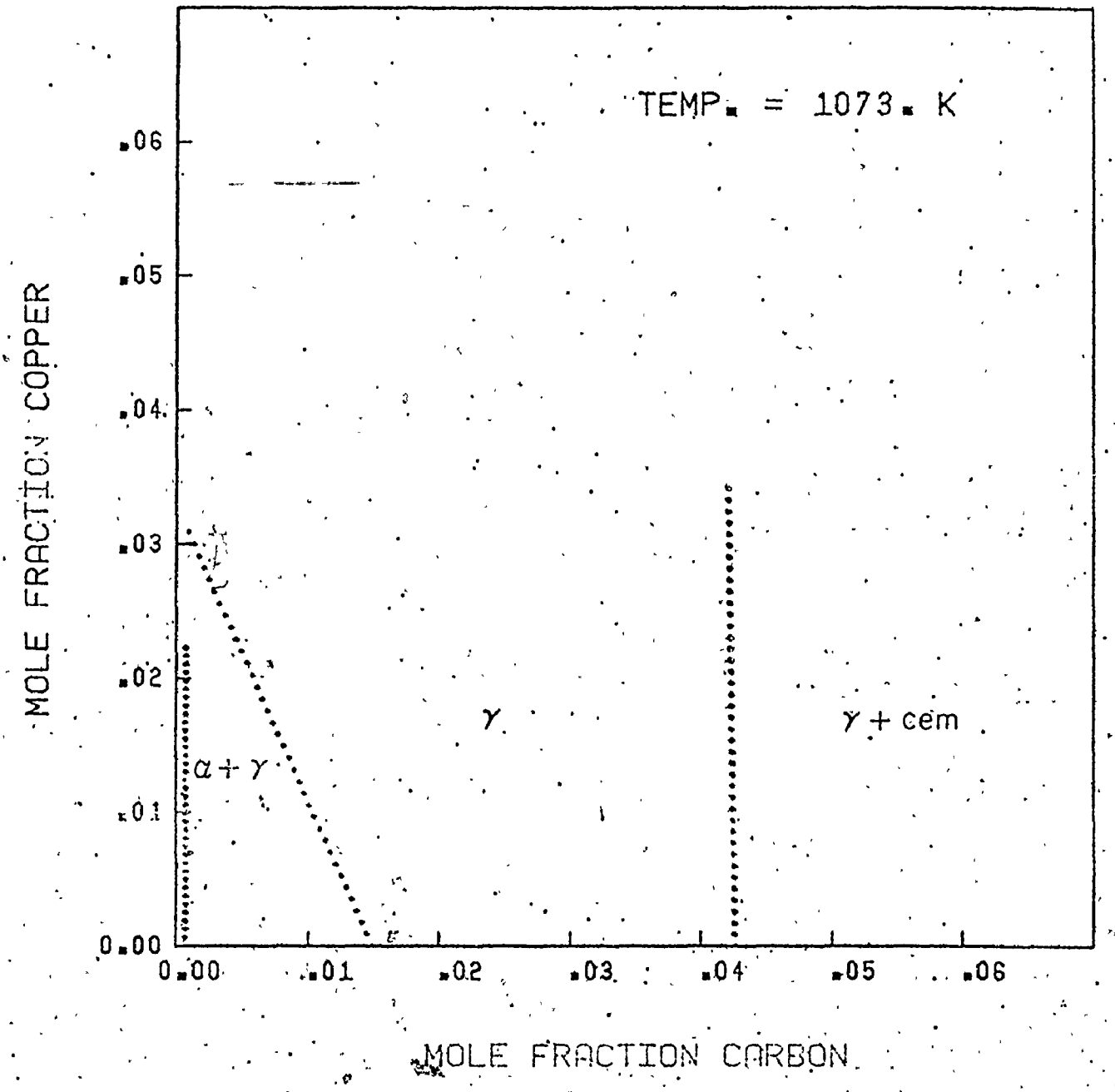

Figure 22 Fe-Cu-C system at 1073 K

TABLE XVI. Fe-Cu-C at 1073 K in wt.%

ELEMENT	GAMMA	CARBIDE	TEMP
.100000	.31496	.946863	1073.00
.200000	.30625	.946842	1073.00
.300000	.29753	.946801	1073.00
.400000	.28882	.946760	1073.00
.500000	.28010	.946719	1073.00
.600000	.27138	.946678	1073.00
.700000	.26265	.946637	1073.00
.800000	.25393	.946596	1073.00
.900000	.24520	.946555	1073.00
1.000000	.23647	.946514	1073.00
1.100000	.22774	.946473	1073.00
1.200000	.21900	.946433	1073.00
1.300000	.21026	.946392	1073.00
1.400000	.20153	.946351	1073.00
1.500000	.19278	.946310	1073.00
1.600000	.18404	.946269	1073.00
1.700000	.17529	.946228	1073.00
1.800000	.16655	.946187	1073.00
1.900000	.15780	.946146	1073.00
2.000000	.14904	.946106	1073.00
2.100000	.14029	.946065	1073.00
2.200000	.13153	.946024	1073.00
2.300000	.12277	.945983	1073.00
2.400000	.11401	.945942	1073.00
2.500000	.10524	.945902	1073.00
2.600000	.09648	.945861	1073.00
2.700000	.08771	.945820	1073.00
2.800000	.07894	.945779	1073.00
2.900000	.07017	.945739	1073.00
3.000000	.06139	.945698	1073.00
3.100000	.05261	.945657	1073.00
3.200000	.04383	.945616	1073.00
3.300000	.03505	.945576	1073.00
3.400000	.02626	.945535	1073.00
3.500000	.01748	.945494	1073.00
3.600000	0.000000	.945453	1073.00
3.700000	0.000000	.945213	1073.00
3.800000	0.000000	.945172	1073.00
3.900000	0.000000	.945131	1073.00
4.000000	0.000000	.945091	1073.00

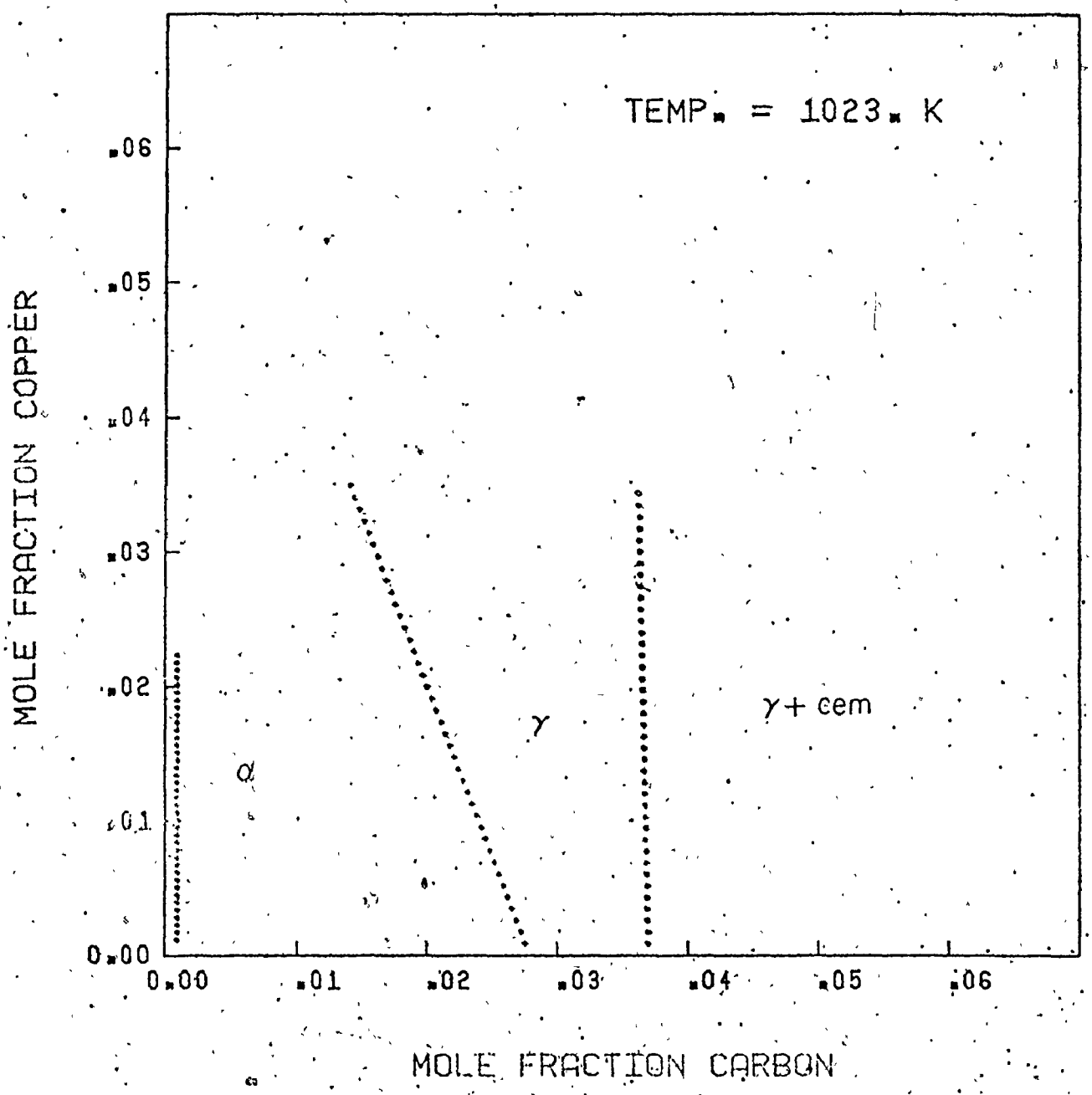

Figure 23 Fe-Cu-C system at 1023 K

TABLE XVII. Fe-Cu-C at 1023 K in wt.%

ELEMENT NO 7

ELEMENT	GAMMA	CARBIDE	TEMP
.100000	.607497	.818398	1023.000
.200000	.597734	.816643	1023.000
.300000	.588971	.817888	1023.000
.400000	.582208	.817133	1023.000
.500000	.577445	.816379	1023.000
.600000	.573682	.816624	1023.000
.700000	.569918	.815869	1023.000
.800000	.566154	.815114	1023.000
.900000	.562390	.814360	1023.000
1.000000	.558626	.813605	1023.000
1.100000	.552862	.813850	1023.000
1.200000	.552097	.812095	1023.000
1.300000	.551332	.812341	1023.000
1.400000	.550567	.811586	1023.000
1.500000	.549802	.811131	1023.000
1.600000	.549037	.810076	1023.000
1.700000	.548271	.810022	1023.000
1.800000	.547505	.809967	1023.000
1.900000	.546739	.809912	1023.000
2.000000	.545973	.809857	1023.000
2.100000	.545206	.809803	1023.000
2.200000	.544440	.809748	1023.000
2.300000	.543673	.809693	1023.000
2.400000	.542906	.809638	1023.000
2.500000	.542139	.809584	1023.000
2.600000	.541371	.809529	1023.000
2.700000	.540603	.809474	1023.000
2.800000	.539835	.809420	1023.000
2.900000	.539067	.809365	1023.000
3.000000	.538299	.809310	1023.000
3.100000	.537530	.809256	1023.000
3.200000	.536762	.809201	1023.000
3.300000	.535993	.809146	1023.000
3.400000	.535224	.809091	1023.000
3.500000	.534454	.809037	1023.000
3.600000	.533685	.808982	1023.000
3.700000	.532915	.808927	1023.000
3.800000	.532146	.808873	1023.000
3.900000	.531375	.808818	1023.000
4.000000	.530605	.808763	1023.000

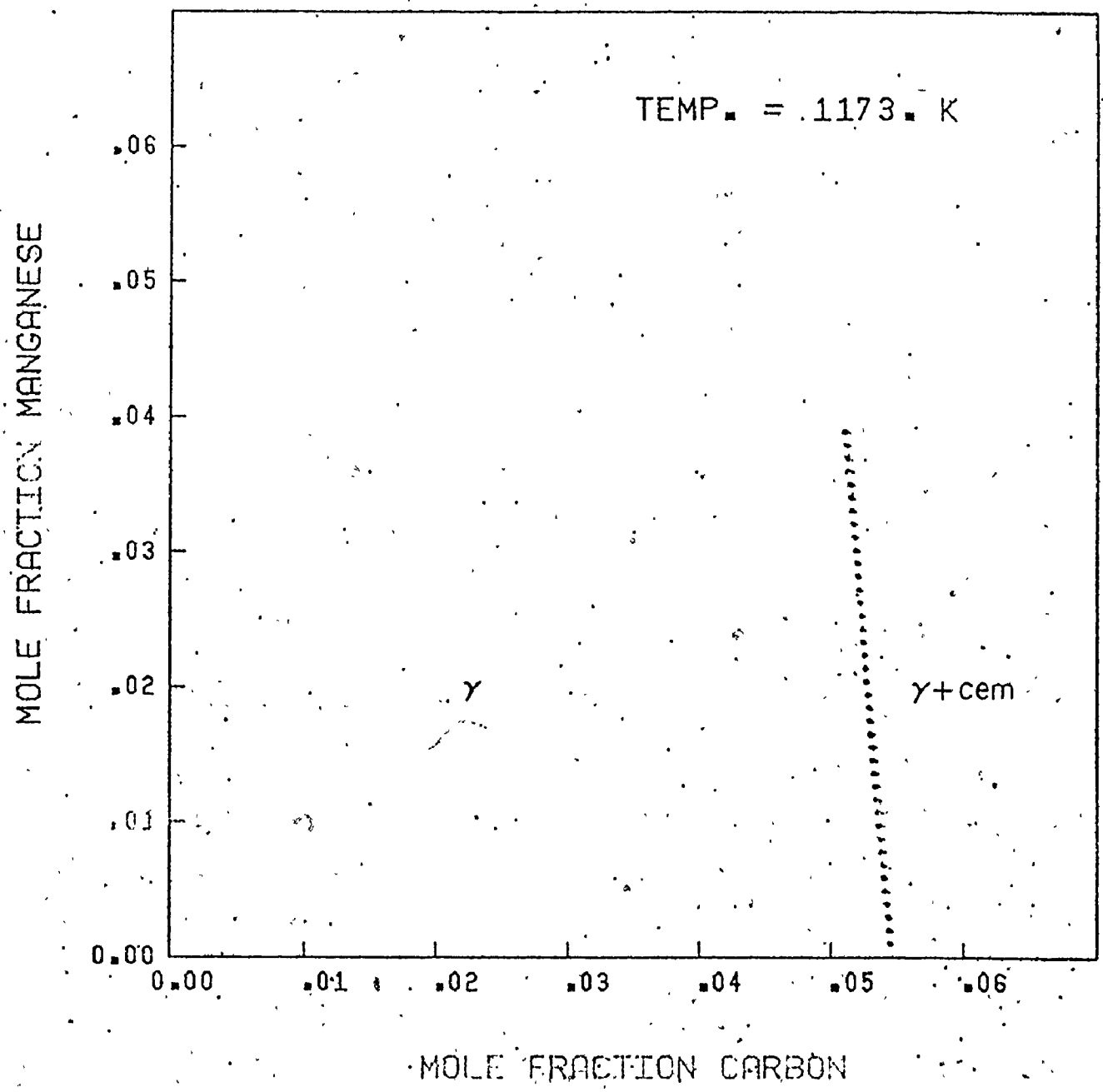

Figure 24. Fe-Mn-C system at 1173 K

TABLE XVIII. Fe-Mn-C at 1173 K in wt.%

ELEMENT NO. 2.

ELEMENT	GAMMA	CARBIDE	TEMP
.100000	0.000000	1.22326	1173.00
.200000	0.000000	1.22126	1173.00
.300000	0.000000	1.21927	1173.00
.400000	0.000000	1.21728	1173.00
.500000	0.000000	1.21529	1173.00
.600000	0.000000	1.21331	1173.00
.700000	0.000000	1.21132	1173.00
.800000	0.000000	1.20933	1173.00
.900000	0.000000	1.20734	1173.00
1.000000	0.000000	1.20536	1173.00
1.100000	0.000000	1.20337	1173.00
1.200000	0.000000	1.20139	1173.00
1.300000	0.000000	1.19940	1173.00
1.400000	0.000000	1.19742	1173.00
1.500000	0.000000	1.19544	1173.00
1.600000	0.000000	1.19346	1173.00
1.700000	0.000000	1.19147	1173.00
1.800000	0.000000	1.18949	1173.00
1.900000	0.000000	1.18751	1173.00
2.000000	0.000000	1.18553	1173.00
2.100000	0.000000	1.18356	1173.00
2.200000	0.000000	1.18158	1173.00
2.300000	0.000000	1.17960	1173.00
2.400000	0.000000	1.17762	1173.00
2.500000	0.000000	1.17565	1173.00
2.600000	0.000000	1.17367	1173.00
2.700000	0.000000	1.17170	1173.00
2.800000	0.000000	1.16972	1173.00
2.900000	0.000000	1.16775	1173.00
3.000000	0.000000	1.16578	1173.00
3.100000	0.000000	1.16381	1173.00
3.200000	0.000000	1.16184	1173.00
3.300000	0.000000	1.15987	1173.00
3.400000	0.000000	1.15790	1173.00
3.500000	0.000000	1.15593	1173.00
3.600000	0.000000	1.15396	1173.00
3.700000	0.000000	1.15199	1173.00
3.800000	0.000000	1.15002	1173.00
3.900000	0.000000	1.14806	1173.00
4.000000	0.000000	1.14609	1173.00

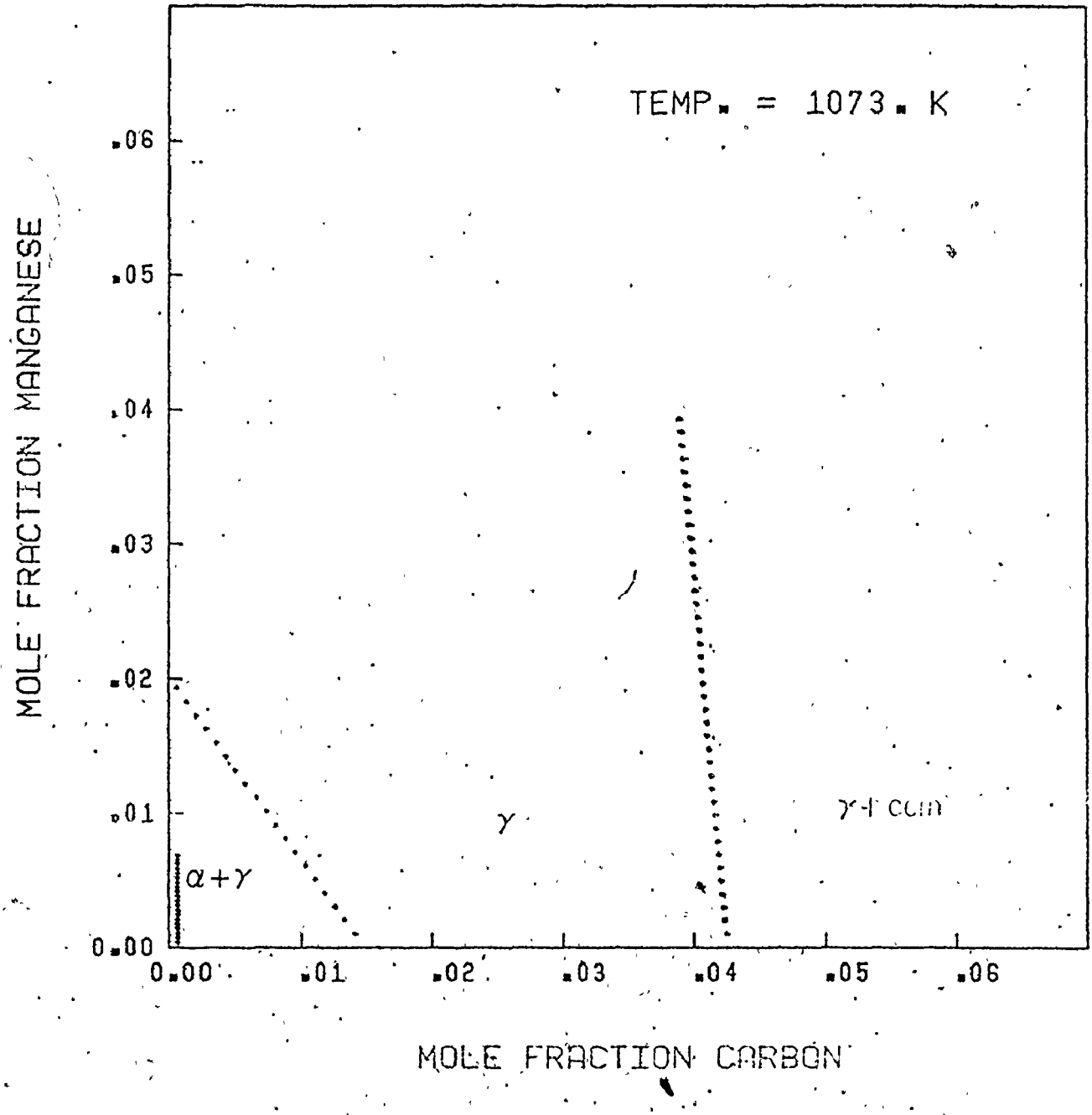

Figure 25 Fe-Mn-C system at 1073 K

TABLE XIX. Fe-Mn-C at 1073 K in wt.%

ELEMENT NO 2

ELEMENT	GAMMA	CARBICE	TEMP
.100000	.31736	.94518	1073.00
.200000	.29106	.94312	1073.00
.300000	.27475	.94106	1073.00
.400000	.25845	.93900	1073.00
.500000	.24214	.93694	1073.00
.600000	.22584	.93488	1073.00
.700000	.20954	.93283	1073.00
.800000	.19323	.93077	1073.00
.900000	.17693	.92871	1073.00
1.000000	.16063	.92666	1073.00
1.100000	.14433	.92461	1073.00
1.200000	.12803	.92255	1073.00
1.300000	.11173	.92050	1073.00
1.400000	.09543	.91845	1073.00
1.500000	.07913	.91640	1073.00
1.600000	.06283	.91435	1073.00
1.700000	.04653	.91230	1073.00
1.800000	.03024	.91025	1073.00
1.900000	.01394	.90820	1073.00
2.000000	0.000000	.90615	1073.00
2.100000	0.000000	.90411	1073.00
2.200000	0.000000	.90206	1073.00
2.300000	0.000000	.90002	1073.00
2.400000	0.000000	.89797	1073.00
2.500000	0.000000	.89593	1073.00
2.600000	0.000000	.89388	1073.00
2.700000	0.000000	.89184	1073.00
2.800000	0.000000	.88980	1073.00
2.900000	0.000000	.88776	1073.00
3.000000	0.000000	.88572	1073.00
3.100000	0.000000	.88368	1073.00
3.200000	0.000000	.88164	1073.00
3.300000	0.000000	.87960	1073.00
3.400000	0.000000	.87757	1073.00
3.500000	0.000000	.87553	1073.00
3.600000	0.000000	.87349	1073.00
3.700000	0.000000	.87146	1073.00
3.800000	0.000000	.86942	1073.00
3.900000	0.000000	.86739	1073.00
4.000000	0.000000	.86536	1073.00

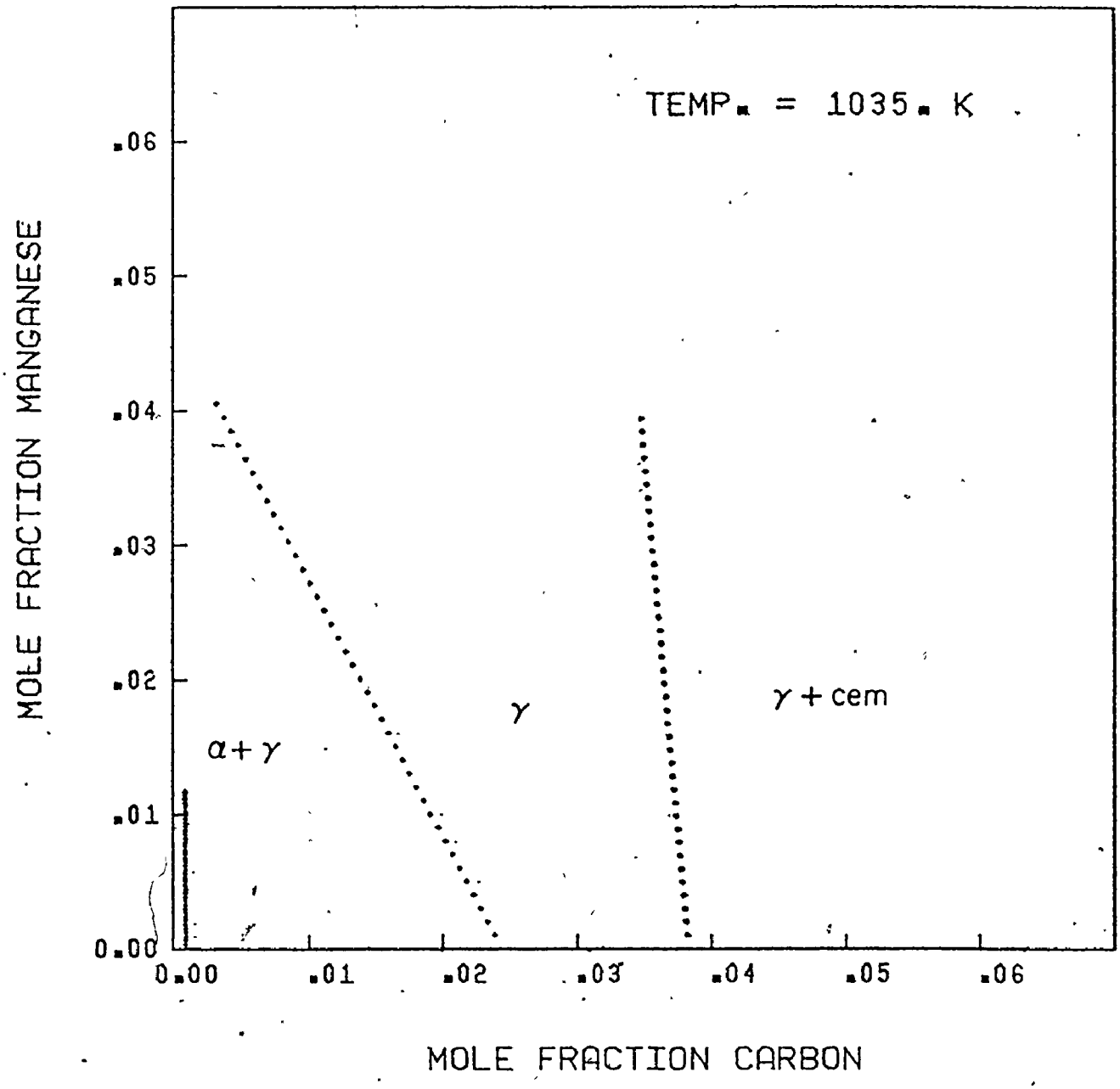

Figure 26 Fe-Mn-C system at 1035 K

TABLE XX. Fe-Mn-C at 1035 K in wt.%

ELEMENT NO 2

ELEMENT	GAMMA	CARBIDE	TEMP
.10000	.52340	.84758	1035.00
.20000	.51179	.84556	1035.00
.30000	.50018	.84355	1035.00
.40000	.48857	.84154	1035.00
.50000	.47697	.83953	1035.00
.60000	.46536	.83752	1035.00
.70000	.45375	.83551	1035.00
.80000	.44214	.83350	1035.00
.90000	.43054	.83149	1035.00
1.00000	.41893	.82949	1035.00
1.10000	.40733	.82748	1035.00
1.20000	.39572	.82547	1035.00
1.30000	.38412	.82347	1035.00
1.40000	.37251	.82146	1035.00
1.50000	.36091	.81946	1035.00
1.60000	.34930	.81746	1035.00
1.70000	.33770	.81546	1035.00
1.80000	.32610	.81346	1035.00
1.90000	.31449	.81145	1035.00
2.00000	.30289	.80945	1035.00
2.10000	.29129	.80746	1035.00
2.20000	.27969	.80546	1035.00
2.30000	.26808	.80346	1035.00
2.40000	.25648	.80146	1035.00
2.50000	.24488	.79947	1035.00
2.60000	.23328	.79747	1035.00
2.70000	.22168	.79548	1035.00
2.80000	.21008	.79348	1035.00
2.90000	.19848	.79149	1035.00
3.00000	.18689	.78950	1035.00
3.10000	.17528	.78751	1035.00
3.20000	.16368	.78551	1035.00
3.30000	.15209	.78352	1035.00
3.40000	.14049	.78153	1035.00
3.50000	.12889	.77954	1035.00
3.60000	.11729	.77755	1035.00
3.70000	.10570	.77557	1035.00
3.80000	.09410	.77358	1035.00
3.90000	.08250	.77159	1035.00
4.00000	.07091	.76961	1035.00

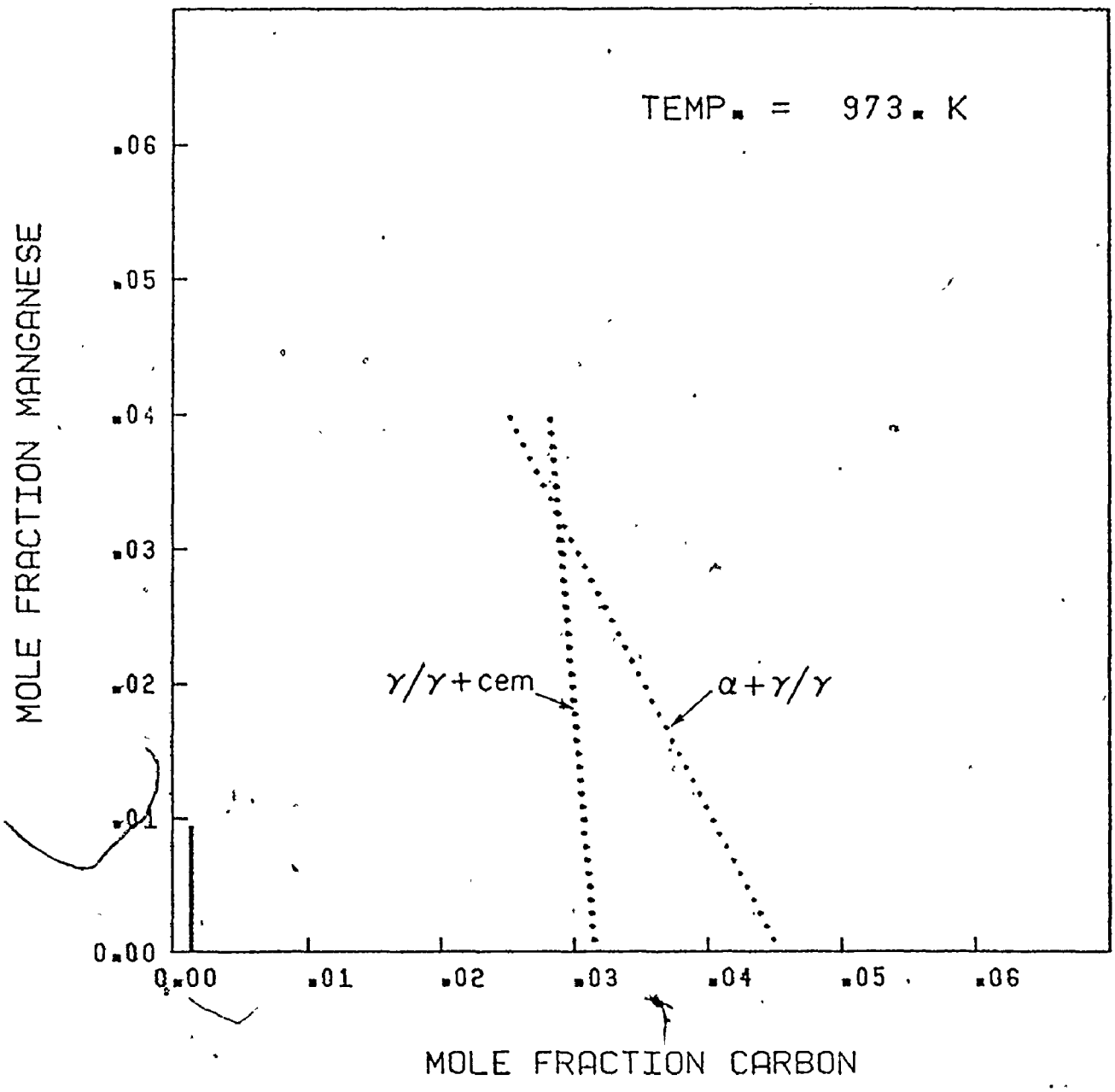

Figure 27 Fe-Mn-C system at 973 K

TABLE XXI. Fe-Mn-C at 973 K in wt.%

ELEMENT NO 2

ELEMENT	GAMMA	CARBIDE	TEMP
.100000	1.00272	.69602	973.00
.200000	.99124	.69416	973.00
.300000	.97975	.69230	973.00
.400000	.96827	.69044	973.00
.500000	.95679	.68858	973.00
.600000	.94531	.68673	973.00
.700000	.93383	.68487	973.00
.800000	.92235	.68301	973.00
.900000	.91087	.68116	973.00
1.000000	.89940	.67930	973.00
1.100000	.88792	.67745	973.00
1.200000	.87644	.67559	973.00
1.300000	.86496	.67374	973.00
1.400000	.85348	.67189	973.00
1.500000	.84200	.67003	973.00
1.600000	.83053	.66818	973.00
1.700000	.81905	.66633	973.00
1.800000	.80757	.66448	973.00
1.900000	.79610	.66263	973.00
2.000000	.78462	.66078	973.00
2.100000	.77315	.65893	973.00
2.200000	.76167	.65709	973.00
2.300000	.75019	.65524	973.00
2.400000	.73872	.65339	973.00
2.500000	.72725	.65155	973.00
2.600000	.71577	.64970	973.00
2.700000	.70430	.64786	973.00
2.800000	.69282	.64601	973.00
2.900000	.68135	.64417	973.00
3.000000	.66988	.64233	973.00
3.100000	.65840	.64049	973.00
3.200000	.64693	.63865	973.00
3.300000	.63546	.63681	973.00
3.400000	.62399	.63497	973.00
3.500000	.61251	.63313	973.00
3.600000	.60104	.63129	973.00
3.700000	.58957	.62945	973.00
3.800000	.57811	.62761	973.00
3.900000	.56663	.62578	973.00
4.000000	.55516	.62394	973.00

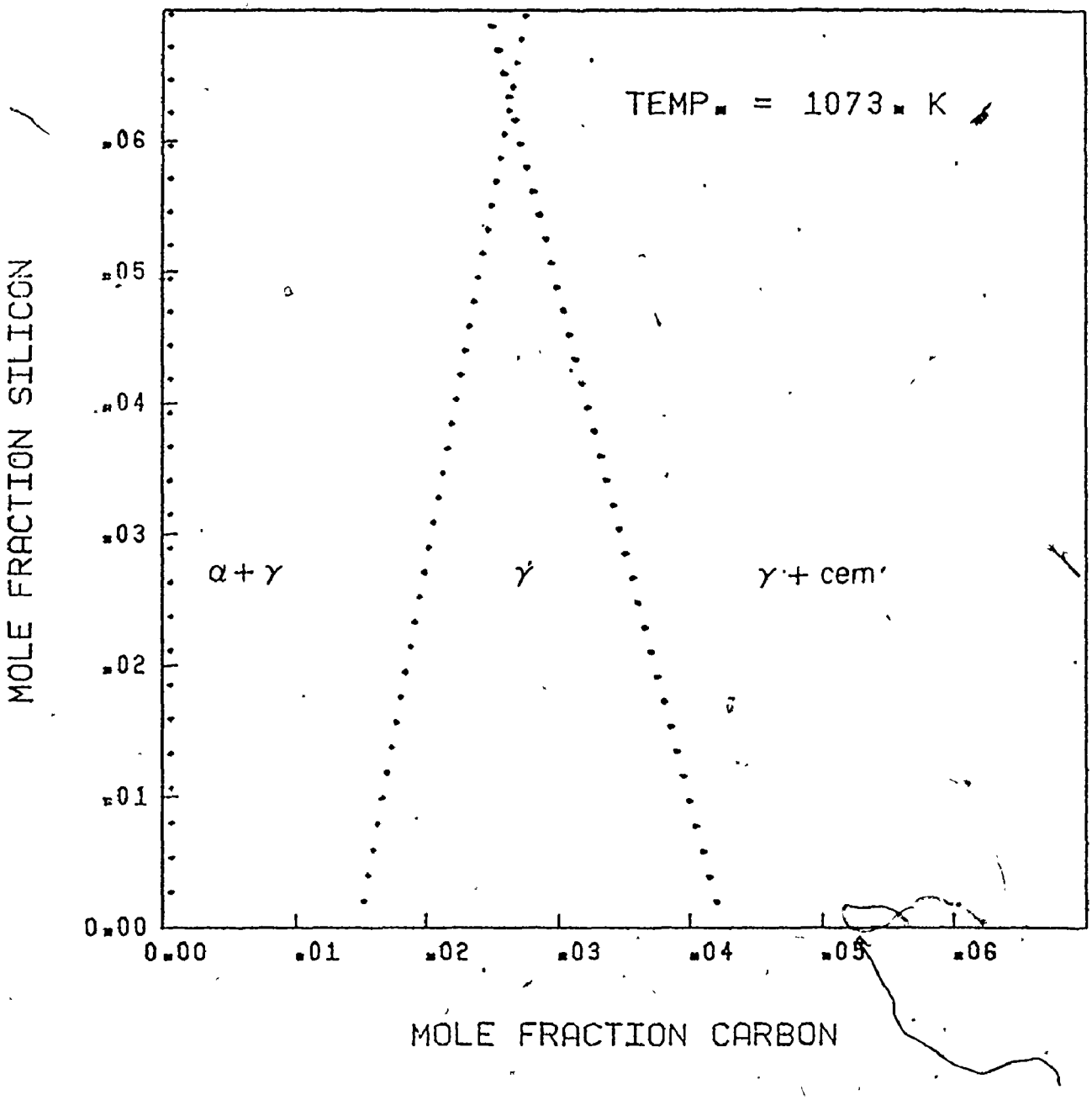

Figure 28 Fe-Si-C system at 1073 K

TABLE XXII. Fe-Si-C at 1073 K in wt.%

ELEMENT NO 3

ELEMENT	GAMMA	CARBIDE	TEMP
.10000	.33229	.93661	1073.00
.20000	.34089	.92599	1073.00
.30000	.34947	.91540	1073.00
.40000	.35802	.90483	1073.00
.50000	.36655	.89428	1073.00
.60000	.37506	.88374	1073.00
.70000	.38354	.87323	1073.00
.80000	.39199	.86274	1073.00
.90000	.40043	.85226	1073.00
.95000	.40884	.84181	1073.00
.10000	.41722	.83137	1073.00
.20000	.42559	.82096	1073.00
.30000	.43393	.81056	1073.00
.40000	.44225	.80018	1073.00
.50000	.45054	.78983	1073.00
.60000	.45881	.77949	1073.00
.70000	.46706	.76917	1073.00
.80000	.47529	.75887	1073.00
.90000	.48349	.74859	1073.00
.95000	.49167	.73833	1073.00
.10000	.49983	.72808	1073.00
.20000	.50797	.71786	1073.00
.30000	.51608	.70765	1073.00
.40000	.52417	.69747	1073.00
.50000	.53224	.68730	1073.00
.55000	.54029	.67715	1073.00
.60000	.54832	.66702	1073.00
.70000	.55632	.65691	1073.00
.80000	.56430	.64682	1073.00
.90000	.57226	.63674	1073.00
.95000	.58020	.62669	1073.00
.10000	.58812	.61665	1073.00
.20000	.59602	.60663	1073.00
.30000	.60388	.59663	1073.00
.40000			

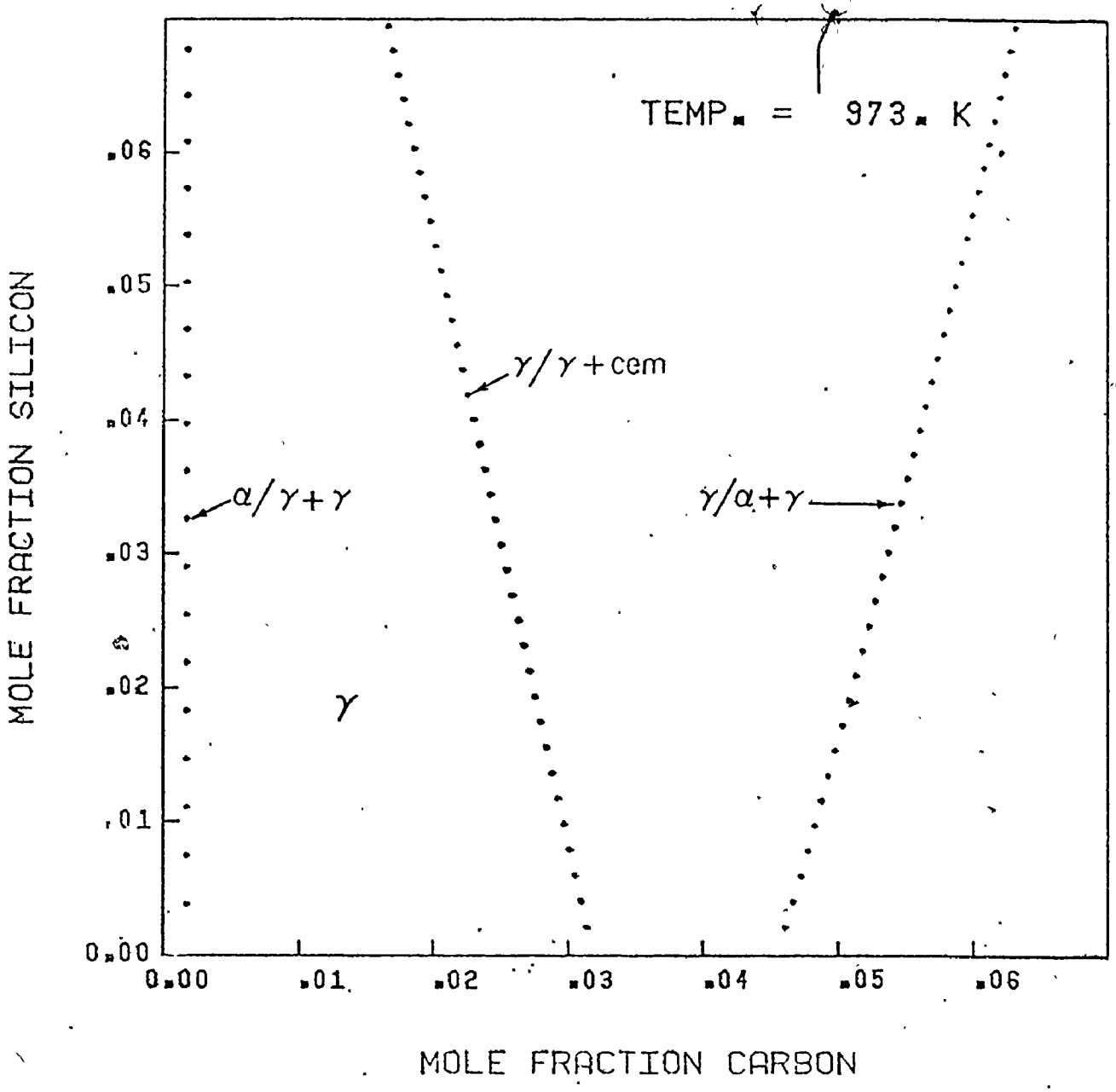

Figure 29 Fe-Si-C system at 973 K

TABLE XXIII. Fe-Si-C at 973 K in wt.%

ELEMENT NO 3

ELEMENT	GAMMA	CARBIDE	TEMP
.100000	1.032756	.688862	973.00
.200000	1.048384	.679337	973.00
.300000	1.054406	.670113	973.00
.400000	1.057721	.660992	973.00
.500000	1.080228	.651172	973.00
.600000	1.089329	.642554	973.00
.700000	1.106623	.633338	973.00
.800000	1.119100	.624240	973.00
.900000	1.131900	.615110	973.00
1.000000	1.144663	.606010	973.00
1.100000	1.157729	.596920	973.00
1.200000	1.169889	.587850	973.00
1.300000	1.182430	.578790	973.00
1.400000	1.194889	.569760	973.00
1.500000	1.207230	.560740	973.00
1.600000	1.219630	.551740	973.00
1.700000	1.231900	.542760	973.00
1.800000	1.244110	.533790	973.00
1.900000	1.256620	.524840	973.00
2.000000	1.268320	.515910	973.00
2.100000	1.280330	.507000	973.00
2.200000	1.292220	.498100	973.00
2.300000	1.304170	.489220	973.00
2.400000	1.315990	.480360	973.00
2.500000	1.327750	.471510	973.00

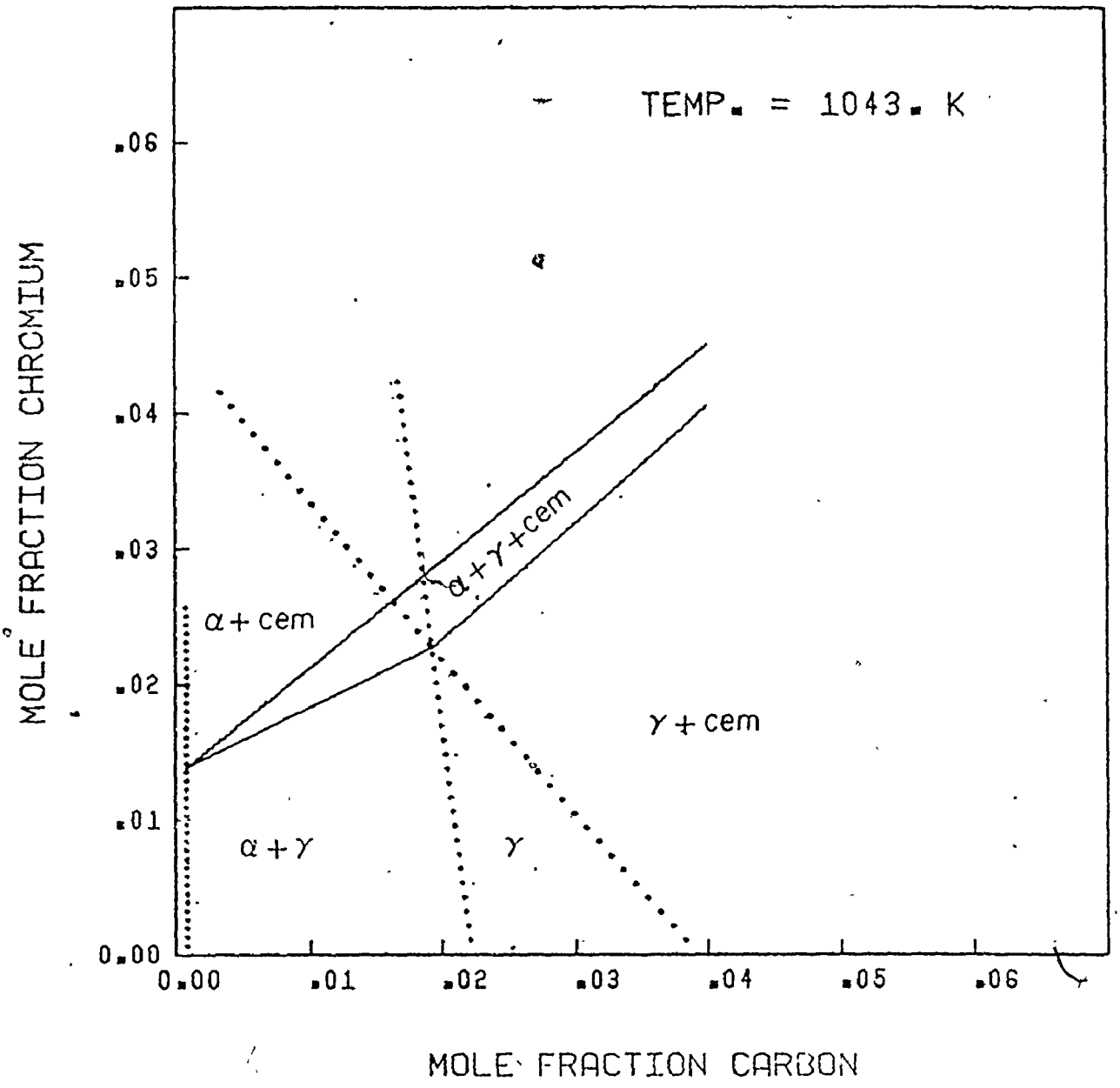

Figure 30 Fe-Cr-C system at 1043 K

TABLE XXIV. Fe-Cr-C at 1043 K in wt.%

ELEMENT NO 5

ELEMENT	GAMMA	CARBIDE	TEMP
.100000	.44233	.84846	1043.00
.200000	.47934	.82717	1043.00
.300000	.47634	.80596	1043.00
.400000	.47335	.78482	1043.00
.500000	.47036	.76376	1043.00
.600000	.46737	.74277	1043.00
.700000	.46438	.72186	1043.00
.800000	.46139	.70102	1043.00
.900000	.45840	.68026	1043.00
1.000000	.45541	.65957	1043.00
1.100000	.45242	.63896	1043.00
1.200000	.44943	.61842	1043.00
1.300000	.44644	.59795	1043.00
1.400000	.44345	.57756	1043.00
1.500000	.44046	.55724	1043.00
1.600000	.43747	.53699	1043.00
1.700000	.43448	.51681	1043.00
1.800000	.43149	.49670	1043.00
1.900000	.42850	.47667	1043.00
2.000000	.42551	.45670	1043.00
2.100000	.42252	.43681	1043.00
2.200000	.41953	.41698	1043.00
2.300000	.41655	.39723	1043.00
2.400000	.41356	.37754	1043.00
2.500000	.41057	.35793	1043.00
2.600000	.40758	.33838	1043.00
2.700000	.40459	.31890	1043.00
2.800000	.40160	.29949	1043.00
2.900000	.39862	.28015	1043.00
3.000000	.39563	.26087	1043.00
3.100000	.39264	.24166	1043.00
3.200000	.38965	.22252	1043.00
3.300000	.38667	.20345	1043.00
3.400000	.38368	.18444	1043.00
3.500000	.38069	.16550	1043.00
3.600000	.37771	.14662	1043.00
3.700000	.37472	.12781	1043.00
3.800000	.37173	.10906	1043.00
3.900000	.36874	.09038	1043.00
4.000000	.36576	.07176	1043.00

Table XXV. Comparison of Partition Coefficients (mole fraction basis) for α/γ in Fe-C-Cr Systems (79)

T °K	$\frac{x^{\gamma}_{Cr}}{x^{\alpha}_{Cr}}$ (expt.)	$\frac{x^{\gamma}_{Cr}}{x^{\alpha}_{Cr}}$ (pred.)
1043	1.66	1.74
1043	1.73	1.74
1023	1.78	1.81

Table XXVI. α/γ Partition Coefficient, $K^{\alpha/\gamma} = x^{\gamma}/x^{\alpha}$

T(K)	Mn	Si	Ni	Cr	Mo	Cu	W	V	Nb	Co
1138	1.17	0.82	1.43	1.25	0.74	1.31	0.36	0.80	1.24	0.99
1104	1.20	0.78	1.49	1.34	0.76	1.35	0.36	0.91	1.54	0.98
1078	1.24	0.75	1.53	1.44	0.78	1.40	0.36	1.04	1.94	0.96
1058	1.28	0.71	1.55	1.55	0.81	1.45	0.36	1.19	2.45	0.95
1041	1.31	0.68	1.57	1.67	0.84	1.50	0.36	1.37	3.10	0.94
1025	1.35	0.65	1.58	1.81	0.87	1.54	0.36	1.57	3.95	0.92
1010	1.39	0.62	1.60	1.97	0.90	1.60	0.37	1.81	5.05	0.91

of this calculation was initially based on the data of Sharma (79) and of Razik et al. (90) for the Fe-C-Cr system as shown in Figure (31). This information was used initially to check the eutectoid intersections predicted between the Ae_3 and carbide lines for the constant composition sections, then to verify equations (IV-1) and (IV-2) for the eutectoid temperature and carbon composition upon the addition of chromium, with salutory results. After the formula was shown to work adequately for additions of chromium, it was used to predict the eutectoid composition and temperature for Si, Cr, Mn and Ni and compared with the data of Bain and Paxton (91) as shown in Figure (32). It is not known if Bain and Paxton restricted their analysis to only Fe_3C-type carbides, so this diagram was limited to 2 wt.pct. alloying element. It is interesting to note that Uhrenius (80) published a similar comparison that showed a deviation comparable to our formulae prediction for Si.

Discussion

As more information on metallic systems becomes available, there is a trend towards developing more complex and comprehensive models (10) in order to explain the findings and to better predict results which are difficult to achieve experimentally. As a result, the calculations can be expensive, demanding long computation times and larger, faster computers.

It was our contention, when embarking on this work, that for most commercially important alloys (i.e.: hardenability steels) it was not necessary and not practical to resort to complex thermodynamic modelling

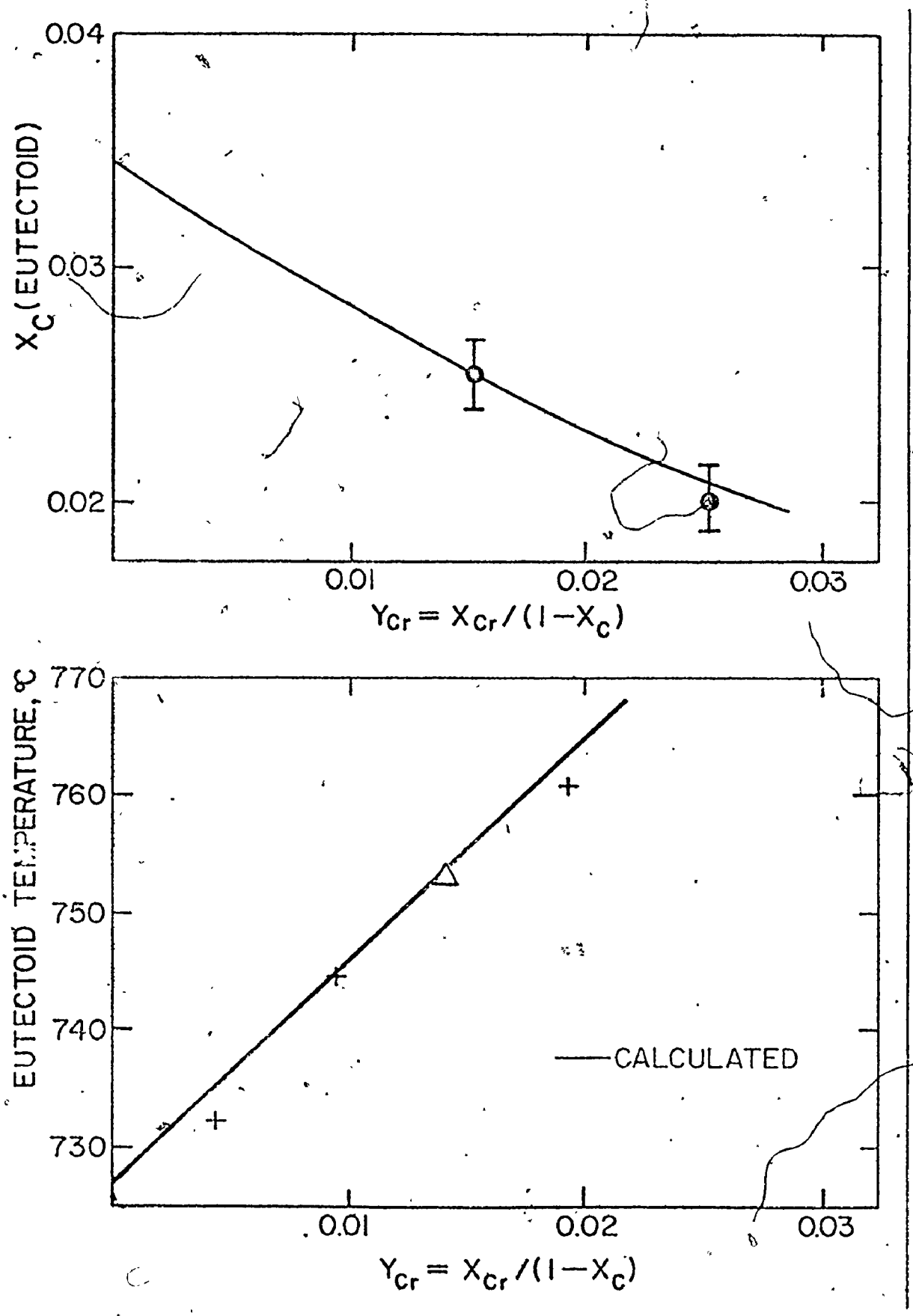

Figure 31 Comparison of predicted and observed variations in the eutectoid temperature and composition with additions of Cr. Experimental points after Sharma (79) +,● and Razik et al. (90)Δ.

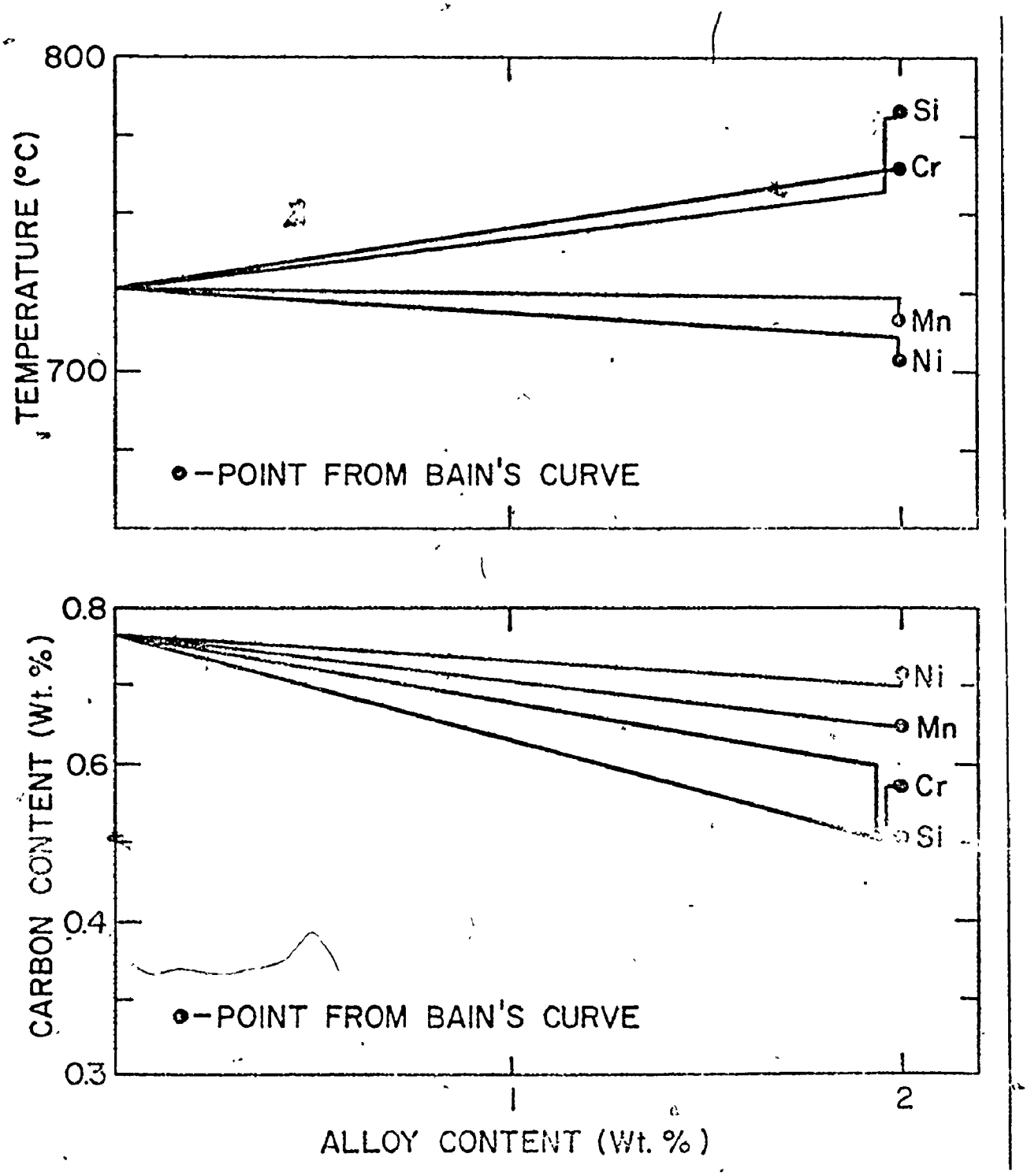

Figure 32 Comparison of predicted and observed variations in the eutectoid temperature and compositon with additions of Mn, Si, Ni and Cr. Single points were taken from Bain's experimental curves (91).

in order to characterize multicomponent dilute alloy phase diagrams. By choosing the Wagner Taylor series expansion as the starting point, we were able to derive equations that are rigorous up to linear terms, that are accurate for small alloy additions and are able to handle efficiently, large numbers of solute additions. Comparison with experimental phase diagrams and phase diagrams computed using more complex models (80) have shown that our formulae give adequate representation of results for quite rich alloys; indeed, to the limits of: 3 wt.pct. Mn, 2.0 wt.pct. Si, 4 wt.pct. Ni, 4 wt.pct. Cr, 1.5 wt.pct. Mo and $\leq$ 1 wt.pct. W, V, Nb and Co. Since for Nb, V, W, Si and Mo, the binary iron phase diagrams contain gamma loops, we assume that the binary loop extents set some kind of limit on the maximum addition which can be accepted in the binary formula.

The above limits apply only to the $\alpha+\gamma$ range which is the only region where quantitative verification is possible. The δ/γ , δ/L, γ/L and γ/carbide fields are also assumed to be qualitatively correct to the same alloy limits although there are unknown inaccuracies due to poorly established thermodynamic data, binary iron phase diagrams and lack of experimental multicomponent observations in these regions. Since the reliability of the information in these areas was questionable, no multi-component quasi-ternary phase diagrams were attempted.

Application of the Wagner Formalism for linearization purposes in our formula required that all variables and standard states be defined at infinite dilution. Although the carbon-carbon and carbon cross interactions are rigorously defined for small solute additions, the values

reported in the literature are actually averages over a wide range of carbon compositions, and usually measured as functions of temperature. The free energy data is referenced at the standard state of infinite dilution but is also an average over a range of composition. These averaging processes in obtaining the thermodynamic parameters could facilitate the extension of the formulae to richer alloys.

It was previously mentioned that the predicted values for the Ae_3 temperatures tended to fall below these experimental ones. Judging by the agreement of our ternary phase diagrams with those predicted and carefully verified by Uhrenius and the experimental ternary phase diagrams of Gilmour (85) and Sharma (79) it is thought that perhaps the experimental results, particularly U.S. Steel contain a systematic error. The experimental Ae_3 temperatures could be affected by segregation, insufficient austenitising temperatures or inadequate holding times. Since the binary and ternary phase diagram determinations were made by holding samples at carefully controlled temperatures for long periods of time, they are probably better than the Ae_3 measurements. The latter fault, too short a holding time, would certainly account for the experimental results being consistently higher than predicted. It is nonetheless thought, because of the behaviour of the Ae_3 and ternary results at low carbon contents, that our manganese and perhaps nickel and chromium free energy data for this region is in error, or that there exists a higher order cross effect which we are unable to account for in our treatment.

Application to Steels

Baganis and Kirkaldy (9) demonstrated that predictive formulae of this type could be used as a boundary condition for the TTT curve as applied in a hardenability predictor. Although this is an indirect use of this type of work, the potential uses in the future are much greater.

At the moment, it is possible for us to predict the solution temperatures of various Fe_3C-type carbides and their solubility limits at any temperature. Given more partition coefficient data and empirical analogues of the Fe-C carbide line, it would be possible to predict the lowest temperature a steel could be held at for the complete dissolution of carbides.

A much more important and promising use of our constant composition sections of the Fe-C binary lies in its applicability to the development and implementation of steels containing a duplex microstructure (92). These steels are manufactured by austenitising then quenching to martensite, followed by cycles of heating in the $\alpha+\gamma$ region then quenching to form a structure of ferrite and dislocated martensite. Since the crucial step is the holding step in the two phase region (during which the alloy segregates into ferrite and austenite along the equilibrium tie-line), we hope our formulae will be instrumental in cutting development time and cost by allowing the prediction of a reasonable carbon composition or temperature starting point. Examples of the types of phase diagrams possible are shown in Figures (33) to (37) for a Fe-1.0 wt.pct. Cr - 1.0 wt.pct. Mo-C alloy.

Figure 33 Fe-1.0 Mo - 1.0 Cr-C constant composition section

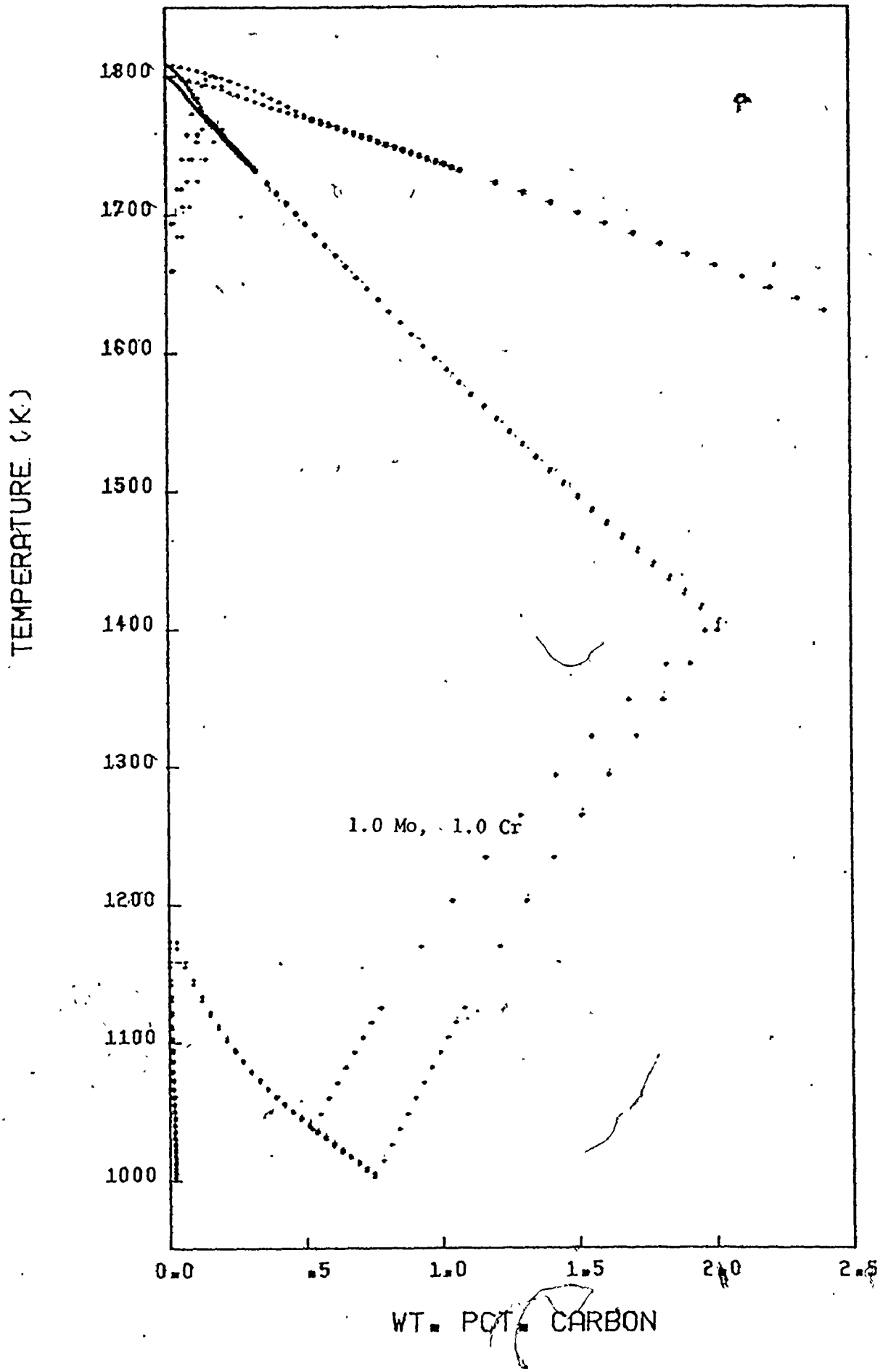

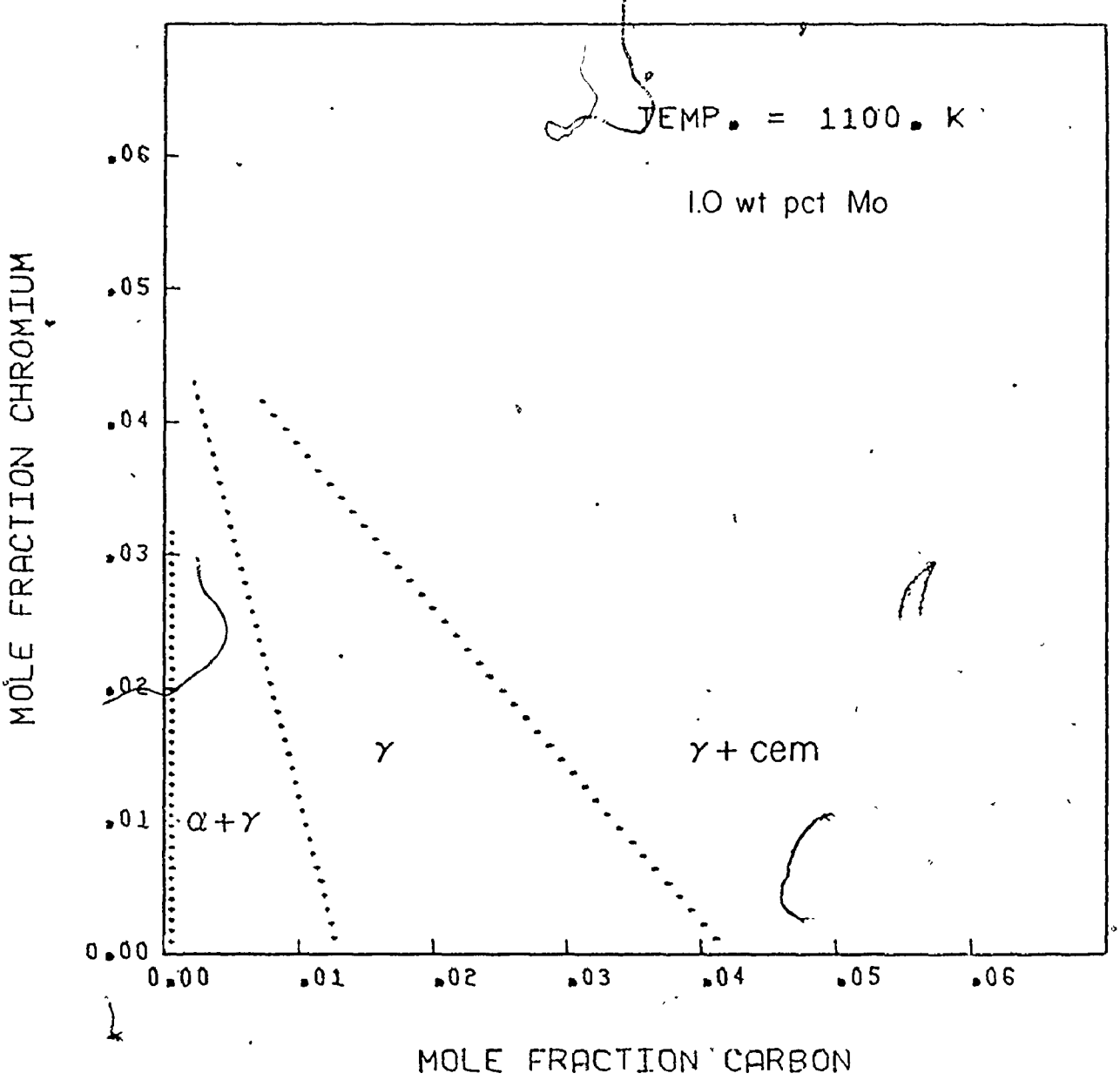

Figure 34 Fe-Cr-C-1.0 Mo isothermal phase diagram at 1100 K

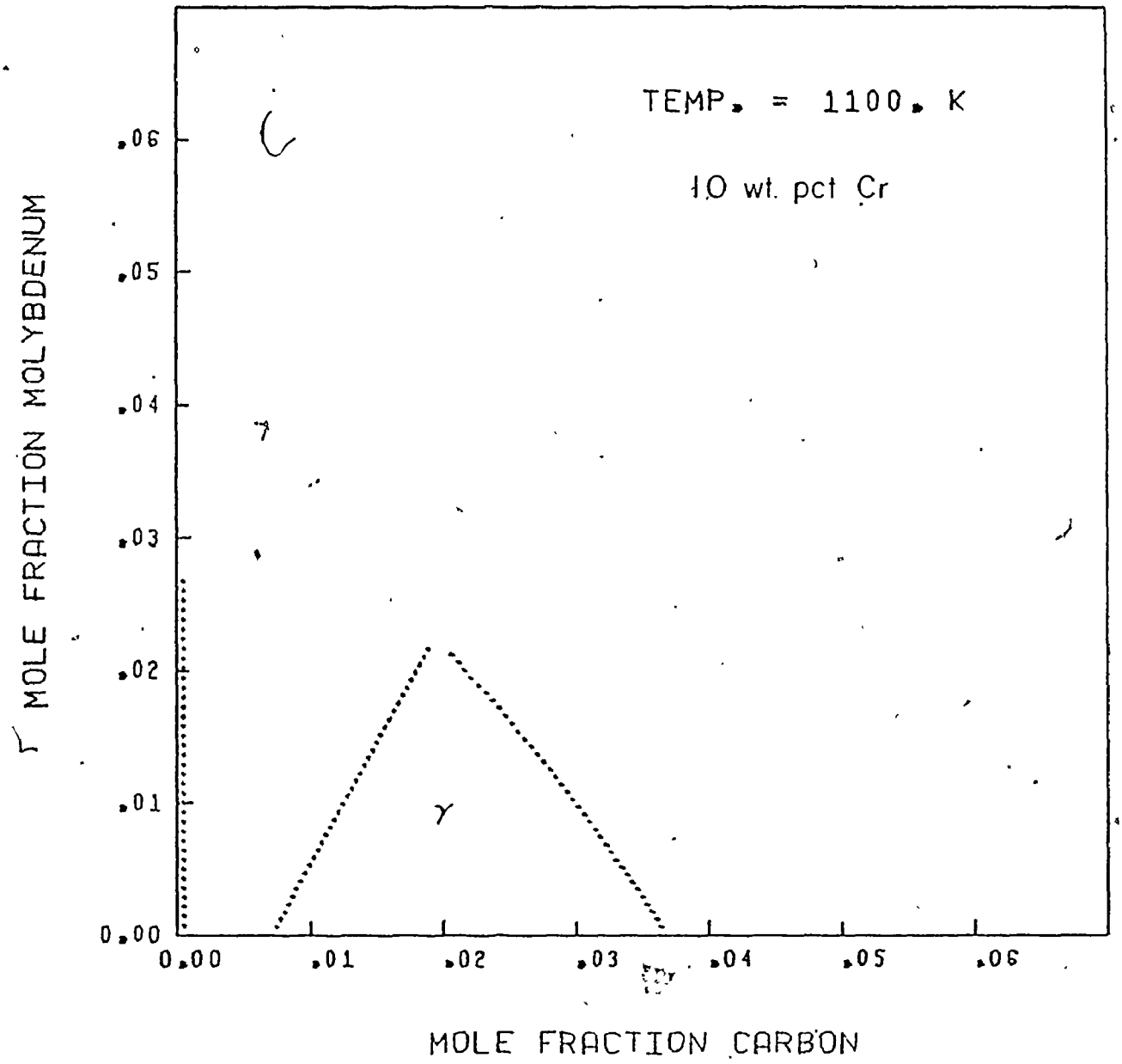

Figure 35 Fe-Mo-C-1.0 Cr isothermal phase diagram at 1100 K

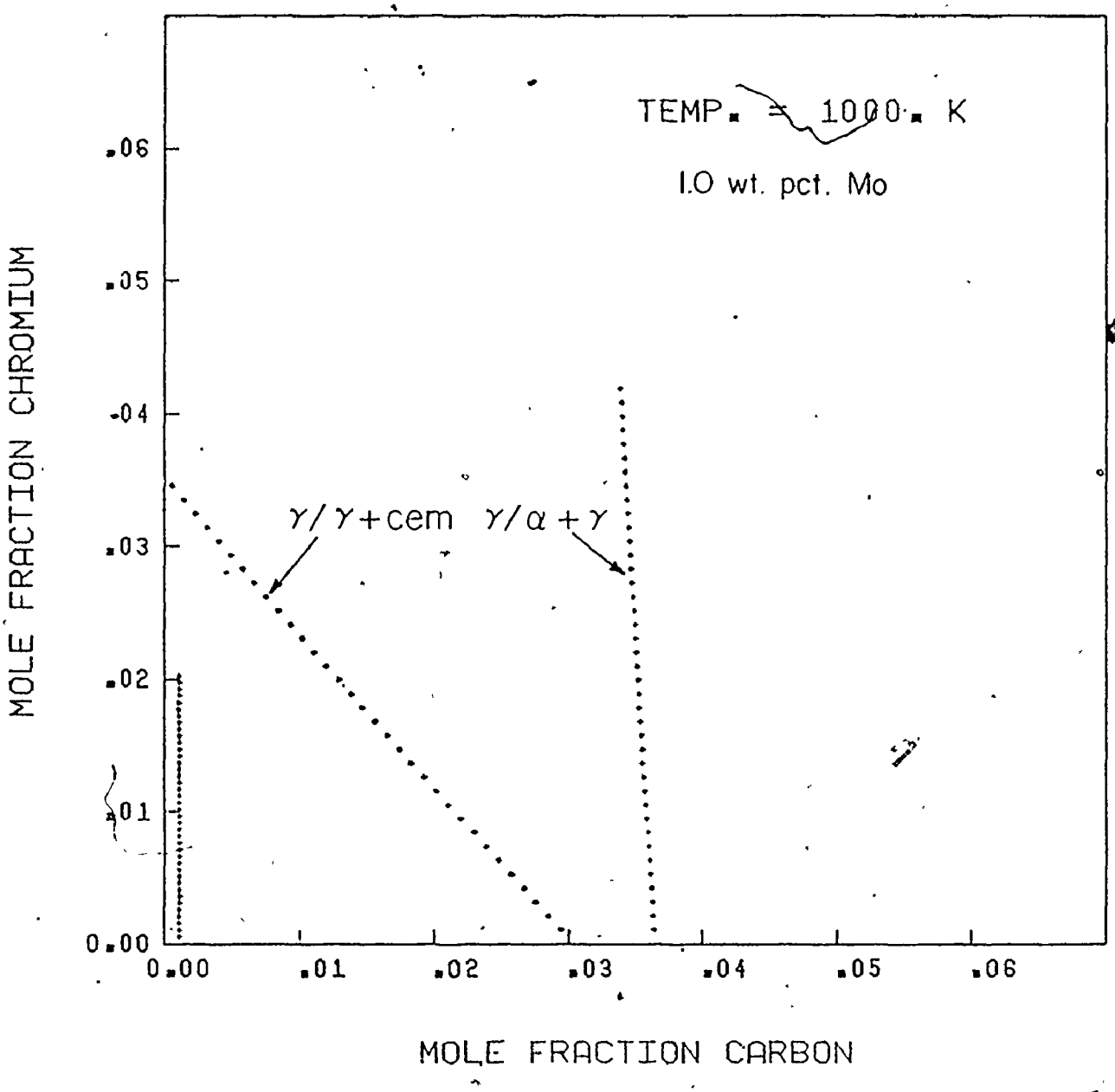

Figure 36 Fe-Cr-C-1.0 Mo isothermal phase diagram at 1000 K

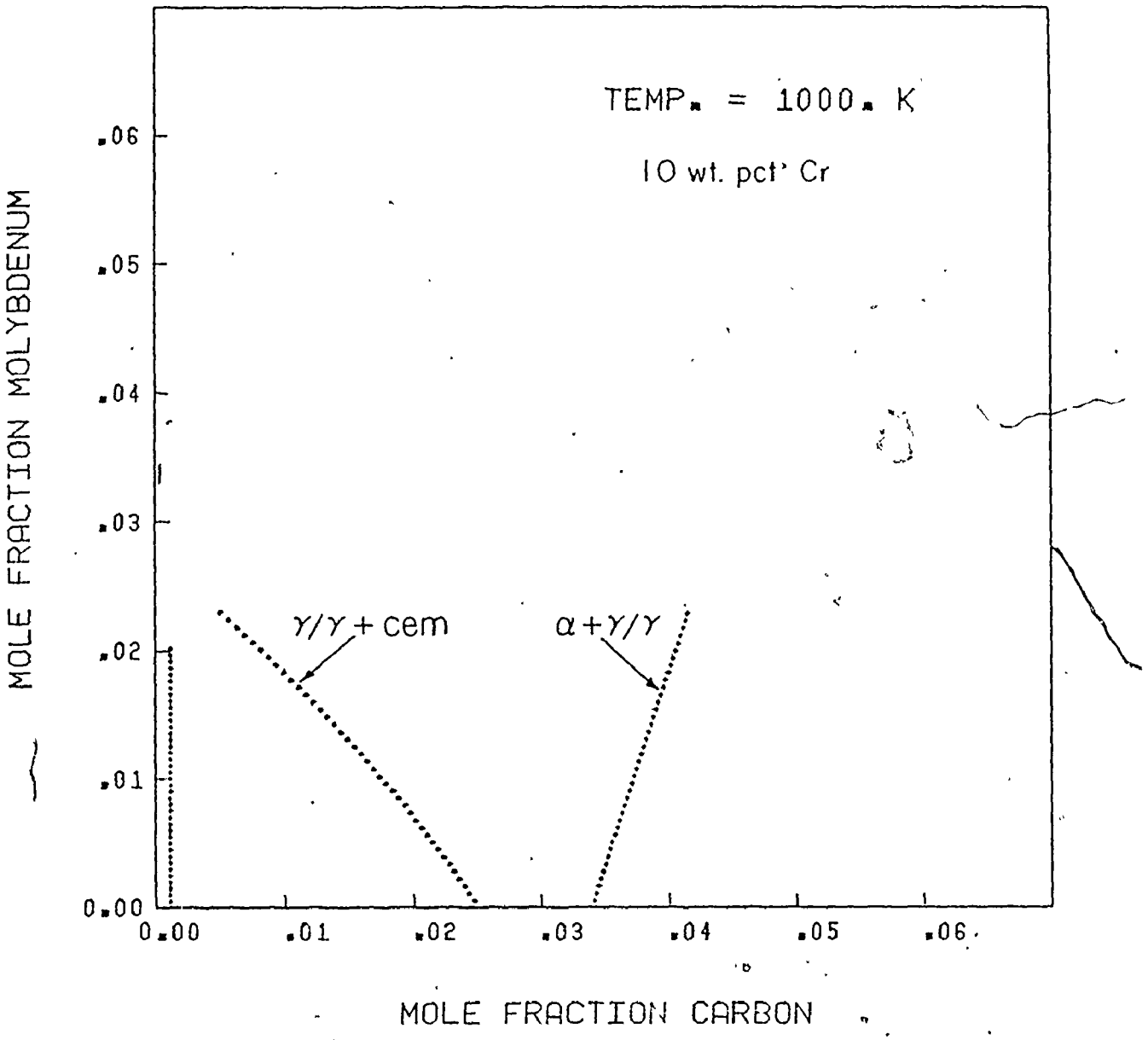

Figure 37 Fe-Mo-C-1.0 Cr isothermal phase diagram at 1000 K

CHAPTER V

CONCLUSION

This thesis describes the derivation of a rigorous formula for the prediction of multicomponent phase diagrams with the following limits: %C < 2 wt%, %Mn < 3 wt%, %Si < 1 wt%, %Ni < 3%, %Cr < 2.5%, %Mo < 2%, %Cu < 3% and W, V, Nb and Co < 1 wt%.

Because the formula is linear in all elements with the exception of carbon, it is capable of describing phase diagrams with any number of components.

The predictive formulae are simple enough to be programmed on a desk calculator.

They can be used to predict constant composition sections of the iron carbon phase diagrams with the composition of the alloying elements held constant and the deviation from the Fe-C binary plotted with respect to different carbon contents. Quasiternary isotherms of any order can be plotted, with any number of elements at constant composition and carbon and another alloying element changing at constant temperature.

We also offer subsidiary formula for the prediction of the multicomponent eutectoid composition and temperature and for the deviation of the T_o line with addition of alloy solutes.

APPENDIX 1

To derive the first phase boundary correction formula we start with the expressions for the equality of chemical potentials. For Fe(n=0) we have

$$\frac{\Delta^o G_o^{\gamma-L}}{RT} = \ln\left[\frac{1-x_1^{\gamma}-\sum_2^n x_i^{\gamma}}{1-x_1^{L}-\sum_2^n x_i^{L}}\right] - x_1^{\gamma}\sum_2^n \varepsilon_{1i}^{\gamma}x_i^{\gamma} + x_1^{L}\sum_2^n \varepsilon_{1i}^{L}x_i^{L} - \frac{\varepsilon_{11}^{\gamma}}{2}(x_1^{\gamma})^2 + \frac{\varepsilon_{11}^{L}}{2}(x_1^{L})^2, \quad (1)$$

For C(n=1) we have

$$\frac{\Delta^o G_1^{\gamma-L}}{RT} = \ln\left[\frac{x_1^{\gamma}}{x_1^{L}}\right] + \varepsilon_{11}^{\gamma}x_1^{\gamma} - \varepsilon_{11}^{L}x_1^{L} \quad (2)$$

and for corponent i we have

$$\frac{\Delta^o G_i^{\gamma-L}}{RT} = \ln\left[\frac{x_i^{\gamma}}{x_i^{L}}\right] + \varepsilon_{1i}^{\gamma}x_1^{\gamma} - \varepsilon_{1i}^{L}x_1^{L} \quad (3)$$

Now rearranging eq. (2)

$$x_1^{\gamma}\exp(\varepsilon_{11}^{\gamma}x_1^{\gamma}) = x_1^{L}\exp\left[\frac{\Delta^o G_1}{RT} + \varepsilon_{11}^{L}x_1^{L}\right] \quad (4)$$

Expanding the exponential and disregarding higher order terms gives

$$x_1^{\gamma}(1+\varepsilon_{11}^{\gamma}x_1^{\gamma}) = x_1^{L}\exp\left[\frac{\Delta^o G_1}{RT} + \varepsilon_{11}^{L}x_1^{L}\right] \quad (5)$$

To a first approximation, for x_1^{L}, x_1^{γ} small

$$x_1^{\gamma} = x_1^{L}\exp\left[\frac{\Delta^o G_1}{RT}\right] \quad (6)$$

Substituting for x_1^{γ} in eq. (5) and rearranging we obtain the next higher order approximation

$$x_1^{\gamma} = \frac{x_1^{L}\exp\left[\frac{\Delta^o G_1}{RT} + \varepsilon_{11}^{L}x_1^{L}\right]}{\left(1+\varepsilon_{11}^{\gamma}x_1^{L}\exp\left[\frac{\Delta^o G_1}{RT}\right]\right)} \quad (7)$$

$$x_i^\gamma(1+\varepsilon_{1i}^\gamma x_1^\gamma) = x_i^L \exp[\frac{\Delta^o G_i}{RT} + \varepsilon_{1i}^L x_1^L] \quad (8)$$

Substituting for x_1^γ from (6) and rearranging we obtain

$$x_i^\gamma = \frac{x_i^L \exp[\frac{\Delta^o G_i}{RT} + \varepsilon_{1i}^L x_1^L]}{(1+\varepsilon_{1i}^\gamma x_1^L \exp[\frac{\Delta^o G_1}{RT}])} \quad (9)$$

Now from (1) we write

$$1-x_1^L - \sum_2^n x_i^L = (1-x_1^\gamma - \sum_2^n x_i^\gamma)$$

$$\cdot \exp[-\frac{\Delta^o G_o}{RT} - x_1^\gamma \sum_2^n \varepsilon_{1i}^\gamma x_i^\gamma + x_1^L \sum_2^n \varepsilon_{1i}^L x_i^L - \frac{\varepsilon_{11}^\gamma}{2}(x_1^\gamma)^2 + \frac{\varepsilon_{11}^L}{2}(x_1^L)^2] \quad (10)$$

and let

$$A_n = \frac{\exp[\frac{\Delta^o G_n}{RT} + \varepsilon_{1n}^L x_1^L]}{1+\varepsilon_{1n}^\gamma x_1^L \exp[\frac{\Delta^o G_1}{RT}]} \quad (11)$$

So that

$$x_1^\gamma = x_1^L A_1 \quad (12)$$

$$x_i^\gamma = x_i^L A_i \quad (13)$$

Next, substituting for x_1^γ and x_i^γ in (10) we obtain

$$1-x_1^L - \sum_2^n x_i^L = \{1-x_1^L A_1 - \sum_2^n x_i^L A_i\}$$

$$\cdot \exp[-\frac{\Delta^o G_o}{RT} - x_1^L A_1 \sum_2^n \varepsilon_{1i}^\gamma x_i^\gamma A_i + x_1^L \sum_2^n \varepsilon_{1i}^L x_i^L - \frac{\varepsilon_{11}^\gamma}{2}(x_1^L A_1)^2 + \frac{\varepsilon_{11}^L}{2}(x_1^L)^2] \quad (14)$$

Now carrying out a first order expansion about the iron carbon line, $T = T_o$, of the quantities $\exp[\frac{\Delta^o G_{o,1}}{RT}]$ in the leading term on the right hand side of (14) (all other temperature-dependent terms appear in higher orders) we obtain

$$\exp\left[\frac{\Delta^o G(T)}{RT}\right] = \exp\left[-\frac{\Delta^o S}{R}\right] \exp\left[\frac{\Delta^o H}{RT_o(1+\frac{\Delta T}{T_o})}\right] = \left(1-\frac{\Delta^o H \Delta T}{RT_o^2}\right) \exp\left[\frac{\Delta^o G}{RT_o}\right] \qquad (15)$$

Following these substitutions we can set all the remaining $A_{1,i}(T) = A^o_{1,i}(T_o) = A^o_{1,i}$. As a subsidiary relation we can evaluate equation (9) at the limit of the Fe-C phase diagram ($x_i=0$; $T=T_o$), viz.,

$$1-x_1^L = \{1-x_1^L A_1^o\} \exp\left[-\frac{\Delta^o G_o}{RT_o} - \frac{\varepsilon_{11}^\gamma}{2}(x_1^L A_1^o)^2 + \frac{\varepsilon_{11}^L}{2}(x_1^L)^2\right] \qquad (16)$$

Next, discarding higher order terms of the type $x_i\Delta T$, $x_i x_j$, (14) becomes

$$1-x_1^L - \sum_2^n x_i = \{1-(1-\frac{\Delta^o H_1 \Delta T}{RT_o^2})\, x_1^L A_1^o - \sum_2^n x_i^L A_i^o\}\, (1+\frac{\Delta^o H_o \Delta T}{RT_o^2})$$

$$\cdot \exp\left[-\frac{\Delta^o G_o}{RT_o} - x_1^L A_1^o \sum_2^n \varepsilon_{1i}^\gamma x_i A_i^o + x_1^L \sum_2^n \varepsilon_{1i}^L x_i^L - \varepsilon_{\frac{11}{2}}^\gamma (x_1^L A_1^o)^2 + \varepsilon_{\frac{11}{2}}^L (x_1^L)^2\right] \qquad (17)$$

Now since the quantity $\left|-x_1^L A_1^o \sum_2^n \varepsilon_{1i}^\gamma x_i A_i^o + x_1^L \sum_2^n \varepsilon_{1i}^L x_i^L\right| \ll 1$ the exponential on the right can be expanded to yield

$$1-x_1^L - \sum_2^n x_i = \{1-(1-\frac{\Delta^o H_1 \Delta T}{RT_o^2}) x_1^L A_1^o - \sum_2^n x_i^L A_i^o\}$$

$$\cdot\{1+(\frac{\Delta^o H_o \Delta T}{RT_o^2} - x_1^L A_1^o \sum_2^n \varepsilon_{1i}^\gamma x_i A_i^o + x_1^L \sum_2^n \varepsilon_{1i}^L x_i^L)\}$$

$$\cdot \exp\left[-\frac{\Delta^o G_o}{RT_o^2} - \varepsilon_{\frac{11}{2}}^\gamma (x_1^L A_1^o)^2 + \varepsilon_{\frac{11}{2}} (x_1^L)^2\right] \qquad (18)$$

Again since the quantity $\left|\frac{\Delta^o H_o \Delta T}{RT_o^2} - x_1^L A_1^o \sum_2^n \varepsilon_{1i}^\gamma x_i A_i^o + x_1^L \sum_2^n \varepsilon_{1i}^L x_i^L\right| \ll 1$, we can rearrange between the left and right hand sides using the binomial theorem to obtain

$$\{1-\frac{\Delta^o H_o \Delta T}{RT_o^2}+x_1 A_1^o \sum_2^n \epsilon_{1i}^{\gamma} x_i A_i^o - x_1^L \sum_2^n \epsilon_{1i}^L x_i^L - x_1^L + x_1^L \frac{\Delta^o H_o \Delta T}{RT_o^2} - \sum_2^n x_1^L + (x_1^L)^2 \sum_2^n \epsilon_{1i}^L x_i^L$$

$$-(x_1^L)^2 A_1^o \sum_2^n \epsilon_{1i}^{\gamma} x_i A_i^o\} \exp[\frac{\Delta^o G_o}{RT_o} + \frac{\epsilon_{11}^{\gamma}}{2}(x_1^L A_1^o)^2 - \frac{\epsilon_{11}^L}{2}(x_1^L)^2]$$

$$= \{1-x_1^L A_1^o + x_1^L A_1^o \frac{\Delta^o H_1 \Delta T}{RT_o^2} - \sum_2^n x_i^L A_i^o\} \qquad (19)$$

But from (16)

$$(1-x_1^L A_1) = (1-x_1^L) \exp[\frac{\Delta^o G_o}{RT_o} + \frac{\epsilon_{11}^{\gamma}}{2}(x_1^L A_1)^2 - \frac{\epsilon_{11}^L}{2}(x_1^L)^2] \qquad (20)$$

Substituting in (19) and rearranging gives

$$\sum_2^n x_i^L A_i^o + \{x_1^L A_1^o \sum_2^n \epsilon_{1i}^{\gamma} x_i^L A_i^o - x_1^L \sum_2^n \epsilon_{1i}^L x_1^L - \sum_2^n x_i^L + (x_1^L)^2 \sum_2^n \epsilon_{1i}^L x_i^L - (x_1^L)^2 A_1^o \sum_2^n \epsilon_{1i}^{\gamma} A_i^o x_i\}$$

$$\cdot \exp[\frac{\Delta^o G_o}{RT_o} + \frac{\epsilon_{11}^{\gamma}}{2}(x_1^L A_1^o)^2 - \frac{\epsilon_{11}^L}{2}(x_1^L)^2]$$

$$= x_1^L A_1 \frac{\Delta^o H_1 \Delta T}{RT_o^2} + (1-x_1^L) \frac{\Delta^o H_o \Delta T}{RT_o^2} \exp[\frac{\Delta^o G_o}{RT_o^2} + \frac{\epsilon_{11}^{\gamma}}{2}(x_1^L A_1^o)^2 - \frac{\epsilon_{11}^L}{2}(x_1^L)^2] \qquad (21)$$

Solving for ΔT and rearranging to obtain the x_i^L's as common factors yields finally

$$\Delta T = RT_o^2 \sum_{i=2}^n \Lambda_i x_i^L$$

where

$$A_i = \frac{[A_i^o - \{1+x_1^L(1-x_1^L)(\epsilon_{1i}^L - \epsilon_{1i}^{\gamma} A_1^o A_i^o)\} \exp\{\frac{\Delta^o G_o}{RT_o} - \frac{(x_1^L)^2}{2}(\epsilon_{1i}^L - \epsilon_{1i}^{\gamma} A_i^{o2})\}]}{x_1^L \Delta^o H_1^o A_1^o + (1-x_1^L)\Delta^o H_o \exp\{\frac{\Delta^o G_o}{RT_o} - \frac{(x_1^L)^2}{2}(\epsilon_{1i}^L - \epsilon_{1i}^{\gamma} A_i^{o2})} \qquad (22)$$

Other than the Wagner expansions we have made no approximations in the carbon variables, $x_1^{\gamma,L}$. If we assume, as is likely, that the empirical determinations of the linear coefficients in the Wagner expansions are actually averages over linear and quadratic effects then we are justified in retaining the quadratic carbon terms in (22). These are marginally

significant for carbon concentrations above the eutectoid.

APPENDIX 2

To derive the metal(I)-carbide(II) correction formula we proceed from the Gibbs-Duhem equation. At constant T and P we have

$$X_o^I d\mu_o + X_1^I d\mu_1 + \sum_2^n X_i^I d\mu_i = 0 \qquad (1)$$

and

$$X_o^{II} d\mu_o + X_1^{II} d\mu_1 + \sum_2^n X_i^{II}\, d\mu_i = 0 \qquad (2)$$

Since $\sum_o^n X_i = 1$ we can subtract and rearrange to obtain

$$(X_1^{II}-X_1^I)(d\mu_1-d\mu_o) + \sum_2^n (X_i^{II}-X_i^I)(d\mu_i-d\mu_o) = 0 \qquad (3)$$

Now using the Wagner expansions with reference states at infinite dilution we have

$$\frac{d\mu_o}{RT} = -\sum_{i=2} dX_i - dX_1 \qquad (4)$$

$$\frac{d\mu_1}{RT} = \frac{dX_1}{X_1} + \epsilon_{11} dX_1 + \sum_{i=2}^n \epsilon_{1i} dX_i \qquad (5)$$

and

$$\frac{d\mu_i}{RT} = \frac{dX_i}{X_i} + \epsilon_{1i} dX_1 + \sum_{k=2}^n \epsilon_{ik}^I dX_k \qquad (6)$$

Substituting into (3), dropping the superscript I and letting all $X_i \to 0$ yields

$$\left\{ \frac{X_1^{II}}{X_1} - 1 + (X_1^{II}-X_1)(1+\epsilon_{11}) \right\} dX_1 + \sum_{i=2}^n \{k_1 - 1 + (1+\epsilon_{i1})(X_1^{II}-X_1)\} dX_i = 0 \qquad (7)$$

Noting that we are seeking a limiting solution wherein ΔX_1 is linear in the X_i we can integrate (7) in the limiting approximation that

$$X_1^{II} - X_1 = X_1^{II} - X_1^c \qquad (8)$$

where X_1^c is the plain carbon limit of the integral. Thus

$$X_1^{II} \ln \frac{X_1}{X_1^c} + \{(X_1^{II}-X_1^c)(1+\epsilon_{11}) - 1\}(X_1 - X_1^c) = -\sum_{i=2}^n \{k_i - 1 + (1+\epsilon_{i1})(X_1^{II}-X_1^c)\} X_i \qquad (9)$$

Letting $X_1 = X_1^c + (X_1 - X_1^c)$ and expanding the logarithm we obtain

$$\Delta X_1 = X_1 - X_1^c = - \frac{X_1^c \sum_{i=2}^{n} X_i \{k_i - 1 + (1+\epsilon_{i1})(X_1^{II} - X_1^c)\}}{X_1^{II} + X_1^c \{(X_1^{II} - X_1^c)(1+\epsilon_{11}) - 1\}} \qquad (10)$$

APPENDIX III

At the T_o temperature:

$$G_i^I = G_i^2 \tag{1}$$

$$x_1^I = x_1^{II} \tag{2}$$

which for the binary gives:

$$x_1^I \mu_1 + x_o^I \mu_2 = x_1^{II} \mu_1^{II} + x_o^{II} \mu_o^{II} \tag{3}$$

but since $x_1^I = x_1^{II}$:

$$x_1^I(\mu_1^I - \mu_1^{II}) + x_o^I(\mu_o^I - \mu_o^{II}) = 0 \tag{4}$$

Therefore:

$$x_1^I\left(\frac{\Delta^o G_1^{I\to II}}{RT}\right) + x_o^I\left(\frac{\Delta^o G_o^{I\to II}}{RT}\right) = 0 \tag{5}$$

Similarly, for a multicomponent system:

$$x_1^I\left(\frac{\Delta^o G_1}{RT}\right) + x_o^I\left(\frac{\Delta G_o^o}{RT}\right) + \sum_2^n \left(\frac{\Delta^o G_i}{RT}\right) = 0 \tag{6}$$

At $T = T_o$, for the binary Fe-C system:

$$x_1^I\left(\frac{\Delta G_1^o(T_o)}{RT_o}\right) + x_o^I\left(\frac{\Delta G_o^o(T_o)}{RT_o}\right) = 0 \qquad (7)$$

Expanding $\frac{\Delta G_i^o}{RT}$ about $T = T_o$:

$$\frac{\Delta^o G(T)}{RT} = \frac{\Delta^o G(T_o)}{RT_o} - \frac{\Delta^o H}{RT_o^2}\Delta T \qquad (8)$$

Substituting (8) into (6) and subtracting (7) yields:

$$-x_1^I\frac{\Delta^o H_1 \Delta T}{RT_o^2} + x_o^I\frac{\Delta^o H_o \Delta T}{RT_o^2} = \sum_2^n\left\{x_i^I\frac{\Delta^o G_i}{RT_o} - x_i^I\frac{\Delta T \Delta H_1^o}{RT_o^2}\right\} \qquad (9)$$

Since, in the dilute limit terms of order $x_i\Delta T$ are negligable:

$$\frac{\Delta T}{RT_o^2}(x_1^I\Delta^o H_1 + x_o^I\Delta^o H_o) = \frac{1}{RT_o}\sum_2^n x_i^I\Delta^o G_i \qquad (10)$$

Thus, in the binary limit, $\sum_2^n x_1 \to 0$, $x_o = 1-x_1$ and

$$\Delta T = \frac{1}{RT_o}\sum_2^n \frac{x_i^1\Delta^o G_i^{I\to II}}{x_1^I\Delta^o H_1 + (1-x_1)\Delta^o H_o} \qquad (11)$$

where T_o is for the binary Fe-C phase diagram. It can be seen, that upon the addition of alloying elements, for dilute alloys that

$$T_o^{alloy} = T_o\{\ 1 + \frac{1}{RT_o^2} \sum_{2}^{n} \frac{x_i^I \Delta^o G_i^{I \rightarrow II}}{x_1^I \Delta^o H_1 + (1-x_1^I)\Delta^o H_o}\ \} \qquad (12)$$

APPENDIX IV

If an alloying element i, is added to an Fe-C binary alloy, the result is to shift the Ae_3 line.

Now at any amount of i added:

$x^x = x_c + \Delta x_1$ where x_c is for the Fe-C binary at T

$T^x = T + \Delta T$ where T_c is for the Fe-C binary at x_c

If m_g is the slope of the Ae_3 $(\alpha+\gamma/\gamma)$ line, it is obvious from the diagram (Fig. L) that

$$x^x = x_c + \frac{\Delta T}{m_g}$$

This means that at any temperature T and amount of alloy addition i, that it is possible to calculate the corresponding shift in x_i. Thus, the coordinates of the $\alpha+\gamma/\gamma$ phase boundary at temperature T and any amount x_i will be in the form:

$$P = P(x_c + \frac{\Delta T}{m_g}, x_i).$$

where ΔT is a function x_i of the previously mentioned type:

$$\Delta T = RT_o^2 \sum_{i=2}^{n} A_i x_i$$

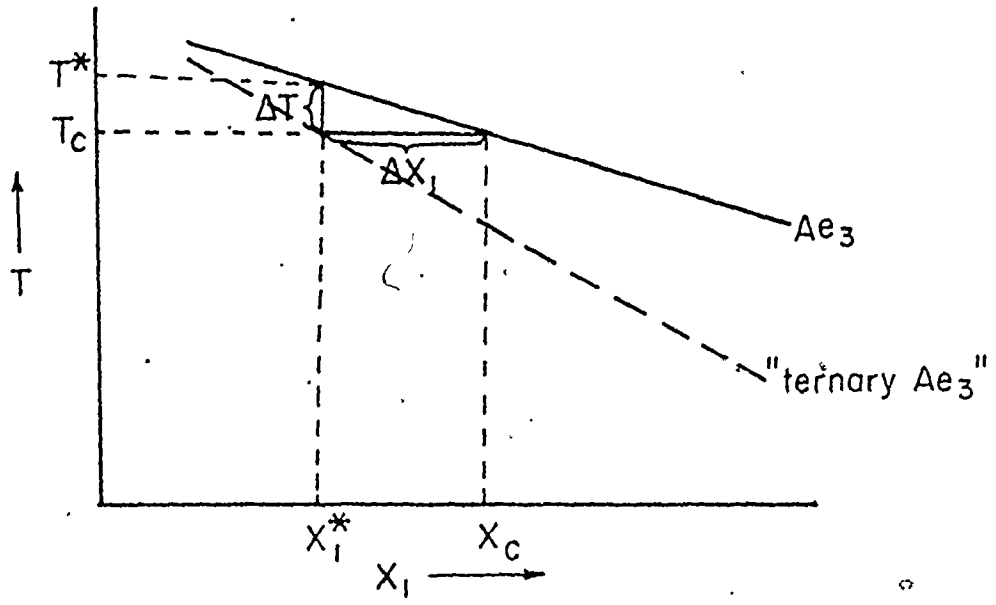

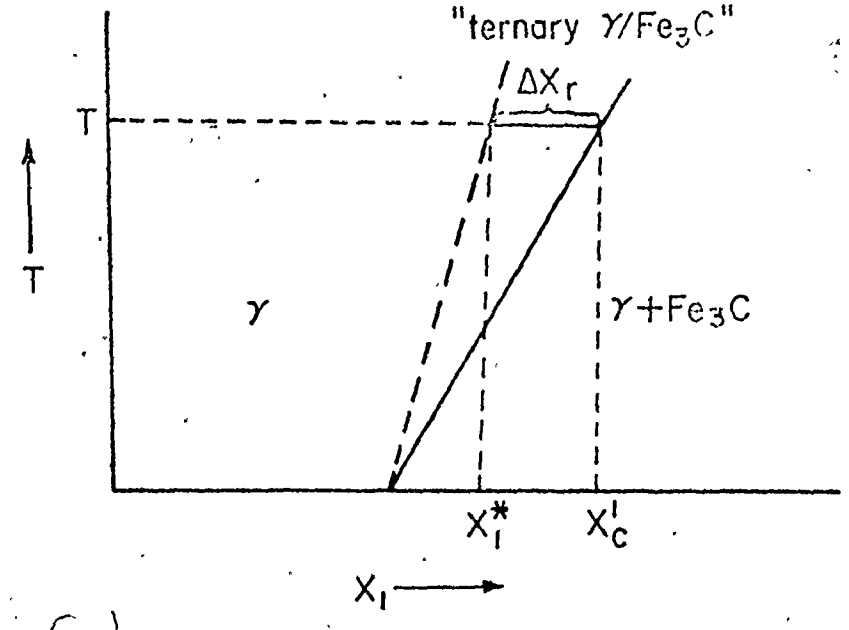

Figure 38 Schematic of deviation of Ae_3 and carbide lines with addition of alloying elements

Similarly, for the carbide line

$$x^* = x_c^1 + \Delta x_1$$

where x_c^1 is the $\gamma/\gamma+Fe_3C$ phase limit in the binary Fe-C system. The coordinates of any point on the isothermal diagram (Fig.J) is thus

$$P = P(x_c^1 + \Delta x_1, x_i)$$

In the same manner it is possible to solve for the intersection of these two points, to calculate the temperature and composition of the eutectic.

Let

GAMMA = $\alpha+\gamma/\gamma$ phase boundary

CARBIDE = $\gamma/\gamma+Fe_3C$ phase boundary

Now, at x_i = constant, the eutectic point lies on the intersection of the two planes, LM at P.

Now, if m_g is the slope of the Ae_3 line (FG) and m_c is the slope of the carbide line (RS) both at the binary eutectic, the transformation to move L' to P is:

$$P = L + \Delta T + \Delta X$$

Now, projecting back to the T-x_1 axis:

$$x_1^* = x_E + \frac{T^*-T_E}{m_c} + \Delta x_1$$

and $$T^* = T_E + (x_1^*-x_E) \cdot m_g + \Delta T$$

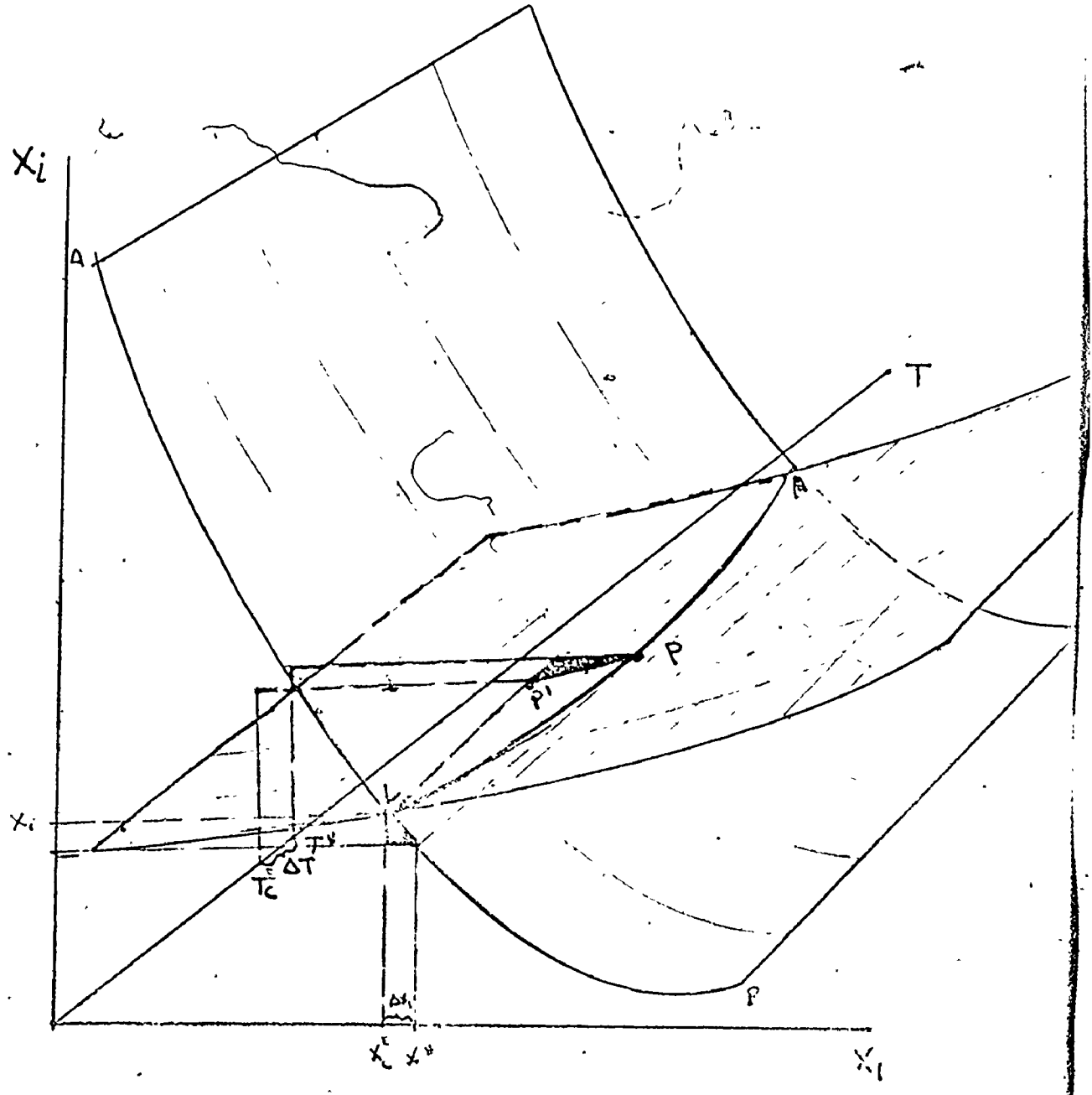

Figure 39 Schematic of multicomponent eutectoid intersection

Hence, at the eutectic, generalizing over all i:

$$x_1^* = \frac{x_E\left(1-\frac{m_g}{m_c}\right) + \frac{\Delta T}{m_c} + \Delta T x_1}{1 - \frac{m_g}{m_c}}$$

and $$T^* = \frac{T_E\left(1 - \frac{m_g}{m_c}\right) + \Delta T + m_g \Delta x_1}{1 - \frac{m_g}{m_c}}$$

APPENDIX V

Program for Calculating Isothermal Quasi-ternary Multicomponent phase diagrams

Variable List

Variables

I,K,KL,M,N	:	indices
CSTORE,DEN,REP1,S, TEST,VIN,VVK,XD,XP, YD,YP,ZA,ZB,ZC,SLOPE ZLS,ZRS	:	dummary variables
J1,J2,J3,J4,J5, NOB, IIM, XNUM	:	counters
A,B,O	:	coefficients of quadratic to be solved
CARK	:	holds γ/cementite partition coefficients of all elements
DT	:	temperature change from Fe-C binary
DTC	:	carbide line temperature of alloy
DTE	:	Ae_3 temperature of alloy
DI	:	slope of Ae_3 line at temperature
GFE	:	$\Delta^o G_o^{\alpha\rightarrow\gamma}$
HC	:	$\Delta^o H_1^{\alpha\rightarrow\gamma}$
Height	:	height of characters to be plotted
HFE	:	$\Delta^o H_o^{\alpha\rightarrow\gamma}$
IER,IERR	:	error messages that equal zero if subroutines operate properly
NUMPLT	:	number of separate phase diagrams to be plotted

Q	:	number of the ternary alloying element to be plotted
R	:	gas constant
SA	:	partition coefficient in calculations
SIGSQ	:	sum of squares of deviations from fitted quadratic
TDGM	:	temperature of isotherm
THETA	:	angle of characters to be plotted
TO	:	temperature from empirical Fe-C phase diagram
XCNEW	:	composition of carbon of carbide line in alloy in mole fraction
XSOL, XSO1X	:	carbon composition in mole fraction of $\alpha/\alpha+\gamma$ boundary
XWCAR	:	carbon composition of carbide line in wt.pct.
ZLG	:	complex, larger root of quadratic containing eutectoid carbon composition in mole fraction
ZLC	:	complex, smaller root of quadratic containing eutectoid carbon composition

Arrays

BX,BZ,C,DXC,WA,WC XWT,Y	:	dummy or working arrays
D,E,F,P,U	:	dummary arrays holding calculated points for curve fitting
W1,W2,W3	:	dummy arrays holding calculated points in wt.pct.
EA	:	gamma phase interaction parameters
EB	:	alpha phase interaction parameters
G	:	$\Delta^{o}G_{i}^{\alpha\rightarrow\gamma}$ data

POLY	:	coefficients of quadratic for Ae_3 line
SARRAY	:	coefficients of quadratic for carbide line
VALP	:	α/γ partition coefficients for all elements
WT	:	composition of elements in wt.pct.
X	:	composition of elements in mole fraction
XW	:	molecular weights of alloying elements
T,V	:	Tabulated $\Delta^{o}G_{o}^{\alpha\rightarrow\gamma}$ data; T(I) holds the temperature and V(I) the $\Delta^{o}G_{o}^{\alpha\rightarrow\gamma}$ value at that temperature

Results: This program, as written was used to calculate and plot the following isothermal phase diagrams:

Fe-Si-C at 973 and 1073 K

Fe-Mn-C at 973, 1035, 1073 and 1173 K

Fe-Ni-C at 973, 1073 and 1173 K

Fe-Cr-C at 1023, 1043, 1073 and 1173 K

Fe-Cu-C at 1023, 1073 and 1173 K

```
C*************************************************************************
      PROGRAM TST(INPUT,OUTPUT,TAPE5=INPUT,TAPE6=OUTPUT)
C
CCCCCCCCCCCCCCCCCCCCCCCCCCCCCCCCCCCCCCCCCCCCCCCCCCCCCCCCCCCCCCCCCCCCCCCCC
C
C     THIS PROGRAM CALCULATES DIRECTLY , ISOTHERMAL PHASE
C     DIAGRAMS OF THE TYPE : FE-C-X-X-X-..., WHERE X IS ONE OF
C     MN,SI,NI,CR,MO,CU,W,V,NB,CO ; OR ANY COMBINATION OF THESE .
C     THE PLOT ROUTINES ARE DESIGNED FOR A BENSON-LEHNER PLOTTER
C     ACCESSED BY A TAPE WRITTEN BY A CDC-6400 COMPUTER . THE
C     ELEMENT TO BE INCREMENTED ALONG THE ORDINATE IS SPECIFIED
C     BY READING IN THE APPROPIATE ELEMENT NUMBER (CALLED Q) .
C      THE REST OF THE ELEMENTS WHICH ARE HELD CONSTANT IN THE
C      CALCULATIONS , ARE READ IN FROM A SINGLE CARD (I.E. WT%)
C     AS IF IT WERE A SINGLE STEEL COMPOSITION BEING ENTERED .
C
C
C       Q=THE NUMBER OF THE ELEMENT TO BE INCREMENTED
C
C      TDGM=THE TEMPERATURE OF THE ISOTHERM REQUIRED
C
C     WT(I)=THE AMOUNT OF ELEMENT I IN WT%
C
C      X(I)=THE AMOUNT OF ELEMENT I IN MOLE FRACTION . THIS
C           IS CALCULATED IN THE PROGRAM AND IS CALLED P(I) FOR
C         THE CARBIDE PHASE .
C
C
C      THE PHASE DIAGRAM IS PLOTTED IN MOLE FRACTION AND THE
C     THREE PHASE REGION IS PLOTTED IF THERE IS A SINGLE THREE
C     PHASE FIELD INTERSECTION IN THE REGION . THIS IS DETERMINED
C     BY FITTING THE GAMMA-CARBIDE AND ALPHA-GAMMA PHASE BOUNDARIES
C     WITH QUADRATICS AND FINDING THEIR INTERSECTION. IF NONE
C     EXISTS THEN THE PHASE REGION CONTAINS NO THREE PHASE TRIANGLE .
C
CCCCCCCCCCCCCCCCCCCCCCCCCCCCCCCCCCCCCCCCCCCCCCCCCCCCCCCCCCCCCCCCCCCCCCCCC
C
      DIMENSION D(200), E(200), F(200), U(200), Z(200), WA(8), C(2)
      DIMENSION X(11), WT(11), XW(11), XNUM(11)
      DIMENSION Y(11), DXC(11), BZ(11), BX(11), WK(600)
      DIMENSION XWT(11), WC(12), BCD(2), W(200), O(11)
      DIMENSION POLY(3), SARRAY(3), P(11)
      DIMENSION W1(200), W2(200), W3(200)
      COMMON /DELG/ G(11),EA(11),EB(11),GFE
      COMMON /TTY/ SA
      COMMON /SSQ/ T(100),V(100)
C     COMMON BLOCK SSQ HOLDS HARVIGS DELTA G-O DATA FOR ALPHA
C     GAMMA FOR  INTERPOLATION USE .
      COMMON /AGPAR/ VALP(11)
      COMMON /XKVAL/ CARK(11)
      COMMON /DTEMP/ TDGM
      COMMON /ACSLP/ D1
      COMPLEX ZSM,ZLG
      INTEGER Q
```

```
      REP1=0.01
      M=94
      NOB=75
      R=1.987
C
CCC    XW CONTAINS THE MOLECULAR WEIGHTS OF THE ELEMENTS
C
      XW(1)=12.011
      XW(2)=54.938
      XW(3)=28.086
      XW(4)=58.71
      XW(5)=51.996
      XW(6)=95.94
      XW(7)=63.54
      XW(8)=183.85
      XW(9)=50.942
      XW(10)=92.906
      XW(11)=58.933
C
CC     READ IN THE DELTA G DATA , THE ELEMENT AND TEMPERATURE REQUIRED
C.
      DO 101 K=1,M
      READ (5,115) T(K),V(K)
101   CONTINUE
      READ (5,116) NUMPLT
      DO 114 IIM=1,NUMPLT
      TSUM=0.0
      J1=J2=J3=0
      READ (5,117) Q,TDGM
C
CC     READ IN THE CONSTANT COMPOSITIONS IN WT. PCT.
C
      READ (5,118) (WT(I),I=1,11)
      WRITE (6,119) Q
      WRITE (6,125)
C
CCC    DRAW THE GRID OUTLINE
C
      CALL GRID (Q)
      WT(Q)=0.0
C
CCC    START TO CALCULATE THE POINTS TO BE PLOTTED
C
      DO 106 KL=1,40
      WT(Q)=WT(Q)+0.10
      W1(KL)=WT(Q)
      XCNEW=1.5
      DTC=50.
      XWT(1)=0.0
C
CCC    CARLIN CALCULATES THE CARBIDE LINE
C
      CALL CARLIN (XW,P,WT,XWT,DTC,XCNEW)
      XWCAR=XWT(1)
      W3(KL)=XWCAR
C
CCCC   TAG CALCULATES THE IRON DATA NEEDED FOR THE TEMPERATURE CHANGE
CCCC   CALCULATIONS
C
      CALL TAG (XW,WT,X,TO,GFE,HC,HFE)
```

```
C
CCC     GAG CALCULATES THE DELTA G AND INTERACTION PARAMETERS NEEDED
C
        CALL GAG (TO)
C
CCC     CALCT DOES THE TEMPERATURE CALCULATIONS
C
        CALL CALCT (TO,X,HC,HFE,DT)
        DTE=DT+TO
        XSOL=X(1)*SA
        J3=J3+1
C
CCC     CALCULATE AND LOOT THE ALPHA/ALPHA+GAMMA BOUNDARY
C
        N=J3
        XSOLX=XSOL
        CALL CHANGE (XSOLX,XW,X,XWT)
        VVT=VALP(C)
        IF (REP1.LT.C.C1) XSOLX=C.C
        D(N)=XSOLX
        XD=XSOLX
        YD=X(C)*VALP(C)
        XD=)D*100
        YD=YD*10C
        IF (REP1.LT.C.01) GO TO 102
        CALL UNITTO (XD,YD,XP,YP)
        CALL GRAF (XP,YP,0.J25,9)
102     CONTINUE
C
CCC     CALCULATE AND PLOT THE AE3 LINE. THE CALCULATIONS MUST BE DONE
        IN WT. PCT. THEN CONVERTED TC MOLE FRACTION
C
        REP1=WT(1)+(TO-DTE)/D1
        IF (REP1.LT.C.C1) REP1=J.J
        WT(1)=REP1
        W2(N)=REP1
        A=1 C).
C       CONVERT WT. PCT. TO ATCN FRACTION
        DEN=(A-WT(1)-WT(2)-WT(3)-WT(4)-WT(5)-WT(6)-WT(7)-WT(8)-WT(9)-WT(10
       1)-WT(11))/55.847+WT(1)/XW(1)+WT(2)/XW(2)+WT(3)/XW(3)+WT(4)/XW(4)+W
       2T(5)/XW(5)+WT(6)/XW(6)+WT(7)/XW(7)+WT(8)/XW(8)+WT(9)/XW(9)+WT(1C)/
       3XW(10)+WT(11)/XW(11)
        DO 103 I=1,11
        X(I)=(WT(I)/XW(I))/DEN
103     CONTINUE
        IF (REP1.LT.C.01) X(1)=C.C
        XD=)(1)
        F(N)=XD
        YD=X(J)
        E(N)=YD
        XD=)D*100
        YD=YD*10C
        IF (REP1.LT.C.C1) GO TO 104
        CALL UNITTO (XD,YD,XP,YP)
        CALL GRAF (XP,YP,0.J25,9)
104     CONTINUE
C
CCC     PLOT THE CARBIDE POINTS
C
        J1=J1+1
```

```
      IF (ABS(DTC-TDGM).GE.1.0) GO TO 105
      J2=J2+1
      M=J2
      VVK=CARK(Q)
      XO=XCNEW
      Z(M)=XCNEW
      YO=P(Q)
      U(M)=P(Q)
      XO=XO*100
      YO=YO*100
      CALL UNITTO (XO,YO,XP,YP)
      CALL GRAF (XP,YP,0.025,1)
105   CONTINUE
C
CC    WRITE THE VALUES PLOTTED IN WEIGHT PCT.
C
      WRITE (6,121) W1(KL),W2(N),W3(KL),TDGM
C
CC    CALCULATE THE EUTECTOID, IF ONE EXISTS
C
      TSUM=TSUM+W2(N)
106   CONTINUE
      IF (TSUM.EQ.0.0) GO TO 113
      IF (Q.EQ.4) GO TO 107
      IF (TDGM.LE.1000.) GO TO 110
107   CONTINUE
      VALP(Q)=VVT
      CARK(Q)=VVK
      VIN=1/VALP(Q)
      WRITE (6,122) Q
      WRITE (6,123) VALP(Q),VIN
      WRITE (6,124) CARK(Q)
C
CC    FIT THE AE3 LINE
C
      W(1)=0.0
      CALL ORLSQ (F,E,W,4,2,WK,SIGSQ,POLY,IERR)
      WRITE (6,125) IERR
      SARRAY(1)=POLY(1)
      SARRAY(2)=POLY(2)
      SARRAY(3)=POLY(3)
C
CC    FIT THE CARBIDE LINE
C
      W(1)=0.0
      CALL ORLSQ (Z,U,W,4,2,WK,SIGSQ,POLY,IERR)
      WRITE (6,126) IERR
      WRITE (6,127) POLY(1),POLY(2),POLY(3),SARRAY(1),SARRAY(2),SARRAY(3
     1)
      A=POLY(1)-SARRAY(1)
      B=(POLY(2)-SARRAY(2))
      C=POLY(3)-SARRAY(3)
      WRITE (6,128) A,B,C
C
CC    SOLVE FOR INTERSECTION
C
      CALL ROOTS(A,B,C,ZLG,ZSM,IER)
      WRITE (6,129) IER
      ZLS=REAL(ZLG)
      ZRS=REAL(ZSM)
```

```
      WRITE (6,130) ZSM,ZLG
      TEST=B**2-A*C
      WRITE (6,131) TEST
      C(1)=ZRS
      C(2)=POLY(3)+POLY(2)*ZRS+POLY(1)*ZRS**2
      CSTORE=C(2)
      J4=0
      IF (C(1).LT.0.0115) GO TO 108
      IF (C(2).LE.0.0) GO TO 108
      IF (C(2).GE.0.06) GO TO 108
      IF (C(1).GE.0.06) GO TO 108
      J4=1
108   CONTINUE
C
CC    CALCULATE AND PLOT THREE PHASE TRIANGLE, IF ONE EXISTS
C
      C(1)=ZLS
      C(2)=POLY(3)+POLY(2)*ZLS+POLY(1)*ZLS**2
      J5=0
      IF (C(1).LT.0.0115) GO TO 109
      IF (C(2).LE.0.0) GO TO 109
      IF (C(1).GE.0.06) GO TO 109
      IF (C(2).GE.0.06) GO TO 109
      J5=1
109   IF (J4+J5.EQ.0) GO TO 112
      IF (J4+J5.EQ.2) GO TO 111
      IF (J4.EQ.1) C(1)=ZRS
      IF (J4.EQ.1) C(2)=CSTORE
      C(1)=C(1)*100.
      C(2)=C(2)*100.0
C     VALP(I) IS THE INVERSE A/G PART COEF FOR ELEMENT I .
      IF (M.GT.6) M=M-6
      D(M)=D(M)*100.
      ZA=VALP(Q)*C(2)
      CALL PLTLN (D(M),ZA,C(1),C(2))
      SLOPE=(CARK(Q)*C(2)-C(2))/(25-C(1))
      ZB=SLOPE*4.0-SLOPE*C(1)+C(2)
      CALL PLTLN (C(1),C(2),4.0,ZB)
      SLOPE=(CARK(Q)*C(2)-C(2))/(25-D(M))
      ZC=SLOPE*4.0-SLOPE*D(M)+ZA
      CALL PLTLN (D(M),ZA,4.0,ZC)
      IF (J4.EQ.1) C(2)=POLY(1)+POLY(2)*ZRS+POLY(3)*ZRS**2
110   CONTINUE
      GO TO 113
111   WRITE (6,132)
112   CONTINUE
113   CONTINUE
C
CC    WRITE NAME AND TEMPERATURE ON PLOT
C
      CALL PLTLET (7,0.325,0.0,3.5,6.2,7HTEMP. =)
      R=4.85
      S=6.2
      HEIGHT=0.325
      THETA=0.0
      ANUM=TOGM
      CALL NUMBER (R,S,HEIGHT,ANUM,THETA,6H(F5.0))
      CALL PLTLET (1,0.325,0.0,5.8,6.2,1HK)
      CALL PLTLET (9,0.75,90.0,-4.0,-2.0,9HB THOMSON)
      CALL PLOT (35.0,0.0,-3)
```

```
114     CONTINUE
        CALL PLOT (X,Y,999)
        STOP
C
115     FORMAT (F5.0,F7.3)
116     FORMAT (I2)
117     FORMAT (I3,F6.1)
118     FORMAT (11F5.0)
119     FORMAT (1H1,///,30X,13HELEMENT NO    ,I3)
120     FORMAT (///,10X,8H ELEMENT,20X,6H  GAMMA ,20X8H CARBIDE,20X,8H  TE
      1MP  ,//)
121     FORMAT (10X,F8.5,2(20X,F8.5),20X,F8.2)
122     FORMAT (1H1,/////,25X,*ELEMENT NO  *,I3)
123     FORMAT (///,10X,*G/A PART COEFF = *,F9.3,10X,*A/G PART COEFF = *,F
      19.3)
124     FORMAT (///,10X,*G/FE3C PART COEFF = *,F9.3,///)
125     FORMAT (//,10X,*IERR = *,I2)
126     FORMAT (//,10X,*IERR = *,I2)
127     FORMAT (//,10X,6F9.4)
128     FORMAT (///,10X,*A=*,F10.5,15X,*B= *,F10.5,15X,*C= *,F10.5)
129     FORMAT (///,10X,*IER = *,I2)
130     FORMAT (///,20X,*ZSH = *,F10.5,F10.5,15X,*ZLG = *,F10.5,F10.5)
131     FORMAT (//,10X,*DISCRIMINANT = *,F10.5)
132     FORMAT (////,15X,*TWO INTERSECTIONS IN REGION , POSSIBLE ERROR*)
        END
C*****************************************************************************
        SUBROUTINE GRID/(Q)
C
CC
C       DRAWS GRID AND WRITES APPROPRIATE CAPTIONS
C
C
        DIMENSION WC(7), Z(7), BCD(1)
        INTEGER Q
        CALL PLOT (X,Y,-20)
        XSCALE=0.5
        YSCALE=0.5
        CALL PLTIN (0.5,0.5,-5.0,-5.0,-5.0,11.0,-5.0,9.0)
        CALL PLTLN (0.0,0.0,7.0,0.0)
        CALL PLTLN (0.0,0.0,0.0,7.0)
        CALL PLTLN (0.0,7.0,7.0,7.0)
        CALL PLTLN (7.0,0.0,7.0,7.0)
        A1=1.0
        B1=0.0
        A2=1.0
        B2=0.2*YSCALE
        DO 1 I=1,6
        CALL PLTLN (A1,B1,A2,B2)
        A1=A1+1.0
        A2=A2+1.0
1       CONTINUE
        A1=0.0
        A2=0.2*XSCALE
        B1=1.0
        B2=1.0
        DO 2 I=1,6
        CALL PLTLN (A1,B1,A2,B2)
        B1=B1+1.0
```

```
      B2=B2+1.0
2     CONTINUE
      WC(1)=0.0
      Z(1)=0.0
      DO 3 I=2,7
      WC(I)=WC(I-1)+0.01
      Z(I)=WC(I)
3     CONTINUE
      R=-0.15
      S=-0.25
      THETA=0.0
      HEIGHT=0.25
      DO 4 I=1,7
      ANUM=WC(I)
      CALL NUMBER (R,S,HEIGHT,ANUM,THETA,6H(F4.2))
      R=R+1.0
4     CONTINUE
      R=-0.5
      S=-0.35
      THETA=0.0
      HEIGHT=0.25
      DO 5 I=1,7
      ANUM=Z(I)
      CALL NUMBER (R,S,HEIGHT,ANUM,THETA,6H(F4.2))
      S=S+1.0
5     CONTINUE
      IF (Q.EQ.2) CALL PLTLET (23,0.325,90.0,-1.0,1.70,23HMOLE FRACTION
     1MANGANESE)
      IF (Q.EQ.3) CALL PLTLET (23,0.325,90.0,-1.0,1.70,23HMOLE FRACTION
     1SILICON  )
      IF (Q.EQ.4) CALL PLTLET (23,0.325,90.0,-1.0,1.70,23HMOLE FRACTION
     1NICKEL   )
      IF (Q.EQ.5) CALL PLTLET (23,0.325,90.0,-1.0,1.70,23HMOLE FRACTION
     1CHROMIUM )
      IF (Q.EQ.6) CALL PLTLET (24,0.325,90.0,-1.0,1.70,24HMOLE FRACTION
     1MOLYBDENUM)
      IF (Q.EQ.7) CALL PLTLET (23,0.325,90.0,-1.0,1.70,23HMOLE FRACTION
     1COPPER   )
      IF (Q.EQ.8) CALL PLTLET (23,0.325,90.0,-1.0,1.70,23HMOLE FRACTION
     1TUNGSTEN )
      IF (Q.EQ.9) CALL PLTLET (23,0.325,90.0,-1.0,1.70,23HMOLE FRACTION
     1VANADIUM )
      IF (Q.EQ.10) CALL PLTLET (23,0.325,90.0,-1.0,1.70,23HMOLE FRACTION
     1 NIOBIUM  )
      IF (Q.EQ.11) CALL PLTLET (23,0.325,90.0,-1.0,1.70,23HMOLE FRACTION
     1 COBALT   )
      CALL PLTLET (20,0.325,0.0,1.83,-0.95,20HMOLE FRACTION CARBON)
      RETURN
      END
C*****************************************************************
      SUBROUTINE NUMBER (R,S,HEIGHT,ANUM,THETA,FMT)
C
CC    ENCODING SUBROUTINE FOR GRID
C
      DIMENSION BCD(1)
      ENCODE (10,FMT,BCD) ANUM
      CALL PLTLET (10,HEIGHT,THETA,R,S,BCD)
      RETURN
```

```
      END
C*****************************************************************************
      SUBROUTINE INTNUM (R,S,HEIGHT,INUM,THETA,FMT)
C
CC    ENCODING SUBROUTINE FOR GRID
C
      DIMENSION BCD(1)
      ENCODE (10,FMT,BCD) INUM
      CALL PLTLET (10,0.25,THETA,R,S,BCD)
      RETURN
      END
C*****************************************************************************
      SUBROUTINE TAG (XW,WT,X,TO,GFE,HC,HFE)
C
CCC
CCCCC
CC    CALCULATES THE POINTS FROM THE EMPIRICAL FE-C PHASE DIAGRAM ,
      THE DELTA G AND DELTA H DATA FOR IRON AND CARBON .
CC
C
      DIMENSION XW(11), WT(11), X(11)
      COMMON /SSQ/ T(100),V(100)
      COMMON /ACSLP/ C1
      COMMON /DTEMP/ TDGM
      REAL HC,HFE
      A=100.
C       CALCULATES TO
      C=0.765
      CT=1.0
      IF (TDGM.LT.1000.) GO TO 2
      DO 1 KKL=1,25
      D1=-150.3-216.0*(0.765-C)**3.26
      B1=1115.0-TDGM-150.3*C+216.0*(0.765-C)**4.26
      A1=C-B1/D1
      C=A1
      IF (ABS(C-CT).LT.0.0005) GO TO 4
      CT=A1
1     CONTINUE
      GO TO 4
2     DO 3 KLK=1,25
      D1=-108.46
      B1=1053.0-TDGM-108.46*C
      A1=C-B1/D1
      C=A1
      IF (ABS(C-CT).LT.0.0005) GO TO 4
      CT=A1
3     CONTINUE
4     D2=530.0-156.78*C
      WT(1)=C
      IF (C.GT.0.765) C=0.765
      TO=1115.-150.3*C+216.*((0.765-C)**4.26)
      IF (C.GT.0.765) TO=1053.-108.46*C
C       CONVERT WT. PCT. TO ATOM FRACTION
      DEN=(A-WT(1)-WT(2)-WT(3)-WT(4)-WT(5)-WT(6)-WT(7)-WT(8)-WT(9)-WT(10
     1)-WT(11))/55.847+WT(1)/XW(1)+WT(2)/XW(2)+WT(3)/XW(3)+WT(4)/XW(4)+W
     2T(5)/XW(5)+WT(6)/XW(6)+WT(7)/XW(7)+WT(8)/XW(8)+WT(9)/XW(9)+WT(10)/
     3XW(10)+WT(11)/XW(11)
```

```
      DO 5 I=1,11
      X(I)=(WT(I)/XW(I))/DEN
5     CONTINUE
C     CALCULATES DELTA G-O FOR FE
      K=INT((TO-800)/10+1)
      GFE=V(K)+(V(K+1)-V(K))*(T(K+1)-TO)/10
      HC=-15323
      TSAVE=TO
      IF (TO.LT.1000.) TO=1000.
      IF (O.GT.0.765) TO=1000.
      HFE=GFE+TC*(0.79-0.0046*(TO-1000.)**0.96)
      HFE=HFE+.058*COS(0.034*(TO-1000.0))*TO
      TO=TSAVE
      RETURN
      END
C*****************************************************************
      SUBROUTINE GAG (TO)
C
C
C     CALCULATES THE DELTA G AND INTERACTION PARAMETER DATA AT A GIVEN
C     TEMPERATURE FOR ELEMENTS 1 TO 11 .
C
C
      COMMON /DELG/ G(11),EA(11),EB(11),GFE
      T=TO
      G(1)=-15323+7.686*T
      G(2)=-26650+42.69*T-0.017*T**2
      G(2)=-5463+3.075*T
      G(3)=38.779*T-4.7244*T*ALOG(T)-5964.
      G(4)=-4545+3.233*T
      G(5)=-367-4.656*T+0.6568*T*ALOG(T)
      G(6)=565+0.15*T
      G(7)=-25500+41.183*T-0.017*T**2
      G(8)=2500-0.15*T
      G(9)=-9367+13.8*T-0.0051*T**2
      G(10)=-14.34+0.0013*(T-273)
      G(11)=0.0
      SA=1100/T
      EA(1)=8.1*SA
      EA(2)=-5070/T
      EA(3)=4.84+7370/T
      EA(4)=4635/T+0.557
      EA(5)=24.4-38400/T
      EA(6)=3.855-17370/T
      EA(7)=3.8*1273/T
      EA(8)=-4.*1323/T
      EA(9)=-19.4*1273/T
      EA(10)=-4.*1273/T
      EA(11)=2.3*1273/T
      DO 1 I=1,11
      EB(I)=0.0
1     CONTINUE
      RETURN
      END
C*****************************************************************
      SUBROUTINE CARLIN (XW,X,WT,XWT,DTC,XCNEW)
```

```
C
CCCCC
CCCCC
CC
      CALCULATES THE CARBON SHIFT FROM THE FE-C BINARY AT A GIVEN
      TEMPERATURE USING PARTITIONING DATA

      DIMENSION WK(11), DXC(11), XW(11), WT(11), X(11), XWT(11)
      DIMENSION Y(11), BX(11), BZ(11)
      COMMON /XKVAL/ CAPK(11)
      COMMON /DELG/ G(11),EA(11),EB(11),GFE
      COMMON /DTEMP/ TDGM
      CT=0.0
      C=0.765
      DO 1 I=1,25
      B1=641.3-TDGM+530*C-78.39*C**2
      D1=530.0-156.78*C
      A1=C-B1/D1
      C=A1
      IF (ABS(C-CT).LT.0.0005) GO TO 2
      CT=A1
1     CONTINUE
2     CONTINUE
      WT(1)=C
      TO=641.3+530*WT(1)-78.39*(WT(1)**2)
      IF (TO.LE.274.0) RETURN
      TT=TO-273.15
      CALL GAG (TO)
      A=100.
C      CONVERT WT. PCT. TO ATOM FRACTION
      DEN=(A-WT(1)-WT(2)-WT(3)-WT(4)-WT(5)-WT(6)-WT(7)-WT(8)-WT(9)-WT(10
     1)-WT(11))/55.847+WT(1)/XW(1)+WT(2)/XW(2)+WT(3)/XW(3)+WT(4)/XW(4)+W
     2T(5)/XW(5)+WT(6)/XW(6)+WT(7)/XW(7)+WT(8)/XW(8)+WT(9)/XW(9)+WT(10)/
     3XW(10)+WT(11)/XW(11)
      DO 3 I=1,11
      X(I)=(WT(I)/XW(I))/DEN
3     CONTINUE
      DO 4 I=1,11
      BZ(I)=WT(I)
      BX(I)=X(I)
      WK(I)=0.0
4     CONTINUE
      DXSUM=0.0
      DXC(1)=0.0
      A=100.0
C
CC    PARTITION COEFFICIENTS AS FUNCTIONS OF TEMPERATURE ,
CC    IN DEGREES CELSIUS .
C
      WK(2)=-0.00284*TO+5.44
      WK(3)=15.14
      WK(4)=0.0004*TO-0.249
      WK(5)=-22.76*ALOG(TT)+163.444
      WK(5)=WK(5)-2.0
      WK(6)=-16.9*ALOG(TT)+121.
      DO 5 I=2,11
      WT(I)=WK(I)*WT(I)
      DEN=(A-WT(1)-WT(2)-WT(3)-WT(4)-WT(5)-WT(6)-WT(7)-WT(8)-WT(9)-WT(10
     1)-WT(11))/55.847+WT(1)/XW(1)+WT(2)/XW(2)+WT(3)/XW(3)+WT(4)/XW(4)+W
     2T(5)/XW(5)+WT(6)/XW(6)+WT(7)/XW(7)+WT(8)/XW(8)+WT(9)/XW(9)+WT(10)/
     3XW(10)+WT(11)/XW(11)
```

```
      Y(I)=(WT(I)/XW(I)/DEN)
      IF (X(I).EQ.0.0) X(I)=1.0E-10
      XK=Y(I)/X(I)
      CARK(I)=XK
      DA=XK-1.0+(1+EA(I))*(0.25-X(1))
      DB=X(1)*((1.0+EA(1))*(0.25-X(1))-1.0)
      DXC(I)=-X(1)*X(I)*DA/(0.25+DB)
      DXSUM=DXSUM+DXC(I)
5     CONTINUE
      X(1)=BX(1)
      XCNEW=X(1)+DXSUM
      CALL CHANGE (XCNEW,XW,X,XWT)
C
CCC   XWT(1)  IS THE ACTUAL CARBON CONTENT IN WT. PCT.
CCC   XCNEW   IS THE ACTUAL CARBON CONTENT IN AT. PCT.
C
      DTC=TO
      DO 6 I=1,11
      WT(I)=BZ(I)
      X(I)=BX(I)
6     CONTINUE
      RETURN
      END
C*****************************************************************************
      SUBROUTINE CHANGE (XSOLX,XW,X,XWT)
C
CCC   CHANGES ALL VALUES FROM MOLE FRACTION TO WT. PCT.
C
      DIMENSION XW(11), X(11), XWT(11)
      DEN=(1-XSOLX-X(2)-X(3)-X(4)-X(5)-X(6)-X(7)-X(8)-X(9)-X(10)-X(11))*
     155.847+XSOLX*XW(1)+X(2)*XW(2)+X(3)*XW(3)+X(4)*XW(4)+X(5)*XW(5)+X(6
     2)*XW(6)+X(7)*XW(7)+X(8)*XW(8)+X(9)*XW(9)+X(10)*XW(10)+X(11)*XW(11)
      XP=100*XSOLX*XW(1)/DEN
      XWT(1)=XP
      DO 1 I=2,11
      XWT(I)=100*X(I)*XW(I)/DEN
1     CONTINUE
      RETURN
      END
C*****************************************************************************
      SUBROUTINE CALCT (TO,X,HC,HFE,DT)
C
CCC   CALCULATES TEMPERATURE DEVIATION FROM FE-C PHASE DIAGRAM
C
      COMMON /TTY/ SA
      DIMENSION X(11), XNUM(11)
      COMMON /DELG/ G(11),EA(11),EB(11),GFE
      COMMON /AGPAR/ VALP(11)
      REAL HC,HFE
C
CCC   CALCULATE NUMERATOR
C
      R=1.987
      RT=1.987*TO
```

```
      FC=G(1)
      XC=X(1)
      EC=EA(1)
      XNUM(1)=0.0
      SUMNUM=0.0
      SA=(EXP(FC/RT+EC*XC)/(1+EB(1)*XC*EXP(FC/RT)))
      PHIC=EXP(GFE/RT-((XC**2)/2.*(EC-EB(1)*SA**2)))
      GG=FC/RT
      DO 1 I=2,11
      F=G(I)
      E=EA(I)
      PA=EXP(F/RT+E*XC)/(1+EB(I)*XC*EXP(GG))
      VALF(I)=PA
C     CALCULATE I-TH TERM
      XNUM(I)=X(I)*(PA-(1+XC*(1-XC)*(E-EB(I)*SA*PA))*PHIC)
C     DOES SUMMATION OF NUMERATOR
      SUMNUM=SUMNUM+XNUM(I)
1     CONTINUE
CC
CC    CALCULATE DENOMINATOR
C
      DEN=(XC*HC*SA)+((1-XC)*HFE*PHIC)
C
CC    CALCULATE TEMPERATURE DIFFERENCE
C
      DT=R*(TO**2)*SUMNUM/DEN.
      RETURN
      END
C     C
C*****************************************************************

      SUBROUTINE OPLSQ (X,Y,W,N,M,WK,SIGSQ,POLY,IERR)
      DIMENSION X(1), Y(1), W(1), POLY(1), WK(1)
C
CC    X IS THE ARRAY OF ABSCISSAE AND Y THE ARRAY OF ORDINATES OF N
CC    W(1).EQ.0. IMPLIES UNIT WEIGHTS ARE TO BE USED. OTHERWISE W IS AN
CC    ARRAY OF WEIGHTS OF SIZE N.
CC    WK IS A WORK SPACE OF SIZE 3N.RESIDUALS ARE RETURNED IN WK(1..N)
CC    M IS THE DEGREE OF POLYNOMIAL TO BE FITTED.
CC    POLY IS AN ARRAY OF SIZE (M+1) AND RETURNS THE COEFFICIENTS OF X
CC    ORDERED FROM HIGHEST POWER TO LOWEST, POLY(M+1) IS CONSTANT TERM
CC    SIGSQ RETURNS THE SUM OF SQUARED DEVIATIONS.
CC    IERR IS INITIALLY SET TO 0.   IF THERE IS AN ILLEGAL VALUE OF M
CC       IERR IS SET TO 1 AND WE RETURN TO THE CALLING PROGRAM
CC    M MUST BE .GT.1 AND .LT.(N-1) AND .LE.15
C
      DIMENSION A(15), U(15), V(15)
      LOGICAL WP
C
CCC   WE USE WP TO SIGNAL WHICH SECTION (2-ND. OR 3-RD. BLOCK OF N WORDS
      C
CCC   OF WK) WHICH CURRENTLY CONTAINS P//M/(X(I)) AND WHICH P//M-1/(X(I
C
      IERR=0
      IF (((M.GT.1).AND.(M.LT.(N-1))).AND.(M.LE.15)) GO TO 1
      IERR=1
      RETURN
1     IF (W(1).EQ.0.) GO TO 3
      S=0.
```

```
C
CC      WE DENOTE  THE WEIGHTS IN WHAT FOLLOWS BY W(I)**2 EVEN THOUGH
CC      THEY CAME FROM THE ARRAY W(I).
C
        DO 2 I=1,N
        WK(I)=W(I)
        S=S+WK(I)
2       CONTINUE
        GO TO 5
3       DO 4 I=1,N
        WK(I)=1.
4       CONTINUE
        S=N
5       D0=S
C
CC      D0,D1 WILL BE USED FOR THE TWO DENOMINATOR TERMS D//M-2/ , D//M-1
CC      RESPECTIVELY
CC
CC      WE CALCULATE U(1)
C
        S=0.
        DO 6 I=1,N
        S=S+X(I)*WK(I)
6       CONTINUE
        T=S/D0
        U(1)=T
        WP=.FALSE.
C
CC      WE CALCULATE THE FIRST POLYNOMIAL EVALUATED AT THE ABSCISSAE IN
CC      THE THIRD BLOCK OF WK AND THE ZERO-TH ORDER POLY-L. IN THE 2-ND.
C
        K=N+N
        DO 7 I=1,N
        KI=K+I
        NI=N+I
        WK(KI)=X(I)-T
        WK(NI)=1.
7       CONTINUE
C
CC      WE EVALUATE V(1),D1,A(1),A(2)
C
        S=0.
        D1=0.
        T=0.
        TT=0.
        DO 8 I=1,N
        KI=K+I
        T1=WK(KI)
        T2=WK(I)
        T3=Y(I)*T2
        S=S+X(I)*T1*T2
        D1=D1+T1*T1*T2
        T=T+T3
        TT=TT+T3*T1
8       CONTINUE
        V(1)=S/D0
        A(1)=T/D0
        A(2)=TT/D1
C
C       WE NOW HAVE...
```

```
C       U1=(SIGMA(  X(I)*W(I)**2  ))/D0
C       D0=SIGMA(   W(I)**2   )
C       P//1/(X(I))=X(I)-U1
C       D1=SIGMA(   P//1/(X(I))**2 *  W(I)**2   )
C       V1=(SIGMA(  X(I)*P//1/(X(I))*W(I)**2  ))/D0
C       A0=(SIGMA(  Y(I)*W(I)**2   ))/D0
C       A1=(SIGMA(  Y(I)*P//1/(X(I))*W(I)**2  ))/D1
C
C       WE GO ON NOW TO THE GENERAL CASE
C
        DO 14 I=2,M
        IF (WP) GO TO 9
        IPP=N+N
        IP=N
        GO TO 10
9       IP=N
        IPP=N+N
C
C       IP IS THE INCREMENT TO BE ADDED TO J TO GET P//M-1/(X(J)),
C       WHILE (IPP+J) YIELDS P//M-2/ (X(J))
C       WE SHALL CALCULATE P//M/ AND OVERWRITE IT ON P//M-2/, REVERSING W
C
10      WP=.NOT.WP
C
C       U//I/=(SIGMA(  X(J)*P//I-1/(X(J))**2 * W(J)**2  ))/(D//I-1/)
        S=0.
        DO 11 J=1,N
        K=IPP+J
        S=S+X(J)*WK(K)*WK(K)*WK(J)
11      CONTINUE
        T=S/D1
        U(I)=T
        S=V(I-1)
C
C       P//I(X(J))=(X(J)-U//I/)*P//I-1/(X(J))-V//I-1/*P//I-2/(X(J))
C       OVERWRITE P//I-2/(X(J)) WITH IT
C
        DO 12 J=1,N
        K=IPP+J
        KI=IP+J
        WK(K)=WK(KI)*(X(J)-T)-WK(K)*S
12      CONTINUE
C
C       WE CALCULATE D//M/=SIGMA(P//M/(X(I))**2 * W(I)**2 ),
C       SHOWING D//M-1/ TO BE AND PLACING D//M/ IN D1
C       V//I/=(SIGMA(  X(J)*P//I/(X(J))*P//I-1/(X(J))*W(J)**2  ))/(D//I-1
C       A//I/=(SIGMA(  Y(J)*P//I/(X(J))*W(J)**2  ))/D//I/
C
        D0=D1
        D1=0.
        S=0.
        T=0.
        DO 13 J=1,N
        K=IPP+J
        KI=IP+J
        T1=WK(K)
        T2=WK(J)*T1
        D1=D1+T1*T2
        S=S+X(J)*WK(KI)*T2
```

```
      T=T+Y(J)*T2
   13 CONTINUE
      V(I)=S/D0
      A(I+1)=T/D1
   14 CONTINUE
C
C     WE HAVE NOW CALCULATED THE ARRAYS U,V, FROM 1 TO M AND
C     A FROM 0 TO M INDEXED 1 TO M+1
C     WE GO ON TO CALCULATE THE COEFFICIENTS OF THE POWERS OF X.
C
      M1=M+1
      WK(1)=1.
      WK(2)=-U(1)
      DO 15 I=2,M
      I1=I-1
      WK(I+1)=-U(I)*WK(I)-V(I1)*WK(I1)
   15 CONTINUE
      S=A(1)
      DO 16 I=2,M1
      S=S+A(I)*WK(I)
   16 CONTINUE
      POLY(M1)=S
      DO 20 I=2,M
      I1=I-1
      DO 17 K=1,M
      L=M1-K
      WK(L+1)=WK(L)
   17 CONTINUE
      WK(I1)=0.
      WK(I)=1.
      DO 18 J=I,M
      K=J-1
      L=K+2
      WK(L)=WK(L)-U(J)*WK(J)-V(K)*WK(K)
   18 CONTINUE
      S=0.
      MMMMM=M1-I1
      DO 19 J=I,M1
      S=S+A(J)*WK(J)
   19 CONTINUE
      POLY(MMMMM)=S
   20 CONTINUE
      POLY(1)=A(M1)
C
C     WE CALCULATE THE RESIDUALS AND SIGSQ
C
      WP=.TRUE.
      IF (W(1).EQ.0.) WP=.FALSE.
      SIGSQ=0.
      DO 23 I=1,N
      S=0.
      DO 21 J=1,M
      K=M1-J
      S=S+POLY(J)*(X(I)**K)
   21 CONTINUE
      T=S+POLY(M1)-Y(I)
      WK(I)=T
      IF (WP) GO TO 22
      SIGSQ=SIGSQ+T*T
      GO TO 23
```

```
22      SIGSQ=SIGSQ+T*T*W(I)
23      CONTINUE
        RETURN
        END
C       C
C*******************************************************************************

        SUBROUTINE ROOTS(A,B,C,ZSM,ZLG,IER)
        SUBROUTINE ROOTS(A,B,C,ZSM,ZLG,IER)
C
C       FIND ROOTS OF THE QUADRATIC EQUATION
C                                          A*X**2 + B*X + C = 0
C
        COMPLEX ZL,ZS,ZSM,ZLG
        DOUBLE PRECISION DIS,DISA
        BS=-B
        IPS=(ALOG(ABS(A))+ALOG(ABS(C))+DLOG(2.D))/(2*DLOG(2.D))
        SCALE=2.D**IPS
        DISA=DBLE(ABS(B))
        DIS=DISA+SCALE
        DIS=DIS-DISA
        IF(SNGL(DIS).EQ.0.0) GO TO 200
        B=0.0
        DIS=DISA+SCALE
        IF(SNGL(DIS).NE.0.0)    B=(BS/SCALE)*2.0
        A=A/SCALE
        C=C/SCALE
        DIS=DIS-SCALE
        DISC=DBLE(B)**2-DBLE(A)*DBLE(C)
        SQDIS=SQRT(ABS(DISC))
        IF(DISC.GT.0.0) GO TO 100
        ZL=CMPLX(B/A,ABS(SQDIS/A))
        ZS=CONJ(ZL)
        IER=1
        GO TO 300
100     B=SIGN(SQDIS,B)+B
200     ZS=CMPLX(C/B,0.0)
        ZL=CMPLX(B/A,0.0)
        IF(ABS(REAL(ZL)).LT.ABS(REAL(ZS))) ZS=-ZL
        IER=0
300     ZSM=ZS
        ZLG=ZL
        RETURN
        END
```

```
800.  217.3
 890. 204.1
 900. 191.1
 910. 178.3
 920. 166.6
 930. 154.1
 940. 142.4
 950. 131.0
 960. 119.9
 970. 109.3
 980. 99.3
 990.  89.6
1000.  80.80
1010.  72.18
1020.  64.16
```

1030.	56.75	
1040.	50.15	
1050.	44.31	
1060.	39.11	
1070.	34.41	
1080.	29.92	
1090.	26.07	
1100.	22.22	0.0
1110.	18.37	
1120.	14.92	
1130.	11.84	
1140.	9.10	
1150.	6.66	
1160.	4.48	
1170.	2.52	
1180.	0.74	
1190.	-0.89	
1200.	-2.40	
1210.	-3.82	
1220.	-5.15	
1230.	-6.39	
1240.	-7.55	
1250.	-8.63	
1260.	-9.63	
1270.	-10.55	
1280.	-11.40	
1290.	-12.17	
1300.	-12.87	
1310.	-13.50	
1320.	-14.06	
1330.	-14.54	
1340.	-14.95	
1350.	-15.29	
1360.	-15.57	
1370.	-15.79	
1380.	-15.95	
1390.	-16.06	
1400.	-16.10	
1410.	-16.10	
1420.	-16.06	
1430.	-15.97	
1440.	-15.83	
1450.	-15.64	
1460.	-15.40	
1470.	-15.11	
1480.	-14.77	
1490.	-14.33	
1500.	-13.95	
1510.	-13.48	
1520.	-12.97	
1530.	-12.41	
1540.	-11.83	
1550.	-11.15	
1560.	-10.45	
1570.	-9.71	
1580.	-9.92	
1590.	-8.98	
1600.	-7.60	
1610.	-6.67	
1620.	-5.30	

```
1630.  -4.28
1640.  -3.22
1650.  -2.11
1660.  -0.96
1670.   0.23
1680.   1.47
1690.   2.75
1700.   4.08
1710.   5.45
1720.   6.86
1730.   8.31
1740.   9.81
1750.  11.36
1760.  12.97
1770.  14.63
1780.  16.35
1790.  18.13
1800.  19.98
1810.  21.90
16
  3 973.
  3 1073.
  2  973.
  2 1035.
  2 1073.
  2 1173.
  4 973.
  4 1073.
  4 1173.
  5 1023.
  5 1043.
  5 1073.
  5 1173.
  7 1023.
  7 1073.
  7 1173.
```

APPENDIX VI

Program for Calculating Constant Composition Sections to the Fe-C Binary Phase Diagram

Variable List

Variables

I,JJ,K,KL,M, NOB	:	indices and counters
A,DEN,DTS,DTT, THELP,XD,XP,YD,YP	:	dummy variables
DT	:	dummy variable returned from CALCT containing the temperature difference
DTA	:	Predicted delta/liquid temperature
DTC	:	Predicted carbide temperature
DTE	:	Predicted Ae_3 temperature
DTG	:	Predicted gamma/liquid temperature
GFE	:	Dummy variable containing $\Delta^{o}G_{o}$
HC	:	Dummy variable containing $\Delta^{o}H_{1}$
HFE	:	Dummy variable containing $\Delta^{o}H_{o}$
NCOUNT	:	Number of constant composition sections to be plotted
R	:	gas constant
SA	:	Dummy variable containing the partition coefficient
TO	:	Dummy variable containing empirical temperature value from the binary Fe-C phase diagram

XCNEW	:	Carbide line carbon content in mole fraction
XSOL	:	dummy variable containing carbon compositions
XSOLA	:	Delta solidus carbon composition
XSOLD	:	Delta/delta + gamma carbon composition
XSOLG	:	Gamma solidus carbon composition
XSOLX	:	Alpha/alpha + gamma carbon composition
XWCAR	:	Carbide line carbon composition in wt.pct.

Arrays

BX,BZ,DXC,WC,WK, XNUM,XWT,Y,Z	:	Dummy arrays
EA	:	Dummy array holding interaction parameters: ϵ_{1i}^{1}
EB	:	Dummy array holding interaction parameters: ϵ_{1i}^{2}
G	:	Dummy array containing $\Delta^{o}G_{i}^{2\rightarrow 1}$
T,V	:	Tabulated $\Delta^{o}G_{o}^{\alpha\rightarrow\gamma}$ values; T(1) holds the temperature and V(I) the $\Delta^{o}G_{o}^{\alpha\rightarrow\gamma}$ value at that temperature
WT	:	Composition of element i in alloy in wt.pct.
X	:	Composition of element i in alloy in mole fraction
XW	:	Molecular weights of the alloying elements

Results: This is a copy of the program utilized to calculate the silicon sections shown in Fig. (8).

```
      PROGRAM TST(INPUT,OUTPUT,TAPE5=INPUT,TAPE6=OUTPUT)
C                                                                     C
C                                                                     C
CCCCCCCCCCCCCCCCCCCCCCCCCCCCCCCCCCCCCCCCCCCCCCCCCCCCCCCCCCCCCCCCCCCCCCC
C                                                                     C
C                                                                     C
C     THIS PROGRAM CALCULATES THE EFFECT OF ADDING ALLOYING ELEMENTS  C
C     TO THE FE-C BINARY AND PLOTS CONSTANT COMPOSITION CONTOURS      C
C     OF THE FE-C PHASE DIAGRAM.THIS PROGRAM IS VALID FOR THE         C
C     TEMPERATURE RANGE : 950 TO 1820 K ;AND FOR THE ELEMENTS :       C
C        MN,SI,NI,CR,MO,CU,W,V,NB AND CO. (ELEMENTS 1 THROUGH 11) .   C
C     AND THEIR RESPECTIVE CONCENTRATIONS IN WT. PCT. MUST BE         C
C     READ IN.                                                        C
C                                                                     C
C     WT(I)= WT. PCT OF ELEMENT I , 0<I<11                            C
C                                                                     C
C     X(I)= MOLE FRACTION OF ELEMENT I , CALCULATED IN THE PROGRAM    C
C                                                                     C
C     XW(I)= MOLECULAR WEIGHTS OF THE ELEMENTS                        C
C                                                                     C
C                                                                     C
CCCCCCCCCCCCCCCCCCCCCCCCCCCCCCCCCCCCCCCCCCCCCCCCCCCCCCCCCCCCCCCCCCCCCCC
C                                                                     C
C                                                                     C
      DIMENSION X(11), WT(11), XW(11), XNUM(11)
      DIMENSION Y(11), WK(11), DXC(11), RZ(11), BX(11)
      DIMENSION XWT(11), HC(12), Z(12), BCD(1)
      COMMON /DELG/ G(11),EA(11),EB(11),GFE
      COMMON /TTY/ SA
      COMMON /SSO/ T(100),V(100)
C     COMMON BLOCK SSO HOLDS HARVIGS DELTA G-O DATA FOR ALPHA
C     GAMMA FOR  INTERPOLATION USE .
      A=100.
      M=94
      N03=75
      THELP=1800.
      R=1.987
C
C     SET THE VALUES OF THE MOLECULAR WEIGHTS
C
      XW(1)=12.011
      XW(2)=54.938
      XW(3)=28.086
      XW(4)=58.71
      XW(5)=51.996
      XW(6)=95.94
      XW(7)=63.54
      XW(8)=183.85
      XW(9)=50.942
      XW(10)=92.906
      XW(11)=58.933
      DO 101 K=1,M
C
C     READ IN THE IRON DELTA G VALUES, NUMBER OF CONTOURS
C
      READ (5,119) T(K),V(K)
101   CONTINUE
      READ (5,120) NCOUNT
      DO 118 JJ=1,NCOUNT
C      READ IN VALUES IN WT. PCT.
```

```
      READ (5,121) (WT(I),I=1,11)
C
CCC   DRAW THE GRID OUTLINE
C
      CALL DRAW
      IF (WT(1).NE.0.00) NOB=1
      IF (WT(1).NE.0.00) WT(1)=-0.329999
      DTC=0.0
      CALL NEWPEN (1)
C
CCC   INCREMENT THE CARBON COMPOSITION
C
      DO 117 KL=1,NOB
      IF (WT(1).LE.1.1) WT(1)=WT(1)+0.03
      IF (WT(1).GT.1.1) WT(1)=WT(1)+0.1
C
CCC    CONVERT WT. PCT. TO ATOM FRACTION
C
      DEN=(A-WT(1)-WT(2)-WT(3)-WT(4)-WT(5)-WT(6)-WT(7)-WT(8)-WT(9)-WT(1
     1)-WT(11))/55.847+WT(1)/XW(1)+WT(2)/XW(2)+WT(3)/XW(3)+WT(4)/XW(4)+W
     2T(5)/XW(5)+WT(6)/XW(6)+WT(7)/XW(7)+WT(8)/XW(8)+WT(9)/XW(9)+WT(10)/
     3XW(10)+WT(11)/XW(11)
      DO 102 I=1,11
      X(I)=(WT(I)/XW(I))/DEN
102   CONTINUE
CCC   CALCULATE THE CARBIDE LINE SHIFT
C
      XCNEW=0.0
      IF (WT(1).LE.0.10.OR.WT(1).GT.2.3) GO TO 103
      CALL CARLIN (XW,X,WT,XWT,DTC,XCNEW)
      XWCAR=XWT(1)
103   CONTINUE
CCCC  CALCULATE THE EMPIRICAL FE-C TEMPERATURE , IRON AND CARBON
      ALPHA-GAMMA
C
      IF (WT(1).GE.0.75) GO TO 114
      CALL TAG (WT,X,TO,GFE,HC,HFE)
C
CCCC  CALCULATE DELTA G AND INTERACTION PARAMETER DATA FOR
      ALPHA-GAMMA
C
      CALL GAG (TO)
C
CCCC  CALCULATE TEMPERATURE SHIFT
C
      CALL CALCT (TO,X,HC,HFE,DT)
      DT=TO+DT
C
CCC   CALCULATE ALPHA/ALPHA+GAMMA LINE
C
      XSOL=X(1)*SA
      DTE=DT
C
CCC   PLOT THE CALCULATED VALUES
C
      IF (DTE.GE.1350) GO TO 107
      XSOLX=XSOL
      CALL CHANGE (XSOLX,XW,X,XWT)
```

```
      XC=XWT(1)
      YC=DTE
C     C
      CALL UNITTO (XD,YD,XP,YP)
      CALL GRAF (XP,YP,0.025,9)
      IF (DTC.GE.DTE) GO TO 105
      XC=WT(1)
      YC=DTE
      CALL UNITTO (XD,YD,XP,YP)
      CALL GRAF (XP,YP,0.025,9)
      GO TO 106
104   CONTINUE
105   CONTINUE
      IF (XWCAR.GT.2.5) GO TO 106
      IF (DTC.GE.DTG) GO TO 106
      IF (DTC.LE.DTE) GO TO 106
      YC=DTC
      XC=XWCAR
      CALL UNITTO (XD,YD,XP,YP)
      CALL GRAF (XP,YP,0.025,9)
106   CONTINUE
107   CONTINUE
C
CCC   CALCULATE THE EMPIRICAL FE-C TEMPERATURE , IRON AND CARBON DATA
CCC   FOR ALPHA-LIQUID
C
      IF (WT(1).GE.2.5) GO TO 108
      CALL TAL (WT,X,TO,GFE,HC,HFE)
C
CCC   CALCULATE DELTA G AND INTERACTION PARAMETER DATA FOR
CCC   FOR ALPHA-LIQUID
C
      CALL GAL (TO)
C
CCC   CALCULATE TEMPERATURE SHIFT
CCC
      CALL CALCT (TO,X,HC,HFE,DT)
      DT=TO+DT
C
CCC   CALCULATE THE SOLIDUS
C
      XSOL=X(1)*SA
      DTA=DT
      XSOLA=XSOL
108   CONTINUE
C
CCC   CALCULATE THE EMPIRICAL FE-C TEMPERATURE , IRON AND CARBON DATA
CCC   GAMMA-LIQUID
C
      CALL TGL (WT,X,TO,GFE,HC,HFE)
C
CCC   CALCULATE DELTA G AND INTERACTION PARAMETER DATA FOR
CCC   GAMMA-LIQUID
C
      CALL GGL (TO)
C
CCC   CALCULATE TEMPERATURE SHIFT
C
      CALL CALCT (TO,X,HC,HFE,DT)
      DT=TO+DT
```

```
C
CC      CALCULATE THE SOLIDUS
C
        XSOL=X(1)*SA
        DTG=DT
        XSOLG=XSOL
C
CCC     DETERMINE AND PLOT THE CORRECT  LIQUIDUS
C
        DTA=DTA
        DTS=DTG
        IF (DTA.GE.DTG) DTG=DTA
        IF (WT(1).GT.2.5) GO TO 109
        XO=WT(1)
        YO=DTG
        CALL UNITTO (XO,YO,XP,YP)
        CALL GRAF (XP,YP,.025,9)
109     CONTINUE
CCC     CALCULATE THE EMPIRICAL FE-C TEMPERATURE , IRON AND CARBON DATA
CC      DELTA-GAMMA
C
        IF (WT(1).GT.0.3) GO TO 110
        IF (THELP.GT.1800.OR.THELP.LT.1350) GO TO 110
        CALL TDG (WT,X,TO,GFE,HC,HFE)
C
CCCC    CALCULATE DELTA G AND INTERACTION PARAMETER DATA FOR
        DELTA-GAMMA
C
        CALL DAG (TO)
C
CCC     CALCULATE TEMPERATURE SHIFT
C
        CALL CALCT (TO,X,HC,HFE,DT)
        DT=TO+DT
        THELP=DT
        CALL PLOTPT (DT,X(1),4)
C
CCC     CALCULATE THE DELTA/GAMMA+DELTA PHASE BOUNDARY
C
        XSOL=X(1)*SA
        DTD=DT
        XSOLD=XSOL
110     CONTINUE
C
CCC     PLOT THE CORRECT SOLIDUS OR DELTA PHASE EXTENT
C
        IF (XCNEW.GT.XSOLG.AND.DTC.GT.DTG) GO TO 111
        CALL CHANGE (YSOLG,XW,X,XWT)
        IF (XWT(1).GE.2.5) GO TO 111
        XO=XWT(1)
        YO=DTG
        CALL UNITTO (XO,YO,XP,YP)
        CALL GRAF (XP,YP,.025,9)
111     CONTINUE
        IF (DTG.LT.DTD) GO TO 113
        IF (DTE.GT.DTC) GO TO 112
        IF (WT(1).GT.0.3) GO TO 112
        XO=WT(1)
        YO=DTD
```

```
      CALL UNITTO (XD,YD,XP,YP)
      CALL GRAF (XP,YP,.025,9)
112   CONTINUE
113   CONTINUE
      IF (X.LT.66669) GO TO 114
      IF (DTA.LT.DTD) GO TO 116
      CALL CHANGE (XSCLA,XW,X,XWT)
      XD=XWT(1)
      YD=DTA
      CALL UNITTO (XD,YD,XP,YP)
      CALL GRAF (XP,YP,.025,9)
114   CONTINUE
      IF (WT(1).GT.0.3) GO TO 115
      IF (DTE.GT.DTD) GO TO 115
      CALL CHANGE (XSCLC,XW,X,XWT)
      XD=XWT(1)
      YD=DTD
      CALL UNITTO (XD,YD,XP,YP)
      CALL GRAF (XP,YP,.025,9)
115   CONTINUE
116   CONTINUE
117   CONTINUE
118   CONTINUE
C
C     END THE PLOT
C
      CALL NEWPEN (2)
      CALL PLTLN (4.0,850.0,4.0,1890.0)
      CALL PLOT (X,Y,999)
      STOP
C
119   FORMAT (F5.0,F7.3)
120   FORMAT (I3)
121   FORMAT (11F5.0)
      END
C*****************************************************************
      SUBROUTINE DRAW
C
C     DRAWS AND LABELS THE GRID
C
      DIMENSION WC(6), Z(3), BCD(1)
      XSCALE=0.2
      YSCALE=40.
      CALL PLOT (X,Y,-20)
      CALL PLTLN (.2,40.0,-1.2,940.0,-1.2,5.0,840.0,1900.0)
      CALL NEWPEN (5)
      CALL PLTLN (2.5,1850.0,2.5,950.0)
      CALL PLTLN (5.0,1850.0,2.5,1850.0)
      CALL PLTLN (5.0,950.0,0.0,1850.0)
      CALL PLTLN (2.5,950.0,0.0,950.0)
      CALL NEWPEN (2)
      A1=.5
      B1=950.0
      A2=1.5
      B2=950.0+1.2*YSCALE
      DO 1 I=1,5
      CALL PLTLN (A1,B1,A2,B2)
      A1=A1+0.5
```

```
      A2=A2+0.5
1     CONTINUE
      A1=0.0
      B1=1000.0
      A2=0.0+2*XSCALE
      B2=1000.0
      DO 2 I=1,9
      CALL PLTLN (A1,B1,A2,B2)
      B1=B1+100.
      B2=B2+100.0
2     CONTINUE
      WC(1)=0.0
      DO 3 I=2,6
      WC(I)=WC(I-1)+0.5
3     CONTINUE
      R=-0.06
      S=900.0
      THETA=0.0
      HEIGHT=0.25
      DO 4 I=1,6
      WC(2)=0.5
      ANUM=WC(I)
      CALL NUMBER (R,S,HEIGHT,ANUM,THETA,6H(F3.1))
      R=R+0.50
4     CONTINUE
      Z(1)=1000.0
      DO 5 I=2,9
      Z(I)=Z(I-1)+100.0
5     CONTINUE
      R=-0.24
      S=1000.0
      DO 6 I=1,9
      INUM=IFIX(Z(I))
      CALL INTNUM (R,S,HEIGHT,INUM,THETA,4H(I4))
      S=S+100.0
6     CONTINUE
      CALL PLTLET (15,0.325,90.0,-0.5,1380.0,15HTEMPERATURE (K))
      CALL PLTLET (15,0.325,0.0,0.8,890.0,15HWT. PCT. CARBON)
      RETURN
      END
C*****************************************************************
      SUBROUTINE NUMBER (R,S,HEIGHT,ANUM,THETA,FMT)
C
C     ENCODING ROUTINE FOR REAL NUMBERS
C
      DIMENSION BCD(1)
      ENCODE (10,FMT,BCD) ANUM
      CALL PLTLET (10,0.25,THETA,R,S,BCD)
      RETURN
      END
C*****************************************************************
      SUBROUTINE INTNUM (R,S,HEIGHT,INUM,THETA,FMT)
C
C     ENCODING ROUTINE FOR INTEGERS
C
      DIMENSION BCD(1)
```

```
      ENCODE (10,FMT,BCD) INUM
      CALL PLTLET (10,0.25,THETA,R,S,BCD)
      RETURN
      END
C*****************************************************************
      SUBROUTINE CHANGE (XSOLX,XW,X,XWT)
C
CC     CHANGES ALL VALUES FROM MOLE FRACTION TO WT. PCT.
C
      DIMENSION XW(11), X(11), XWT(11)
      DEN=(1-XSOLX-X(2)-X(3)-X(4)-X(5)-X(6)-X(7)-X(8)-X(9)-X(10)-X(11))
     155.847+XSOLX*XW(1)+X(2)*XW(2)+X(3)*XW(3)+X(4)*XW(4)+X(5)*XW(5)+X(
     2)*XW(6)+X(7)*XW(7)+X(8)*XW(8)+X(9)*XW(9)+X(10)*XW(10)+X(11)*XW(11
      XP=100*XSOLX*XW(1)/DEN
      XWT(1)=XP
      DO 1 I=2,11
      XWT(I)=100*X(I)*XW(I)/DEN
1     CONTINUE
      RETURN
      END
C*****************************************************************
      SUBROUTINE TAG (WT,X,TO,GFE,HC,HFE)
C
CCCC
CCCCCC
CCCC
C
      DIMENSION WT(11), X(11)
      COMMON /SSO/ T(100),V(100)
      REAL HC,HFE
C      CALCULATES TO
      C=WT(1)
      TO=1115.-153.3*C+216.*((0.765-C)**4.26)
C     CALCULATES DELTA G-J FOR FE
      K=INT((TO-900)/10+1)
      GFE=V(K)+(V(K+1)-V(K))*(T(K+1)-TO)/10
      HC=-15323
      HFE=GFE+TO*(0.85-0.0046*(TO-1000.)**0.96)
      HFE=HFE+.058*COS(0.034*(TO-1000.0))*TO
      RETURN
      END
C*****************************************************************
      SUBROUTINE GAG (TO)
C
CCCC
CCCCCC
CCCC
C
      COMMON /DELG/ G(11),EA(11),EB(11),GFE
      T=TO
```

```
      G(1)=-15323+7.666*T
      G(2)=-34795+62.137*T-0.0255*T**2
      G(2)=G(2)*0.667
      G(3)=38.779*T-4.7244*T*ALOG(T)-5964.
      G(4)=-4545+3.237*T
      G(5)=-367-4.656*T+0.6562*T*ALOG(T)
      G(6)=565+0.15*T
      G(7)=-25500+41.183*T-0.017*T**2
      G(8)=25000-0.15*T
      G(9)=-8357+13.8*T-0.0051*T**2
      G(10)=-14.34+0.0013*(T-273)
      G(11)=0.0
      SA=1100/T
      EA(1)=6.1*SA
      EA(2)=-5070/T
      EA(3)=4.84+7370/T
      EA(4)=4535/T+0.557
      EA(5)=24.4-32400/T
      EA(6)=7.83-15930/T
      EA(7)=3.8*1273/T
      EA(8)=-4.0*1323/T
      EA(9)=-19.4*1273/T
      EA(10)=-40*1273/T
      EA(11)=2.3*1273/T
      DO 1 I=1,11
      EB(I)=0.0
1     CONTINUE
      RETURN
      END
C*****************************************************************
      SUBROUTINE TDG (WT,X,TC,GFE,HC,HFE)
C
C
C     CALCULATES THE DELTA G FOR IRON , THE DELTA H FOR IRON AND
C     CARBON AND THE EMPIRICAL TEMPERATURE FROM THE FE-C PHASE DIAGRAM
C     FOR DELTA/GAMMA
C
C
      DIMENSION WT(11), X(11)
      COMMON /SSO/ T(100),V(100)
      REAL HC,HFE
      XC=WT(1)
C       CALCULATES TO
      TC=1666+981*XC-179.0*XC**2
C     CALCULATES DELTA G-O FOR FE
      K=INT((TO-900)/10+1)
      GFE=V(K)+(V(K+1)-V(K))*(T(K+1)-TO)/10
      GFE=-GFE
      HC=15323
      HFE=200
      RETURN
      END
C*****************************************************************
      SUBROUTINE DAG (TO)
C
C
```

```
C       CALCULATES THE DELTA G AND INTERACTION PARAMETER DATA FOR
CC      DELTA/GAMMA
CC
C
        COMMON /DELG/ G(11),EA(11),EB(11),GFE
        T=TO
        G(1)=-5.3*T+7840
        G(2)=650-0.305*T
        G(3)=5364-38.779*T+4.7244*T*ALOG(T)
        G(4)=4545-3.233*T
        G(5)=367+4.556*T-0.6568*T*ALOG(T)
        G(6)=-565-0.15*T
        G(7)=25500-41.183*T+0.017*T**2
        G(8)=-2500+0.15*T
        G(9)=8357-1398*T+.0151*T**2
        G(10)=14.34-0.0013*(T-273)
        G(11)=0.00
        SA=1100/T
        EA(1)=0.1*SA
        EA(2)=-5070/T
        EA(3)=4.64+7370/T
        EA(4)=4835/T+0.557
        EA(5)=24.64-38400/T
        EA(6)=7.03-15930/T
        EA(7)=3.8*1273/T
        EA(8)=-4.0*1323/T
        EA(9)=-19.4*1273/T
        EA(10)=-4.0*1273/T
        EA(11)=2.3*1273/T
        DO 1 I=1,11
        EB(I)=EA(I)
1       CONTINUE
        RETURN
        END
C*******************************************************************************
        SUBROUTINE TGL (WT,X,TO,GFE,HC,HFE)
C
CC      CALCULATES THE DELTA G FOR IRON , THE DELTA H FOR IRON AND
CC      CARBON AND THE EMPIRICAL TEMPERATURE FROM THE FE-C PHASE DIAGRAM
CC      FOR GAMMA/LIQUID
CCC
C
        DIMENSION WT(11), X(11)
        REAL HC,HFE
C       CALCULATE TO
        C=WT(1)
        TO=1534.3-61.3*C-4.6*C**2
C       CALCULATE GFE
        GFE=-2646+39.1693*TO-5.27*TO*ALOG(TO)+0.001*TO**2
        HC=5430.
        HFE=3524.
        RETURN
        END
C*******************************************************************************
        SUBROUTINE GGL (TC)
```

```
C
CCCCC
      CALCULATES THE DELTA G AND INTERACTION PARAMETER DATA FOR
      GAMMA/LIQUID
CCCCC
C
      COMMON /DELG/ G(11),EA(11),EB(11),GFE
      T=TO
      XX=1800/T
      G(1)=-5633+0.6*T
      G(2)=2860-2.63*T
      G(3)=-2236-34.6*T+4.7244*T*ALOG(T)
      G(3)=3.9*T-8200
      G(4)=-790-0.64*T
      G(5)=4600-2.19*T
      G(6)=2.14*T-7165
      G(7)=9000-2.37*T
      G(8)=6190-2.45*T
      G(9)=-4995-1.93*T
      G(10)=5500-2.3*T
      G(11)=4110-2.19*T
      EA(1)=7510/T+0.389
      EA(2)=-2.79*XX
      EA(3)=18476/T-0.429
      EA(4)=2.85*XX
      EA(5)=-5.37*XX
      EA(6)=-4*XX
      EA(7)=4.05*XX
      EA(8)=-6.53*XX
      EA(9)=-16.07*XX
      EA(10)=-23.62*XX
      EA(11)=1.79*XX
      EB(1)=8.1*1100/T
      EB(2)=-5070/T
      EB(3)=4.84+7370/T
      EB(4)=4835/T+0.557
      EB(5)=24.4-38400/T
      EB(6)=7.63-15930/T
      EB(7)=3.8*1273/T
      EB(8)=-4.0*1323/T
      EB(9)=-19.4*1273/T
      EB(10)=-4.0*1273/T
      EB(11)=2.3*1273/T
      RETURN
      END
C*****************************************************************
      SUBROUTINE TAL (WT,X,TO,GFE,HC,HFE)
C
CCC
      CALCULATES THE DELTA G FOR IRON , THE DELTA H FOR IRON AND
C     CARBON AND THE EMPIRICAL TEMPERATURE FROM THE FE-C PHASE DIAGRAM
C     FOR DELTA/LIQUID
CCC
C
      COMMON /SSO/ T(100),V(100)
      DIMENSION WT(11), X(11)
      REAL HC,HFE
C     CALCULATE TO
```

```
      C=W1(1)
      TC=1809-29.56*C-86.*C**2
C       CALCULATE GFE
      K=INT((TO-900)/10+1)
      GAA=V(K)+(V(K+1)-V(K))*(T(K+1)-TO)/10
      GBB=-2646+39.1693*TO-5.27*TO*ALOG(TO)+0.001*TO**2
      GFE=GAA+GBB
      HC=5400.
      HFE=3524.
      RETURN
      END
C*****************************************************************
      SUBROUTINE GAL (TO)
C
CCCCCC
      CALCULATES THE DELTA G AND INTERACTION PARAMETER DATA FOR
      DELTA/LIQUID
C
      COMMON /DELG/ G(11),EA(11),EB(11),GFE
      T=TO
      XX=1000/T
      G(1)=-21300+6.3*T
      G(2)=3100-2.308*T
      G(3)=3.9*T-8200
      G(4)=-2120-0.38*T
      G(5)=2.19*T-4600
      G(6)=2.29*T-6600
      G(7)=9000-2.37*T
      G(8)=6190-2.45*T
      G(9)=-4950-1.93*T
      G(10)=5500-2.3*T
      G(11)=3550-2.19*T
      EA(1)=7810/T+0.389
      EA(2)=-2.70*XX
      EA(3)=18476/T-0.428
      EA(4)=2.85*XX
      EA(5)=-5.07*XX
      EA(6)=-4*XX
      EA(7)=-5.07*XX
      EA(8)=-4*XX
      EA(9)=4.05*XX
      EA(10)=-6.53*XX
      EA(11)=-16.07*XX
      EA(12)=-23.82*XX
      EA(13)=1.79*XX
      EB(1)=8.1*1100/T
      EB(2)=-5070/T
      EB(3)=4.64+7370/T
      EB(4)=4635/T+0.557
      EB(5)=24.4-38400/T
      EB(6)=7.83-15930/T
      EB(7)=3.8*1273/T
      EB(8)=-4.0*1323/T
      EB(9)=-19.4*1273/T
      EB(10)=-4.0*1273/T
      EB(11)=2.3*1273/T
      RETURN
```

```
      END
C*****************************************************************
      SUBROUTINE CARLIN (XW,X,WT,XWT,DTC,XCNEW)
C
CCC
CCC    CARLIN CALCULATES THE SHIFT IN THE CARBON CONTENT OF THE
CCC    CARBIDE LINE ,AT ANY GIVEN TEMPERATURE, WITH THE ADDITION
CCC    OF ALLOYING ELEMENTS
CCC
C
      DIMENSION WK(11), DXC(11), XW(11), WT(11), X(11), XWT(11)
      DIMENSION Y(11), BX(11), BZ(11)
      COMMON /CELG/ G(11),EA(11),EB(11),GFE
      TO=1000.*(0.673+0.485*WT(1)-0.062*WT(1)**2)
      CALL GAG (TO)
      T=TO
      EA(2)=4.64+7370/T
      TT=TO-273.15
      CALL GAG (TO)
      DO 1 I=1,11
      BZ(I)=WT(I)
      BX(I)=X(I)
      WK(I)=0.0
1     CONTINUE
      DXSUM=0.0
      DXC(1)=0.0
      A=100.0
C
CCC   PARTITION COEFFICIENTS , CALCULATED AT TEMPERATURE
C
      WK(2)=-0.00284*TO+5.44
      WK(3)=1E-34
      WK(4)=0.0004*TO-0.249
      WK(5)=-22.78*ALOG(TT)+163.444
      WK(5)=WK(5)-2.0
      WK(6)=-16.9*ALOG(TT)+121.
      DO 2 I=2,11
      WT(I)=WK(I)*WT(I)
      DEN=(A-WT(1)-WT(2)-WT(3)-WT(4)-WT(5)-WT(6)-WT(7)-WT(8)-WT(9)-WT(1
     1)-WT(11))/55.847+WT(1)/XW(1)+WT(2)/XW(2)+WT(3)/XW(3)+WT(4)/XW(4)+
     2T(5)/XW(5)+WT(6)/XW(6)+WT(7)/XW(7)+WT(8)/XW(8)+WT(9)/XW(9)+WT(10)/
     3XW(10)+WT(11)/XW(11)
      Y(I)=(WT(I)/XW(I))/DEN
      IF (X(I).EQ.0.0) X(I)=1.0E-10
      XK=Y(I)/X(I)
      DA=XK-1.0+(1+EA(I))*(0.25-X(1))
      DB=X(1)*((1.0+EA(1))*(0.25-X(1))-1.0)
      DXC(I)=-X(1)*X(I)*DA/(0.25+DB)
      DXSUM=DXSUM+DXC(I)
2     CONTINUE
      X(1)=3X(1)
      XCNEW=X(1)+DXSUM
      CALL CHANGE (XCNEW,XW,X,XWT)
C
CCC   XWT(1) IS THE ACTUAL CARBON CONTENT IN WT. PCT.
CCC   XCNEW  IS THE ACTUAL CARBON CONTENT IN AT. PCT.
C
      DTC=TO
```

```
      DO 3 I=1,11
      WT(I)=BZ(I)
      X(I)=BX(I)
3     CONTINUE
      RETURN
      END
C*****************************************************************
      SUBROUTINE CALCT (TO,X,HC,HFE,DT)
C
CCC
CCC   CALCT DETERMINES THE SHIFT IN TEMPERATURE CAUSED BY THE
C     ADDITION OF ALLOYING ELEMENTS
CCC
C
      COMMON /TTY/ SA
      DIMENSION X(11), XNUM(11)
      COMMON /DELG/ G(11),EA(11),EB(11),GFE
      REAL HC,HFE
C
CCC   CALCULATE NUMERATOR
C
      R=1.987
      RT=1.987*TO
      FC=G(1)
      XC=X(1)
      EC=EA(1)
      XNUM(1)=0.0
      SUMNUM=0.0
      SA=(EXP(FC/RT+EC*XC)/(1+EB(1)*XC*EXP(FC/RT)))
      PHIC=EXP(GFE/RT-((XC**2)/2*(EC-EB(1)*SA**2)))
      GG=FC/RT
      DO 1 I=2,11
      F=G(I)
      E=EA(I)
      PA=EXP(F/RT+E*XC)/(1+EB(I)*XC*EXP(GG))
C     CALCULATE I-TH TERM
      XNUM(I)=X(I)*(PA-(1+XC*(1-XC)*(E-EB(I)*SA*PA))*PHIC)
C
CCC   DOES SUMMATION OF NUMERATOR
CC
      SUMNUM=SUMNUM+XNUM(I)
1     CONTINUE
CCC
CCC   CALCULATE DENOMINATOR
C
      DEN=(XC*HC*SA)+((1-XC)*HFE*PHIC)
C
CCC   CALCULATE TEMPERATURE DIFFERENCE
CC
      DT=R*(TO**2)*SUMNUM/DEN
      RETURN
      END
C*****************************************************************
      SUBROUTINE NEWPEN (U)
C
C     DUMMY ROUTINE NECESSARY IN ORDER TO ACCOMMODATE DIFFERENT PLOTTER
```

```
C
      RETURN
      END

*          6400 END OF RECORD
  980.  99.3
  990.  89.6
 1000.  80.80
 1010.  72.18
 1020.  64.15
 1030.  56.75
 1040.  50.15
 1050.  44.21
 1060.  39.11
 1070.  34.21
 1080.  29.92
 1090.  26.07
 1100.  22.22   0.0
 1110.  18.37
 1120.  14.82
 1130.  11.54
 1140.   9.11
 1150.   6.66
 1160.   4.48
 1170.   2.52
 1180.   0.74
 1190.  -0.89
 1200.  -2.40
 1210.  -3.82
 1220.  -5.15
 1230.  -6.39
 1240.  -7.55
 1250.  -8.63
 1260.  -9.63
 1270.  -10.55
 1280.  -11.41
 1290.  -12.17
 1300.  -12.87
 1310.  -13.50
 1320.  -14.06
 1330.  -14.54
 1340.  -14.95
 1350.  -15.29
 1360.  -15.57
 1370.  -15.79
 1380.  -15.95
 1390.  -16.05
 1400.  -16.11
 1410.  -16.11
 1420.  -16.06
 1430.  -15.97
 1440.  -15.83
 1450.  -15.64
 1460.  -15.43
 1470.  -15.11
 1480.  -14.77
 1490.  -14.38
 1500.  -13.95
 1510.  -13.48
```

```
1520.  -12.97
1530.  -12.41
1540.  -11.83
1550.  -11.15
1560.  -10.45
1570.  -9.71
1580.  -8.92
1590.  -8.08
1600.  -7.20
1610.  -6.27
1620.  -5.30
1630.  -4.28
1640.  -3.22
1650.  -2.11
1660.  -0.96
1670.   0.23
1680.   1.47
1690.   2.75
1700.   4.08
1710.   5.45
1720.   6.86
1730.   8.31
1740.   9.81
1750.  11.36
1760.  12.97
1770.  14.63
1780.  16.35
1790.  18.13
1800.  19.98
1810.  21.90
   3
                1.0
                2.0
```

References

1. E.A. Baganis, Private Communication.
2. K.W. Andrews, J.I.S.I., 203, (1965), p. 721.
3. T. Kunitaki and H. Ohtani, The Sumitomo Search, Vol. 2 (1969), p. 18.
4. R.A. Grange, Met. Progress, 79 (1961), No. 4, p. 73.
5. F. Wever, Arch. Eisenhuttenwesen, 2 (1928/29), pp. 739-748.
6. F. Wever, Mitt. K.W.I. Eisenforsch., 13 (1931), pp. 193-197.
7. F. Wever, Ergebnisse der Technischen Röntgenkunde, 2 (1931), pp. 240-250.
8. C. Zener, Trans. Amer. Inst. Min. Met. Eng., 167 (1946), p. 513.
9. E. Baganis and J.S. Kirkaldy, Met. Trans. A, in press (1978).
10. M. Hillert, "Calculation of Phase Equilibria", Phase Transformations, 1968 Seminar, ASM, Metals Park, Ohio, pp. 181-218.
11. M. Hillert and L.J. Staffansson, Acta. Chem. Scand., 24 (1970), pp. 3618.
12. J.F. Elliott, M. Gleiser and V. Ramakrishna, Thermochemistry for Steelmaking, Vol. II, Addison-Wesley, Mass. (1963).
13. D.R. Gaskell, Introduction to Metallurgical Thermodynamics, McGraw-Hill, New York (1973), p. 394.
14. H. Harvig, Jernkont. Ann., 155 (1971), pp. 157-161.
15. R.L. Orr and J. Chipman, Trans. TMS-A.I.M.E., 239 (1967), pp. 630-633.
16. T. Wada, H. Wada, J.F. Elliott and J. Chipman, Met. Trans., 3 (1973), pp. 1657-1662.

17. R.C. Sharma and J.S. Kirkaldy, Can. Met. Quart., 12 (1973), pp. 391.

18. G.K. Sigworth and J.F. Elliott, Metal Science, 8 (1974), pp. 298-310.

19. J. Chipman, Met. Trans., 1 (1970), pp. 2163-2168.

20. M.G. Benz and J.F. Elliott, Trans. TMS-A.I.M.E., 221 (1961), pp. 323-331.

21. W.A. Fischer, K. Lorenz, H. Fabritius and D. Schlegel, Arch. Eisenhüttenwesen, 41 (1970), pp. 489-498.

22. W.A. Dench and O. Kubaschewski, J.I.S.I., 201 (1963), pp. 140-143.

23. A. Ferrier and M. Olette, Compt. Rend., 254 (1962), pp. 2322-2324.

24. J.P. Morris, E.F. Foerster, C.W. Schultz and G.R. Zellars, U.S. Bureau of Mines, Rept. Invest. No. 6723 (1966).

25. O. Vollmer, R. Kohlhass and M. Braun, Z. Naturforschg., 21 (1966), pp. 181-182.

26. A.R. Troiano and F.T. McGuire, Trans. ASM, 31 (1943) pp. 340.

27. G. Kirchner, T. Nishizawa and B. Uhrenius, Met. Trans., 4 (1973), pp. 167-174.

28. E.A. Baganis, M. Eng. Thesis, McMaster University (1976).

29. A. Hellawell and W. Hume-Rothery, Phil. Trans. Roy. Soc., 249 (1957), pp. 417-459.

30. M. Hillert and L. Staffansson, Met. Trans. B, 7B (1976), pg. 2040.

31. E. Übelacker, Compt. Rend., 261 (1967), pp. 976-979.

32. J. Fridberg and H. Harvig, TRITA-MAC-0007, Materials Centre, Royal Institute of Technology, 5100 44 Stockholm 70 (1971).

33. L. Kaufman, in "Phase Stability in Metals and Alloys", P.S. Rudman, J. Stringer and R.I. Jaffe, eds., McGraw-Hill, New York (1967).

34. L. Kaufman, in "Phase Stability in Metals and Alloys", P.S. Rudman, J: Stringer and R.I. Jaffe, eds., McGraw-Hill, New York (1967).

35. R.B. Reese, R.A. Rapp and G.R. St. Pierre, Trans. A.I.M.E., 242 (1968). pp. 1719-1726.

36. G. Belton and R. Fruehan, Met. Trans., 1 (1970), pp. 781-787.

37. G. Kirchner, H. Harvig and B. Uhrenius, Met. Trans., 4 (1973), pp. 1059-1067.

38. A.K. Sinha, R.A. Buckley and W. Hume-Rothery, J.I.S.I., 205 (1967), pp. 191-195.

39. W.S. Gibson, J.R. Lee and W. Hume-Rothery, J.I.S.I., 198 (1961), pp. 64-66.

40. R.J. Weiss and K.J. Tauer, Phys. Rev., 102 (1956), pg. 1490.

41. H. Harvig, G. Kirchner and M. Hillert, Met. Trans., 3 (1972), pp. 329-333.

42. L. Kaufman, Report PB144220, Office of Technical Services, Cambridge, Mass.

43. J.P. Morris and G.R. Zellars, TMS-A.I.M.E., 206 (1956), pp. 1086-1090.

44. F. Wooley and J.F. Elliott, Trans. A.I.M.E., 234 (1967), pp. 1872-1883.

45. W. Oelsen, E. Schürmann and C. Florin, Arch. Eisenhuttenwesen, 32 (1961), pp. 719-728.

46. A.K. Sinha and W. Hume-Rothery, J.I.S.I., 205 (1967), pp. 1145-1149.

47. G. Kirchner and G. Gemmel, "Fördelning av Vanadin Mellan Ferrit och Austenit, Teknisa Hogskolan (1970).

48. W.R. Lucas and W.P. Fishel, Trans. A.I.M.E., 46 (1954), pp. 277-282.

49. T. Wada, H. Wada, J.F. Elliott and J. Chipman, Met. Trans., 3 (1972), pp. 2865-2872.

50. K.M. Myles and A.T. Aldred, J. Phys. Chem., 68 (1964), pp. 64-69.

51. J. Fruehan, Met. Trans., 1 (1970), pp. 2083-2088.

52. R.C. Hudd, A. Jones and M.N. Kale, J.I.S.I., 209 (1971), pp. 121-125.

53. A. Ferrier, E. Übelacker and E. Wachtel, Compt. Rend., 258, (1964), pp. 5424-5427.

54. G.B. Harris and W. Hume-Rothery, J.I.S.I., 170 (1953), pp. 212-217.

55. J.B. Gilmour, G.R. Purdy and J.S. Kirkaldy, Met. Trans., 3 (1972), pp. 1455-1462.

56. R. Ebeling and N. Wever, Arch. Eisenhuttenwesen, 40 (1969), pp. 551-555.

57. L. Kaufman, Prog. Mater. Sci., 14 (1969), pp. 55-96.

58. C.H.P. Lupis and J.F. Elliott, Trans. TMS-A.I.M.E., 233 (1965), pp. 257-258.

59. J.M. Dealy and R.D. Pehlke, Trans. TMS-A.I.M.E., 227 (1963), pp. 88-91.

60. T. Nishizawa, Scand. J. Metal., 1 (1972), pp. 41-48.

61. T. Nishizawa, "Thermodynamics of Fe-C-Mn, Fe-C-Cr and Fe-C-Mo Systems", Report 4602, Swedish Board for Technical Development, Stockholm (1967).

62. J.C. Greenbank, J.I.S.I., 209 (1971), pp. 986-990.

63. K. Bungardt, E. Schümann, H. Preisendonz, P. Schüler and H.J. Osing, DEW-Tech-Ber., 9 (1969), pg. 439.

64. J.A. Lobo and G.H. Geiger, Met. Trans. A, 7A (1976), pp. 1347-1357.

65. O. Nyquist, K.W.K. Lange and J. Chipman, Trans. A.I.M.E., 224 (1962), pp. 714-718.

66. H. Wada, K. Gunji, T. Wada, Trans. Nat. Res. Inst. for Metals, 9 (1967), pp. 22-26.

67. T. Fuwa and J. Chipman, Trans. A.I.M.E., 215 (1959), pp. 708-716.

68. R. Smith, J. Am. Chem. Soc., 70 (1948), pp. 2724-2729.

69. T. Wada, H. Wada, J.F. Elliott and J. Chipman, Met. Trans. 3 (1972), pp. 1657-1662.

70. J.C. Greenbank, J.I.S.I., 209 (1971), pp. 819-825.

71. K. Natesan and T.F. Kassner, Met. Trans., 4 (1974), pp. 2557-2566.

72. A.J. Heckler and P.G. Winchell, Trans. TMS-A.I.M.E., 227 (1963), pg. 732.

73. R. Smith, Trans. TMS-A.I.M.E., 218 (1960), pg. 62.

74. R.J. Brigham and J.S. Kirkaldy, Trans. TMS-A.I.M.E., 227 (1963), pp. 538-539.

75. L.C. Brown and J.S. Kirkaldy, Trans. TMS-A.I.M.E., 227 (1963), pg. 1461.

76. V.K. Chandhok, J.P. Hirth and E.J. Dulis, Trans. TMS-A.I.M.E., 224 (1962), pp. 858-864.

77. R. Smith, Trans. A.I.M.E., 233 (1965), pp. 397-401.

78. B. Uhrenius, Sandvik Internal Report, Reg. No. FF1775 (1973).

79. R. Sharma, Ph.D. Thesis, McMaster University (1976).

80. B. Uhrenius, to be published in "Hardenability with Application to Steels", The Metal Society, Metals Park, Ohio (1978).

81. L. Kaufman, S.V. Radcliffe and M. Cohen, in: Decomposition of Austenite by Diffusional Processes, V.F. Zackay and H.I. Aaronson, ed., John Wiley and Sons, New York (1962), pp. 313-351.

82. S. Ban-Ya, J.F. Elliott and J. Chipman, Met. Trans., 1 (1970), pp. 1313-1320.

83. H.I. Aaronson and H.I. Domion, Trans. TMS-A.I.M.E., 236 (1966), p. 781.

84. M.G. Hall, K.R. Kinsman and H.I. Aaronson, Met. Trans., 3 (1972), p. 1320.

85. J.B. Gilmour, The Role of Manganese in the Formation of Proeutectoid Ferrite, Ph.D. Thesis, McMaster University (1970).

86. G. Kirchner and B. Uhrenius, Acta Met., 22 (1974), p. 391.

87. D. Swinden and J. Woodhead, J.I.S.I., 209 (1971), p. 883.

88. Atlas of Isothermal Transformation Diagrams, U.S. Steel, Pittsburgh U.S.A., Third Edition (1963). Also supplement to Second Edition (1953).

89. A.S.M. Metal Progress Data Sheets, Metal Progress Reprint Service, American Society for Metals, Metals Park, Ohio, U.S.A.

90. N.A. Razik, G.W. Lorimer and N. Ridley, Met. Trans., 7A (1976), pp. 209-214.

91. E.G. Bain and H.W. Paxton, Alloying Elements in Steels, A.S.M., Metals Park, Ohio (1961).

92. G. Thomas, from: Fundamental Aspects of Structural Alloy Design, R.I. Jaffe and B.A. Wilcox, eds., Plenum Publishing Corp. (1977).

93. J.S. Kirkaldy, B.A. Thomson and E.A. Baganis, to be published in "Hardenability with Application to Steels", The Metal Society, Metals Park, Ohio, (1978).

94. J.S. Kirkaldy and G.R. Purdy, Can. J. of Physics, 40 (1962), p. 202.

95. B. Brion, P. Desre and E. Bonnier, J. Chim. Phys. et Phys-Chim. Biolog., 65 (1968), p. 1321.